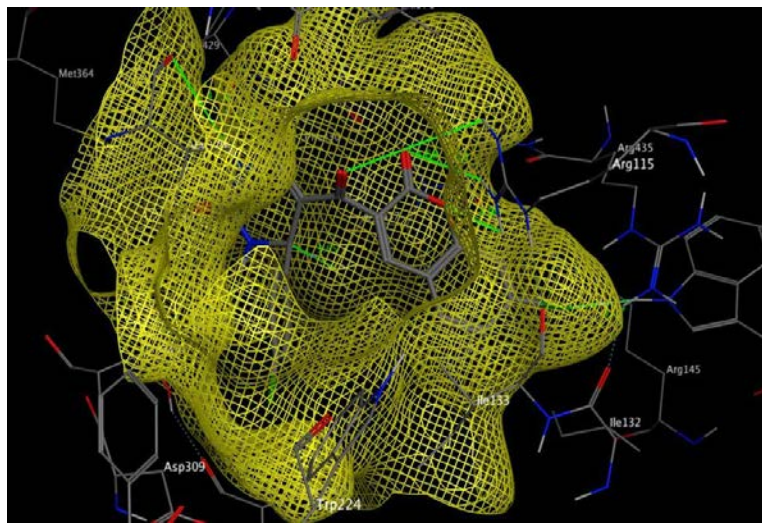


# Chapter 4



## Results and Discussion

## CHAPTER 4: RESULTS AND DISCUSSION

### 4.1 *In silico* screening studies

#### 4.1.1 Molecular docking of coumarin-quinoxaline hybrids

Molecular docking studies of designed molecules were carried out against human aromatase (PDB Id: 3S7S) and human epidermal growth receptor-2 (PDB Id: 3WSQ) in order to evaluate the binding patterns of the molecules with the receptor. Various docking scores of designed molecules RB1-RB90 (Figure 4.1) calculated by MOE software against both the protein IDs have been displayed in Table 4.1. The docking protocol was validated by re-docking of internal ligand over the co-crystallized ligand and the RMSD value was found to be 0.34. The docking scores of all the designed hybrids were compared to the standard drugs Exemestane (aromatase inhibitor) and Trastuzumab (HER2 inhibitor).

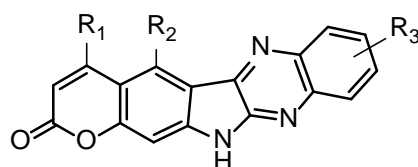


Figure 4.1: Designed compounds RB1-RB90

Table 4.1: Docking scores of designed library of compounds

| Compound No. | R <sub>1</sub>   | R <sub>2</sub> | R <sub>3</sub>                       | Docking Score (PDB Id: 3S7S) | Docking Score (PDB Id: 3WSQ) |
|--------------|------------------|----------------|--------------------------------------|------------------------------|------------------------------|
| RB1          | H                | H              | H                                    | -7.63                        | -6.99                        |
| RB2          | H                | H              | 4-CH <sub>3</sub>                    | -7.12                        | -6.82                        |
| RB3          | H                | H              | 4-F                                  | -7.28                        | -6.72                        |
| RB4          | H                | H              | 4-CF <sub>3</sub>                    | -7.04                        | -6.98                        |
| RB5          | H                | H              | 4,5-(CH <sub>3</sub> ) <sub>2</sub>  | -6.99                        | -6.63                        |
| RB6          | H                | H              | 3-OCH <sub>3</sub>                   | -6.82                        | -6.12                        |
| RB7          | H                | H              | 3,4-(OCH <sub>3</sub> ) <sub>2</sub> | -7.18                        | -6.28                        |
| RB8          | H                | H              | 4-Cl                                 | -6.72                        | -6.04                        |
| RB9          | H                | H              | 4-Br                                 | -6.98                        | -5.98                        |
| RB10         | H                | H              | 4-NO <sub>2</sub>                    | -7.14                        | -5.76                        |
| RB11         | OCH <sub>3</sub> | H              | H                                    | -7.22                        | -5.78                        |
| RB12         | OCH <sub>3</sub> | H              | 3-CH <sub>3</sub>                    | -7.28                        | -5.92                        |
| RB13         | OCH <sub>3</sub> | H              | 4-F                                  | -8.72                        | -7.48                        |
| RB14         | OCH <sub>3</sub> | H              | 4-CF <sub>3</sub>                    | -8.92                        | -7.58                        |

|      |                               |                 |                                      |       |       |
|------|-------------------------------|-----------------|--------------------------------------|-------|-------|
| RB15 | OCH <sub>3</sub>              | H               | 2,3-(CH <sub>3</sub> ) <sub>2</sub>  | -7.69 | -7.26 |
| RB16 | OCH <sub>3</sub>              | H               | 3-OCH <sub>3</sub>                   | -8.68 | -7.76 |
| RB17 | OCH <sub>3</sub>              | H               | 3,4-(OCH <sub>3</sub> ) <sub>2</sub> | -8.82 | -7.68 |
| RB18 | OCH <sub>3</sub>              | H               | 4-Cl                                 | -8.42 | -7.44 |
| RB19 | OCH <sub>3</sub>              | H               | 4-Br                                 | -8.66 | -7.52 |
| RB20 | OCH <sub>3</sub>              | H               | 4-NO <sub>2</sub>                    | -8.12 | -7.13 |
| RB21 | OH                            | H               | H                                    | -7.96 | -6.88 |
| RB22 | OH                            | H               | 4-CH <sub>3</sub>                    | -7.88 | -6.08 |
| RB23 | OH                            | H               | 4-F                                  | -7.62 | -6.38 |
| RB24 | OH                            | H               | 4-CF <sub>3</sub>                    | -7.74 | -6.22 |
| RB25 | OH                            | H               | 4,5-(CH <sub>3</sub> ) <sub>2</sub>  | -7.19 | -5.76 |
| RB26 | OH                            | H               | 3-OCH <sub>3</sub>                   | -7.32 | -5.89 |
| RB27 | OH                            | H               | 3,4-(OCH <sub>3</sub> ) <sub>2</sub> | -8.02 | -5.98 |
| RB28 | OH                            | H               | 4-Cl                                 | -7.84 | -6.48 |
| RB29 | OH                            | H               | 4-Br                                 | -7.86 | -6.56 |
| RB30 | OH                            | H               | 4-NO <sub>2</sub>                    | -7.12 | -5.42 |
| RB31 | C <sub>6</sub> H <sub>5</sub> | H               | H                                    | -6.78 | -5.12 |
| RB32 | C <sub>6</sub> H <sub>5</sub> | H               | 4-CH <sub>3</sub>                    | -6.98 | -5.08 |
| RB33 | C <sub>6</sub> H <sub>5</sub> | H               | 4-F                                  | -7.42 | -6.14 |
| RB34 | C <sub>6</sub> H <sub>5</sub> | H               | 4-CF <sub>3</sub>                    | -7.56 | -6.66 |
| RB35 | C <sub>6</sub> H <sub>5</sub> | H               | 4,5-(CH <sub>3</sub> ) <sub>2</sub>  | -7.96 | -6.92 |
| RB36 | C <sub>6</sub> H <sub>5</sub> | H               | 3-OCH <sub>3</sub>                   | -8.76 | -7.98 |
| RB37 | C <sub>6</sub> H <sub>5</sub> | H               | 3,4-(OCH <sub>3</sub> ) <sub>2</sub> | -7.98 | -6.88 |
| RB38 | C <sub>6</sub> H <sub>5</sub> | H               | 4-Cl                                 | -6.72 | -5.62 |
| RB39 | C <sub>6</sub> H <sub>5</sub> | H               | 4-Br                                 | -6.88 | -5.87 |
| RB40 | C <sub>6</sub> H <sub>5</sub> | H               | 4-NO <sub>2</sub>                    | -6.78 | -5.73 |
| RB41 | H                             | CH <sub>3</sub> | H                                    | -7.22 | -6.42 |
| RB42 | H                             | CH <sub>3</sub> | 4-CH <sub>3</sub>                    | -7.16 | -6.26 |
| RB43 | H                             | CH <sub>3</sub> | 4-F                                  | -7.62 | -6.60 |
| RB44 | H                             | CH <sub>3</sub> | 4-CF <sub>3</sub>                    | -7.76 | -6.86 |
| RB45 | H                             | CH <sub>3</sub> | 4,5-(CH <sub>3</sub> ) <sub>2</sub>  | -7.82 | -7.82 |
| RB46 | H                             | CH <sub>3</sub> | 3-OCH <sub>3</sub>                   | -7.89 | -7.89 |
| RB47 | H                             | CH <sub>3</sub> | 3,4-(OCH <sub>3</sub> ) <sub>2</sub> | -7.66 | -7.66 |
| RB48 | H                             | CH <sub>3</sub> | 4-Cl                                 | -6.18 | -6.18 |
| RB49 | H                             | CH <sub>3</sub> | 4-Br                                 | -6.99 | -6.99 |
| RB50 | H                             | CH <sub>3</sub> | 4-NO <sub>2</sub>                    | -6.76 | -6.76 |
| RB51 | CH <sub>3</sub>               | CH <sub>3</sub> | H                                    | -6.56 | -6.56 |
| RB52 | CH <sub>3</sub>               | CH <sub>3</sub> | 4-CH <sub>3</sub>                    | -6.65 | -6.65 |

|      |                 |                  |                                      |       |       |
|------|-----------------|------------------|--------------------------------------|-------|-------|
| RB53 | CH <sub>3</sub> | CH <sub>3</sub>  | 4-F                                  | -6.79 | -6.79 |
| RB54 | CH <sub>3</sub> | CH <sub>3</sub>  | 4-CF <sub>3</sub>                    | -7.13 | -6.52 |
| RB55 | CH <sub>3</sub> | CH <sub>3</sub>  | 4,5-(CH <sub>3</sub> ) <sub>2</sub>  | -7.14 | -5.74 |
| RB56 | CH <sub>3</sub> | CH <sub>3</sub>  | 3-OCH <sub>3</sub>                   | -7.78 | -6.67 |
| RB57 | CH <sub>3</sub> | CH <sub>3</sub>  | 3,4-(OCH <sub>3</sub> ) <sub>2</sub> | -7.84 | -6.72 |
| RB58 | CH <sub>3</sub> | CH <sub>3</sub>  | 4-Cl                                 | -7.04 | -5.18 |
| RB59 | CH <sub>3</sub> | CH <sub>3</sub>  | 4-Br                                 | -7.08 | -5.62 |
| RB60 | CH <sub>3</sub> | CH <sub>3</sub>  | 4-NO <sub>2</sub>                    | -7.16 | -5.98 |
| RB61 | OH              | CH <sub>3</sub>  | H                                    | -5.99 | -5.12 |
| RB62 | OH              | CH <sub>3</sub>  | 4-CH <sub>3</sub>                    | -6.14 | -5.13 |
| RB63 | OH              | CH <sub>3</sub>  | 4-F                                  | -6.13 | -5.02 |
| RB64 | OH              | CH <sub>3</sub>  | 4-CF <sub>3</sub>                    | -6.34 | -5.16 |
| RB65 | OH              | CH <sub>3</sub>  | 4,5-(CH <sub>3</sub> ) <sub>2</sub>  | -6.42 | -5.34 |
| RB66 | OH              | CH <sub>3</sub>  | 3-OCH <sub>3</sub>                   | -6.98 | -5.72 |
| RB67 | OH              | CH <sub>3</sub>  | 3,4-(OCH <sub>3</sub> ) <sub>2</sub> | -7.02 | -6.14 |
| RB68 | OH              | CH <sub>3</sub>  | 4-Cl                                 | -6.86 | -5.78 |
| RB69 | OH              | CH <sub>3</sub>  | 4-Br                                 | -6.82 | -5.72 |
| RB70 | OH              | CH <sub>3</sub>  | 4-NO <sub>2</sub>                    | -6.92 | -5.88 |
| RB71 | H               | OCH <sub>3</sub> | H                                    | -6.73 | -5.64 |
| RB72 | H               | OCH <sub>3</sub> | 4-CH <sub>3</sub>                    | -6.98 | -5.34 |
| RB73 | H               | OCH <sub>3</sub> | 4-F                                  | -8.02 | -6.78 |
| RB74 | H               | OCH <sub>3</sub> | 4-CF <sub>3</sub>                    | -7.88 | -6.62 |
| RB75 | H               | OCH <sub>3</sub> | 4,5-(CH <sub>3</sub> ) <sub>2</sub>  | -7.14 | -5.67 |
| RB76 | H               | OCH <sub>3</sub> | 3-OCH <sub>3</sub>                   | -7.26 | -5.99 |
| RB77 | H               | OCH <sub>3</sub> | 3,4-(OCH <sub>3</sub> ) <sub>2</sub> | -7.98 | -6.12 |
| RB78 | H               | OCH <sub>3</sub> | 4-Cl                                 | -7.24 | -5.78 |
| RB79 | H               | OCH <sub>3</sub> | 4-Br                                 | -7.12 | -5.42 |
| RB80 | H               | OCH <sub>3</sub> | 4-NO <sub>2</sub>                    | -7.24 | -5.48 |
| RB81 | OH              | OCH <sub>3</sub> | H                                    | -7.98 | -5.93 |
| RB82 | OH              | OCH <sub>3</sub> | 4-CH <sub>3</sub>                    | -7.73 | -5.78 |
| RB83 | OH              | OCH <sub>3</sub> | 4-F                                  | -7.76 | -5.52 |
| RB84 | OH              | OCH <sub>3</sub> | 4-CF <sub>3</sub>                    | -7.89 | -5.79 |
| RB85 | OH              | OCH <sub>3</sub> | 4,5-(CH <sub>3</sub> ) <sub>2</sub>  | -7.56 | -5.86 |
| RB86 | OH              | OCH <sub>3</sub> | 3-OCH <sub>3</sub>                   | -9.21 | -7.31 |
| RB87 | OH              | OCH <sub>3</sub> | 3,4-(OCH <sub>3</sub> ) <sub>2</sub> | -8.14 | -6.99 |
| RB88 | OH              | OCH <sub>3</sub> | 4-Cl                                 | -8.12 | -6.88 |
| RB89 | OH              | OCH <sub>3</sub> | 4-Br                                 | -8.06 | -6.76 |
| RB90 | OH              | OCH <sub>3</sub> | 4-NO <sub>2</sub>                    | -8.16 | -6.18 |

|             |  |  |  |       |       |
|-------------|--|--|--|-------|-------|
| Exemestane  |  |  |  | -9.18 |       |
| Trastuzumab |  |  |  |       | -7.38 |

Among the ninety designed molecules, twelve (RB13-14, RB16-19, RB36-37, RB86-89) displayed maximum docking scores which were comparable to the standard drugs (Table 4.2). These twelve were predicted to have maximum inhibitory potentials against both the receptors. The selected twelve hybrid molecules were further analysed for the binding patterns within the cavities of the receptors. Various interactions displayed by the twelve best compounds at particular distances, have been depicted in Table 4.3. The interaction poses of best six compounds against PDB Id:3S7S and for PDB Id: 3WSQ have been presented in Figures 4.2 to 4.15. The main amino residues involved in bonding in the pocket of aromatase were Val370, Met311, Gly439, Met303, Ala307 and Ser314 whereas in the pocket of HER2 Val164, Arg143, Pro41, Pro172, Ala173, Gly42, Ala85, Glu162 and Tyr181. The major interaction types were hydrogen bonding, arene-cation and arene-H interactions. It is evident that the pattern of binding in case of standard drug Exemestane involved similar amino acid residues and functional groups as in case of best compounds against aromatase (Figure 4.16). The same trend was observed in case of HER2 receptor where the standard drug Trastuzumab was used (Figure 4.17). The overlay pose of internal ligand of aromatase and re-docked ligand has been depicted in Figure 4.18.

**Table 4.2: Docking scores of best 12 coumarin-quinoxaline Hybrids**

| Compound | R <sub>1</sub>                | R <sub>2</sub> | R <sub>3</sub>                       | Docking Score (3S7S) | Docking Score (3WSQ) |
|----------|-------------------------------|----------------|--------------------------------------|----------------------|----------------------|
| RB13     | CH <sub>3</sub>               | H              | 4-F                                  | -8.72                | -7.48                |
| RB14     | CH <sub>3</sub>               | H              | 4-CF <sub>3</sub>                    | -8.92                | -7.58                |
| RB16     | CH <sub>3</sub>               | H              | 3-OCH <sub>3</sub>                   | -8.68                | -7.76                |
| RB17     | CH <sub>3</sub>               | H              | 3,4-(OCH <sub>3</sub> ) <sub>2</sub> | -8.82                | -7.68                |
| RB18     | CH <sub>3</sub>               | H              | 4-Cl                                 | -8.42                | -7.44                |
| RB19     | CH <sub>3</sub>               | H              | 4-Br                                 | -8.66                | -7.52                |
| RB36     | C <sub>6</sub> H <sub>5</sub> | H              | 3-OCH <sub>3</sub>                   | -8.76                | -7.98                |
| RB37     | C <sub>6</sub> H <sub>5</sub> | H              | 3,4-(OCH <sub>3</sub> ) <sub>2</sub> | -7.98                | -7.28                |

|             |    |                  |                                      |       |       |
|-------------|----|------------------|--------------------------------------|-------|-------|
| RB86        | OH | OCH <sub>3</sub> | 3-OCH <sub>3</sub>                   | -9.21 | -7.31 |
| RB87        | OH | OCH <sub>3</sub> | 3,4-(OCH <sub>3</sub> ) <sub>2</sub> | -8.14 | -6.99 |
| RB88        | OH | OCH <sub>3</sub> | 4-Cl                                 | -8.12 | -6.88 |
| RB89        | OH | OCH <sub>3</sub> | 4-Br                                 | -8.06 | -6.96 |
| Exemestane  |    |                  |                                      | -9.18 |       |
| Trastuzumab |    |                  |                                      |       | -7.38 |

Table 4.3: Various interactions revealed by best twelve designed hybrids

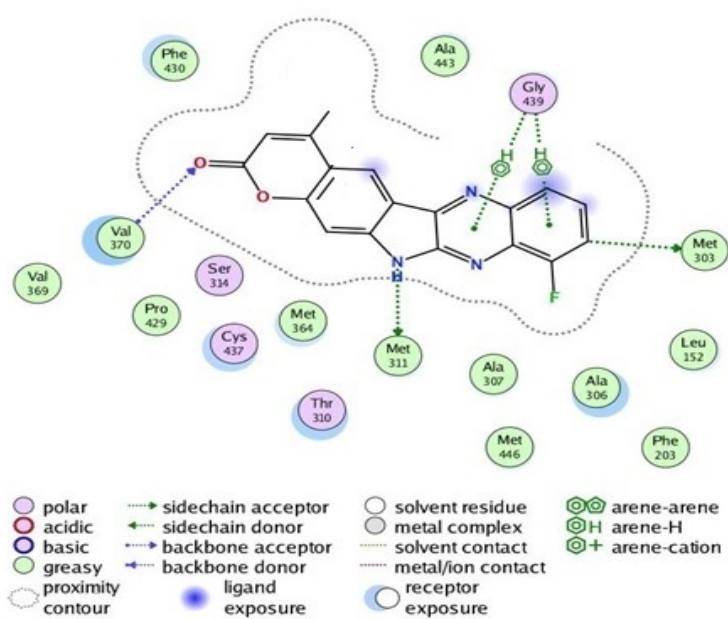
| Compound | Docking Scores |       | Type of Interactions & Distances  |  |
|----------|----------------|-------|---|--|
|          | 3S7S           | 3WSQ  | 3S7S  | 3WSQ   |
|          | RB13           | -8.72 | -7.48   | Val370 (H-bond with =O; 2.41Å), Ser314(H-bond with =O; 3.96Å), Met311(H-bond with –NH; 2.19Å), Gly439(H-bond with N; 3.79Å), Met303(Bond between S and H; 3.80Å), Gly439(Two Arene-H interactions) |
| RB14     | -8.92          | -7.58 | Met311(H-bond with –NH; 2.64Å), Gly439(Two Arene-H interactions), Met303(Bond between S and H; 3.95Å), Gly439(H bond with N; 3.65Å), Met364(H bond with =O; 2.93Å), Val370(H-bond with O; 4.40Å), Ala307(H-bond | Valine174(Two Arene-H interactions), Leu175(H bond with N; 3.67Å), Ala173(H bond with NH; 3.88Å), Pro172(H bond with NH; 4.76Å)  |

|      |       |       |   |  |
|------|-------|-------|---|--|
|      |       |       | with N; 4.64Å)  |  |
| RB16 | -8.68 | -7.76 | Val370(H-bond with =O; 2.17Å), Val370(H-bond with =O; 2.54Å), Met311(H-bond with –NH; 2.05Å), Gly439(Arene-H interaction), Gly439(H bond with N; 3.92Å), THR310(H-bond with –NH; 4.10Å), Ser314(H-bond with O; 3.86Å) | Arg143 (Two arene-cation interactions), Thr165(H-bond with –NH; 3.67Å), Val164(H bond with N; 3.33Å), Gly42(H bond with N; 3.99Å), Ala85(H bond with =O; 3.59Å), Arg143 (H-bond with –NH; 2.86Å) |
| RB17 | -8.82 | -7.68 | Met311(H-bond with –NH; 2.24Å), Ala307(H-bond with =O; 3.24Å), Gly439(H bond with O; 3.81Å), Val370(H bond with O; 4.62Å)   | Valine174(Two Arene-H interactions), Ala173(H-bond with –NH; 3.47Å), Val164(H-bond with O; 2.47Å), Glu162(H-bond with O; 4.46Å), Tyr181(H-bond with O; 3.68Å)                                    |
| RB18 | -8.42 | -7.44 | Met311(H-bond with –NH; 2.46Å), Ser314(Bond between H and Cl; 3.19Å), Met303(Bond between S and H; 3.72Å), Ala307(H bond with =O; 3.55Å)  | Valine174(Two Arene-H interactions), Leu175(H-bond with N; 2.47Å), Ala173(H-bond with –NH; 3.98Å),   |
| RB19 | -8.66 | -7.52 | Gly439(Two Arene-H interactions), Met311(H-bond with –NH; 2.37Å), Met303(Bond between S and H; 3.86Å),  | Valine174(Two Arene-H interactions), Val164(H-bond with Br; 2.48Å), Ala173(H-bond with –NH; 3.972Å), Leu175(H-   |

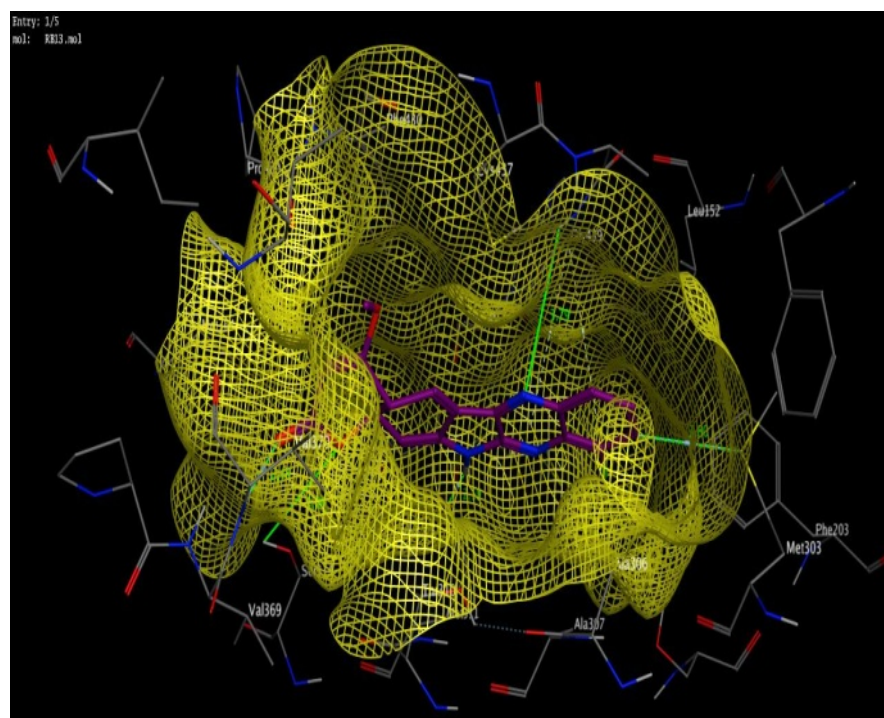
|      |       |       |  |   |
|------|-------|-------|--|---|
|      |       |       | Gly439(H bond with N; 3.72Å), Val370(H bond with =O; 2.73Å)  | bond with N; 3.79Å), Tyr181(H-bond with =O; 3.60Å),   |
| RB36 | -8.76 | -7.98 | Met311(H-bond with –NH; 2.26Å), Met303(Bond between S and H; 4.05Å), Thr310(Arene-H interaction), Ala307(H bond with =O; 4.45Å)  | Pro8(Arene-H interaction), Gly44(H bond with =O; 4.19Å), Arg143(H bond with N; 2.96Å), Gln167(H bond with O; 3.15Å)                                   |
| RB37 | -7.98 | -7.28 | Met311(H-bond with –NH; 2.36Å), Met303(Bond between S and H; 4.15Å), Thr310(Arene-H interaction),  | Pro8(Arene-H interaction), Gly44(H bond with =O; 4.29Å), Arg143(H bond with N; 2.67Å),  |
| RB86 | -9.21 | -7.31 | Met311(H-bond with NH; 2.19Å), Met303(Bond between S and H; 3.75Å), Ser199(H bond with =O; 3.1Å), Ala307(H bond with O; 3.46Å), Ser314(H bond with O; 2.66Å), Ala438(H bond with O; 3.66Å) | Thr43(H bond with NH; 2.42Å), Ala4(H bond with OH; 1.79Å), Tyr95(H bond with N; 2.98Å), Gly42(H bond with O; 3.81Å), Gln43(H bond with =O; 3.92Å)     |
| RB87 | -8.14 | -6.99 | Met311(H-bond with NH; 2.19Å), Met303(Bond between S and H; 3.75Å), Ser199(H bond with =O; 3.1Å)   | Thr43(H bond with NH; 2.42Å), Ala4(H bond with OH; 1.79Å), Ala173(H-bond with –NH; 3.98Å), Glu162(H-bond with O; 4.46Å), Tyr181(H-bond with O; 3.68Å) |

|             |       |       |  |  |
|-------------|-------|-------|--|--|
| RB88        | -8.12 | -6.88 | Met311(H-bond with NH; 2.19Å), Met303(Bond between S and H; 3.75Å), Ser199(H bond with =O; 3.1Å), Ser314(Bond between H and Cl; 3.12Å) | Thr43(H bond with NH; 2.42Å), Ala4(H bond with OH; 1.89Å), Ala173(H-bond with -NH; 3.98Å),   |
| RB89        | -8.06 | -6.96 | Met311(H-bond with NH; 2.29Å), Met303(Bond between S and H; 3.53Å), Ser199(H bond with =O; 3.12Å), Val370(H bond with =O; 2.73Å)       | Thr43(H bond with NH; 2.42Å), Ala4(H bond with OH; 1.73Å), Val164(H-bond with Br; 2.48Å),  |
| Exemestane  | -9.18 |       | Met374(H bond with =O; 1.97Å), Arg115(H bond with =O; 2.67Å), Ala306(H bond with =O; 4.30Å)  |  |
| Trastuzumab |       | -7.38 |  | Val164(Arene-H interaction), Val164(H-bond with NH; 2.02Å), Arg143(Arene-cation interaction), Arg143(H-bond with O; 2.33Å), Glu166(H bond with OH; 1.88Å), Ser163(H bond with NH; 2.30Å) |

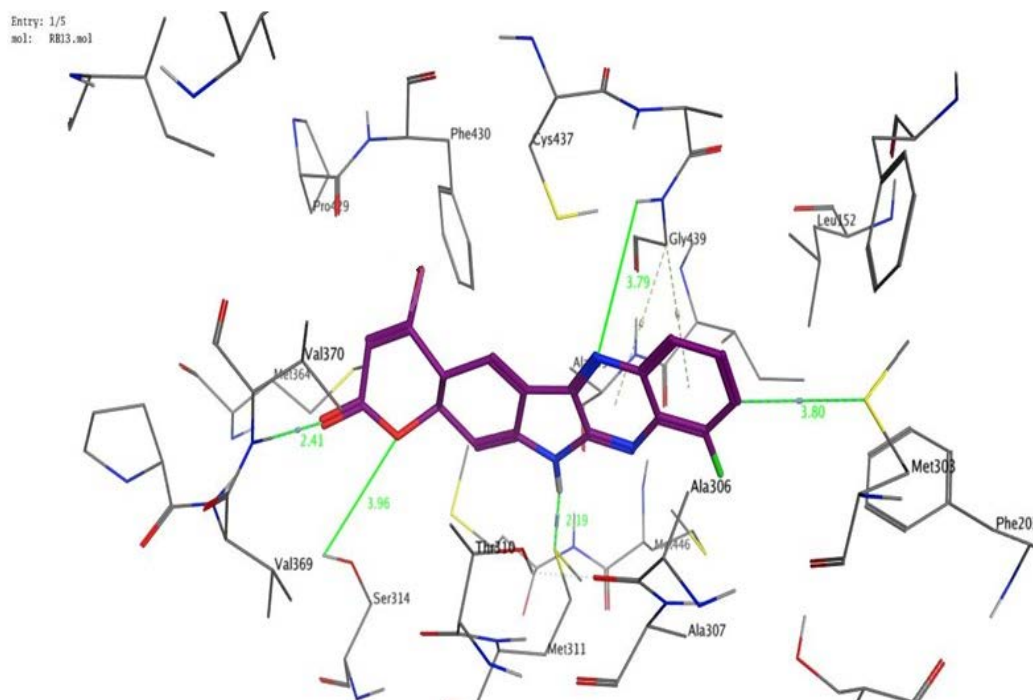
Compound RB13



(a)

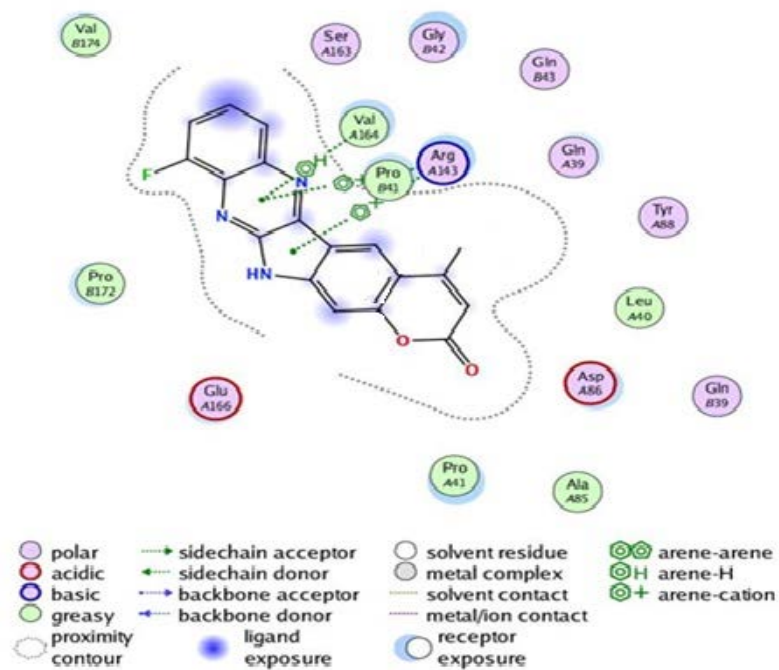


(b)

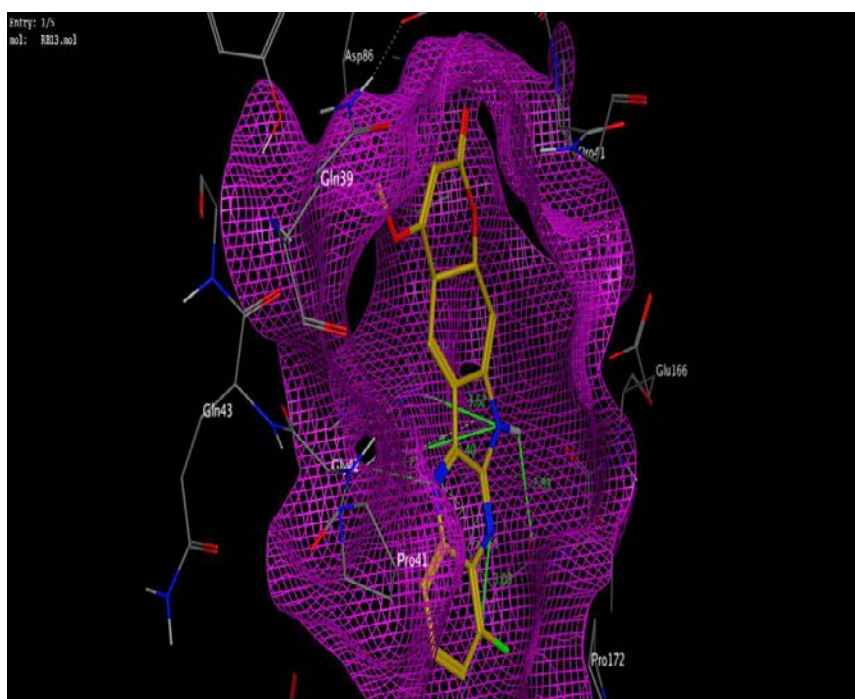


(c)

Figure 4.2: Interaction poses of compound RB13 with aromatase (a) 2D interactions (b) RB13 embedded in receptor pocket (c) Interactions along with distances



(a)



(b)

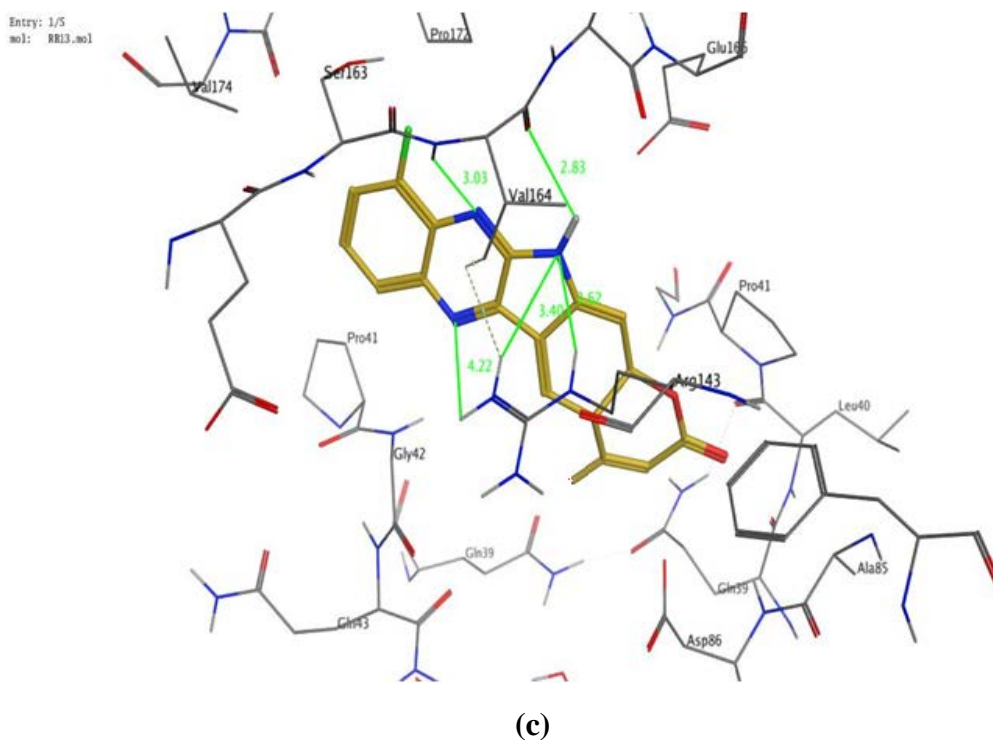
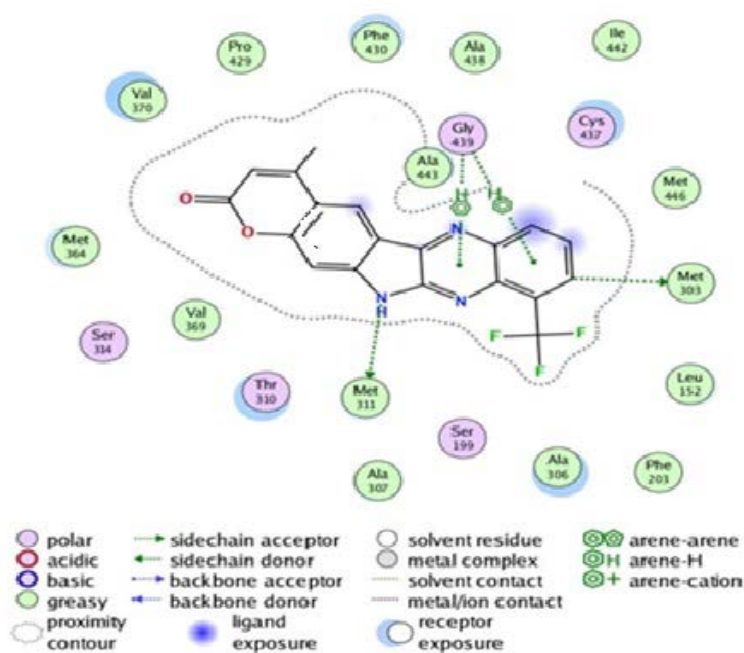
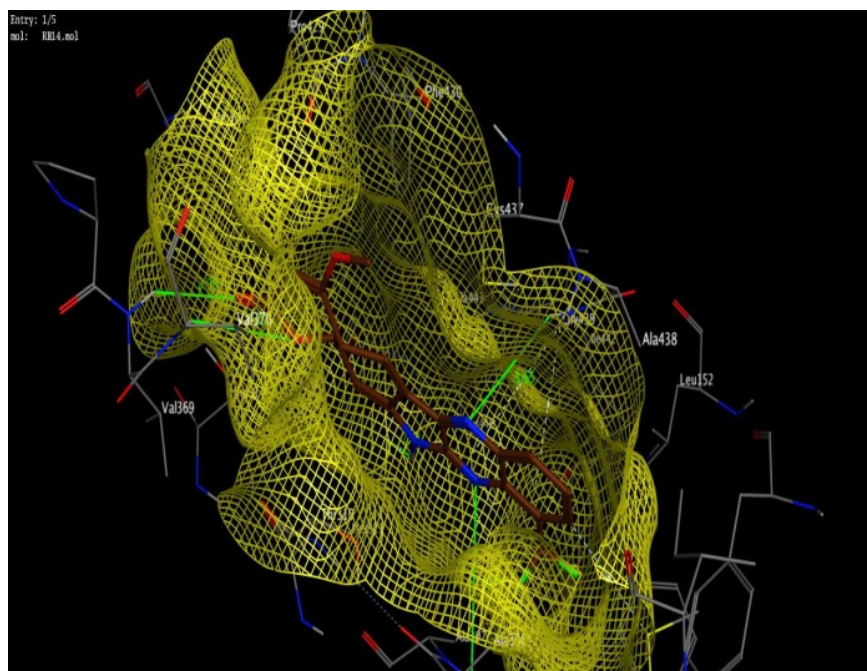


Figure 4.3: Interaction poses of compound RB13 with HER2 (a) 2D interactions (b) RB13 embedded in receptor pocket (c) Interactions along with distances

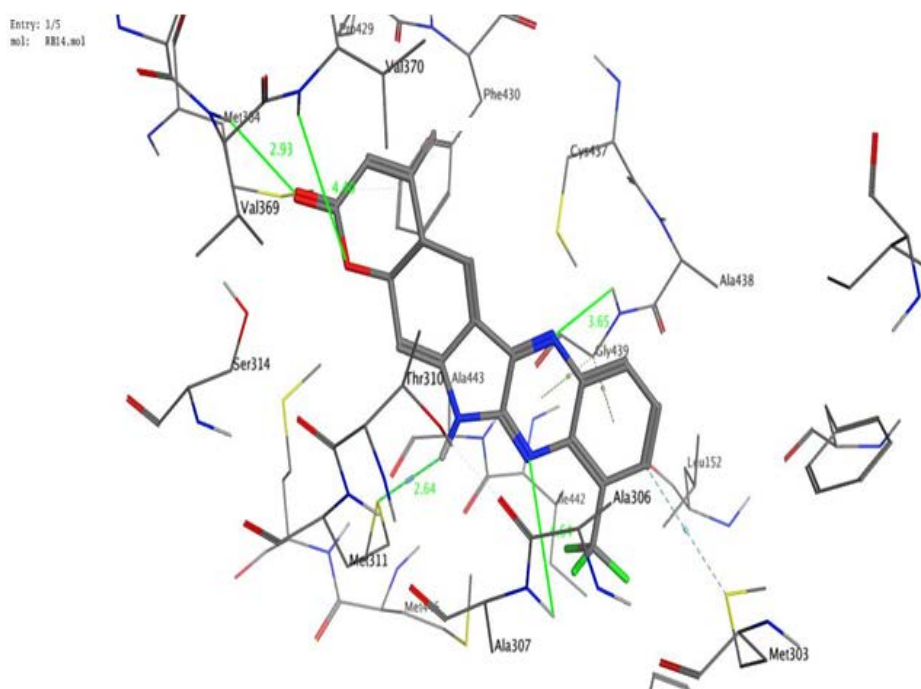
### Compound RB14



(a)

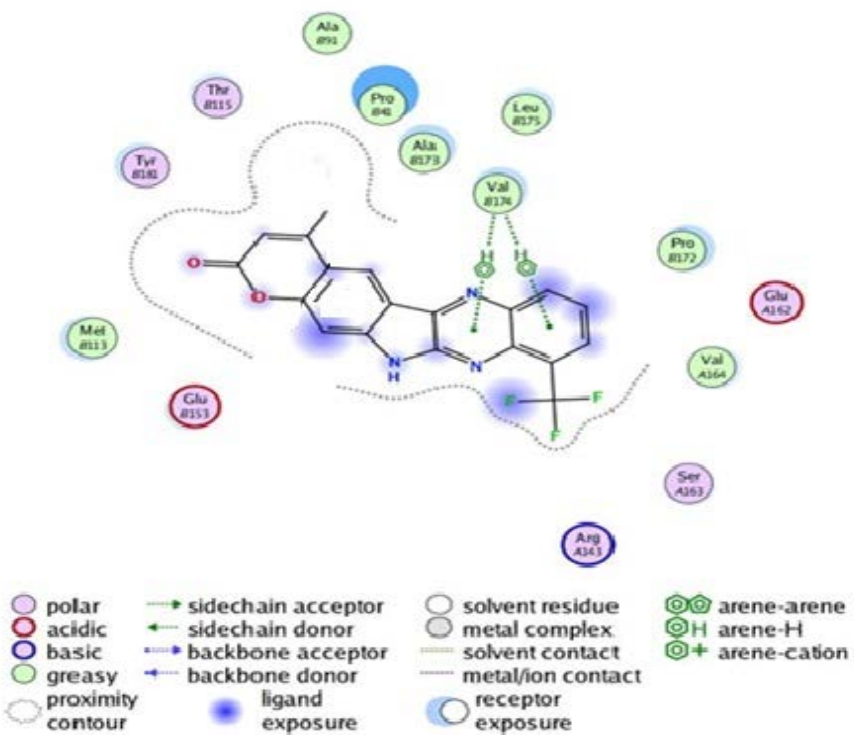


(b)

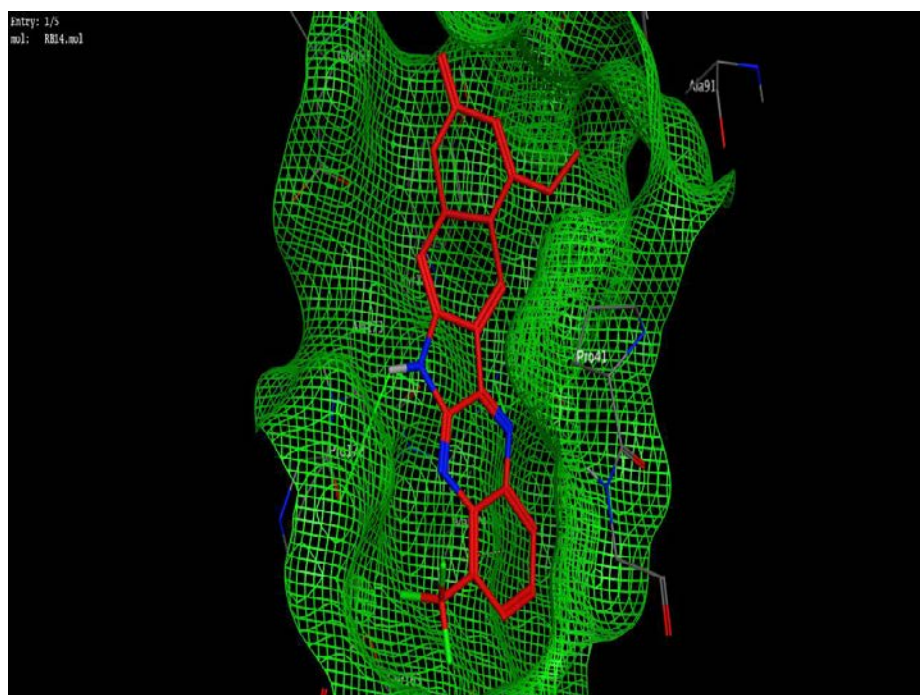


(c)

**Figure 4.4: Interaction poses of compound RB14 with Aromatase (a) 2D interactions (b) RB14 embedded in receptor pocket (c) Interactions along with distances**

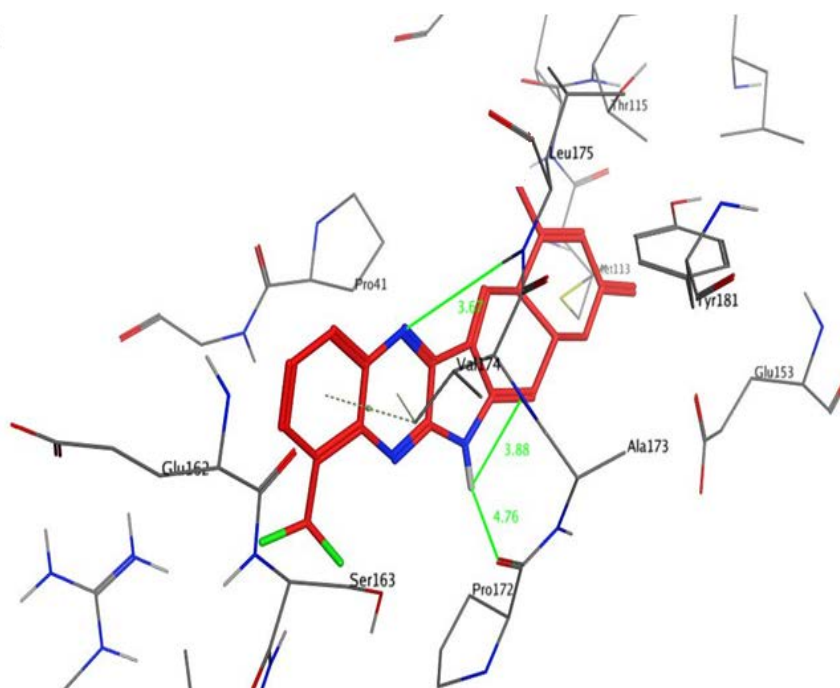


(a)



(b)

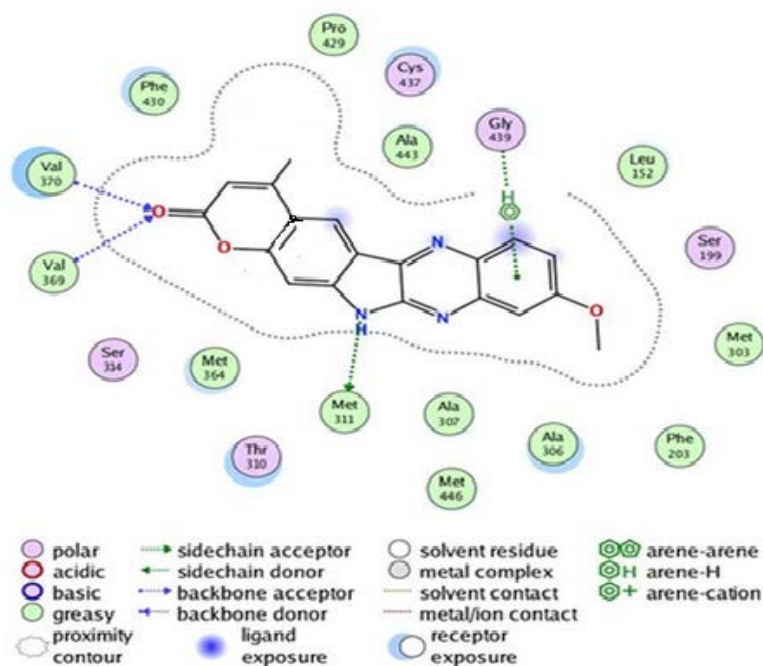
Entry: 1/5  
mol: RB14.mol



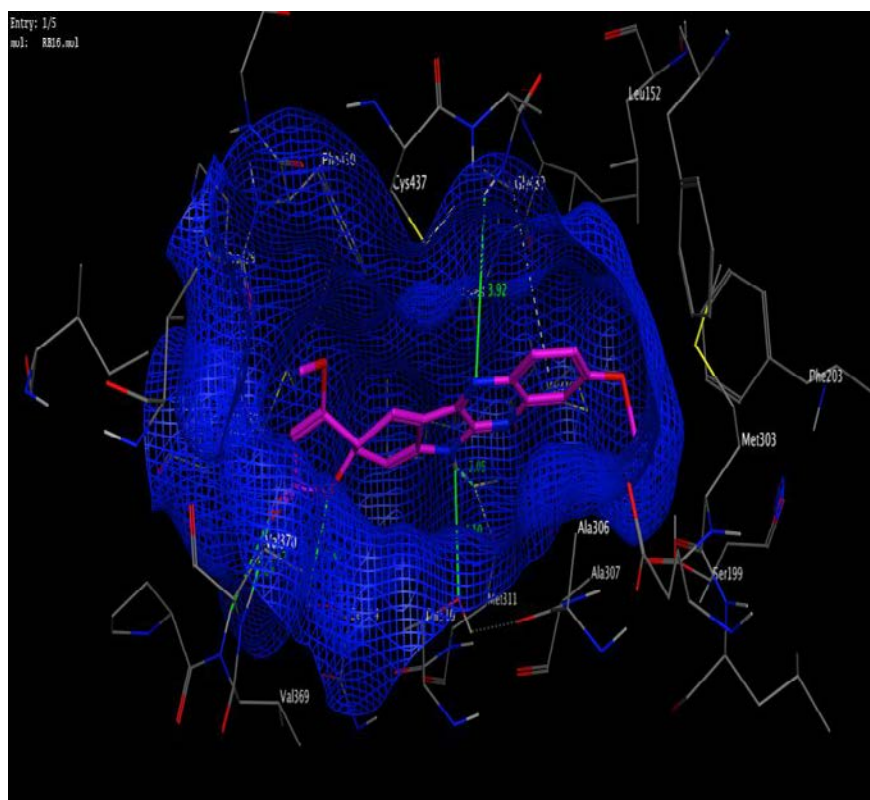
(c)

Figure 4.5: Interaction poses of compound RB14 with HER2 (a) 2D interactions (b) RB14 embedded in receptor pocket (c) Interactions along with distances

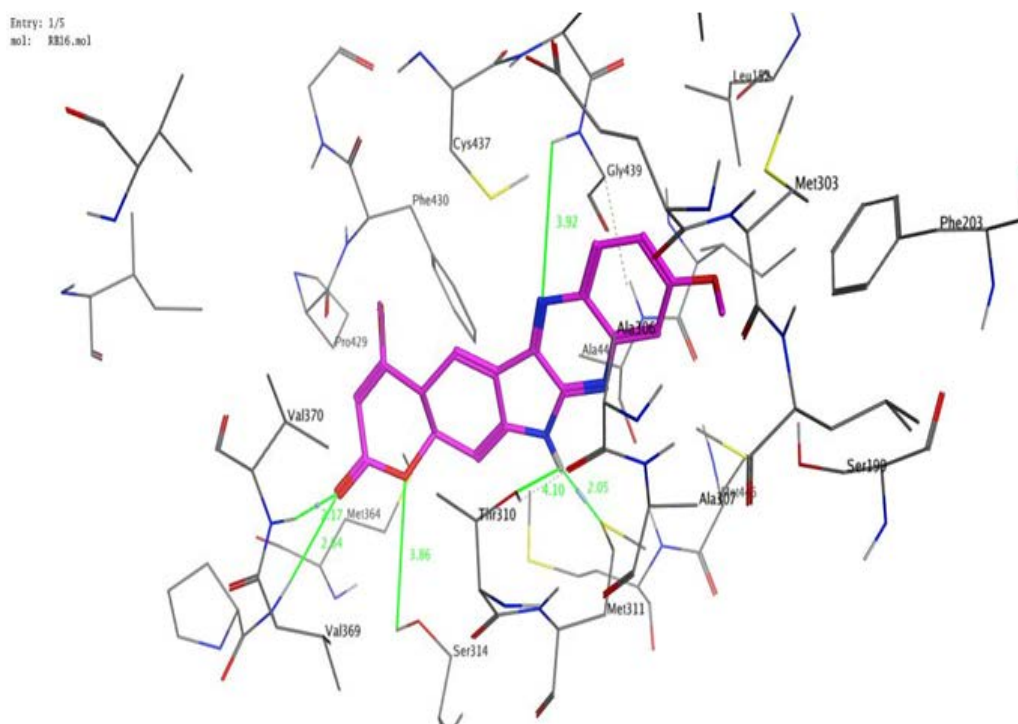
### Compound RB16



(a)

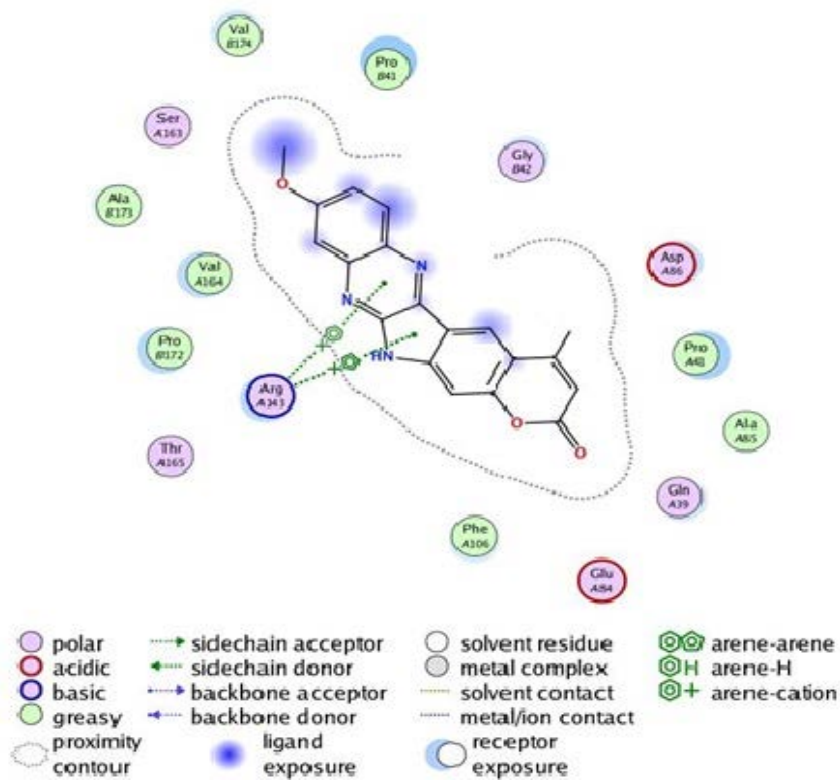


(b)

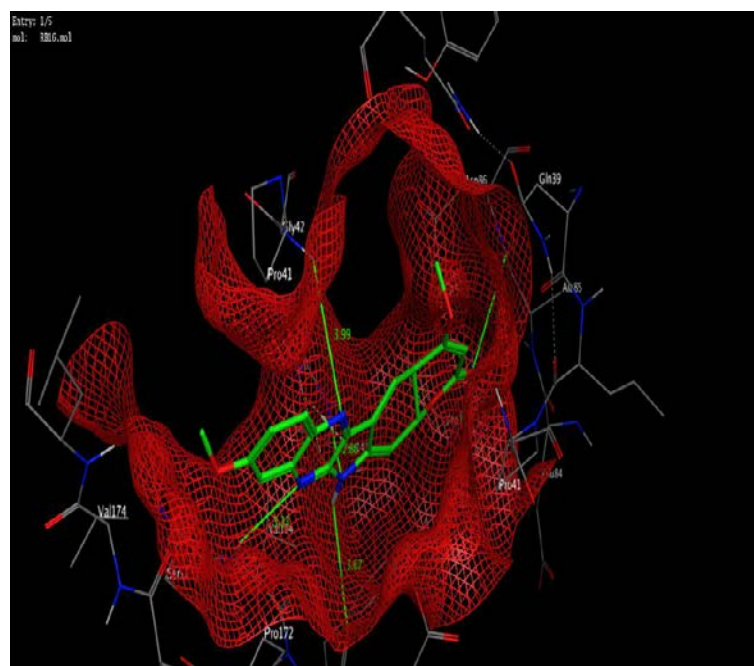


(c)

**Figure 4.6:** Interaction poses of compound RB16 with Aromatase (a) 2D interactions (b) RB16 embedded in receptor pocket (c) Interactions along with distances

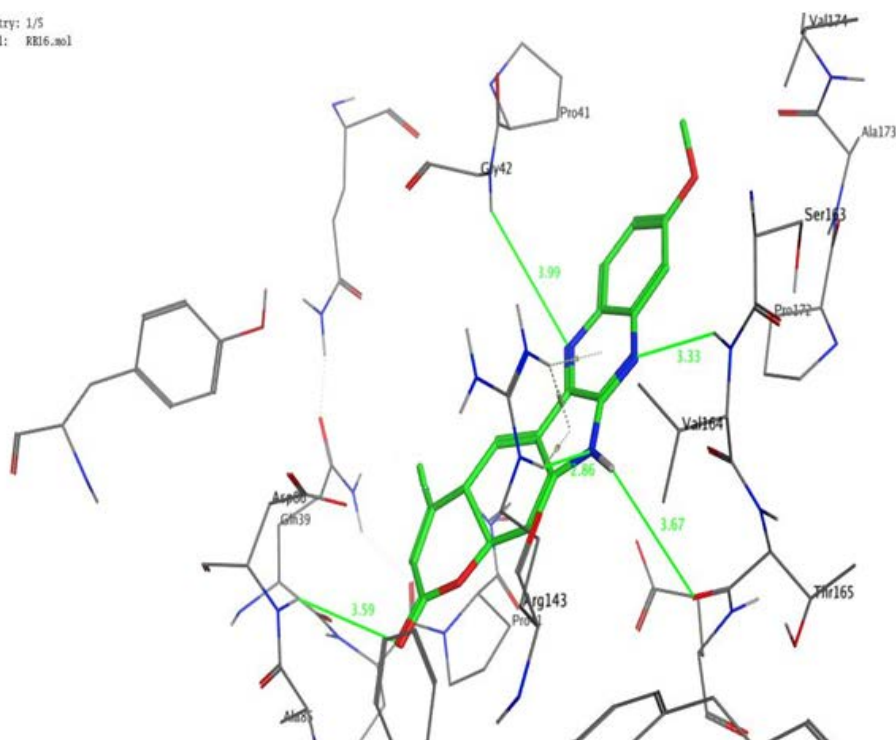


(a)



(b)

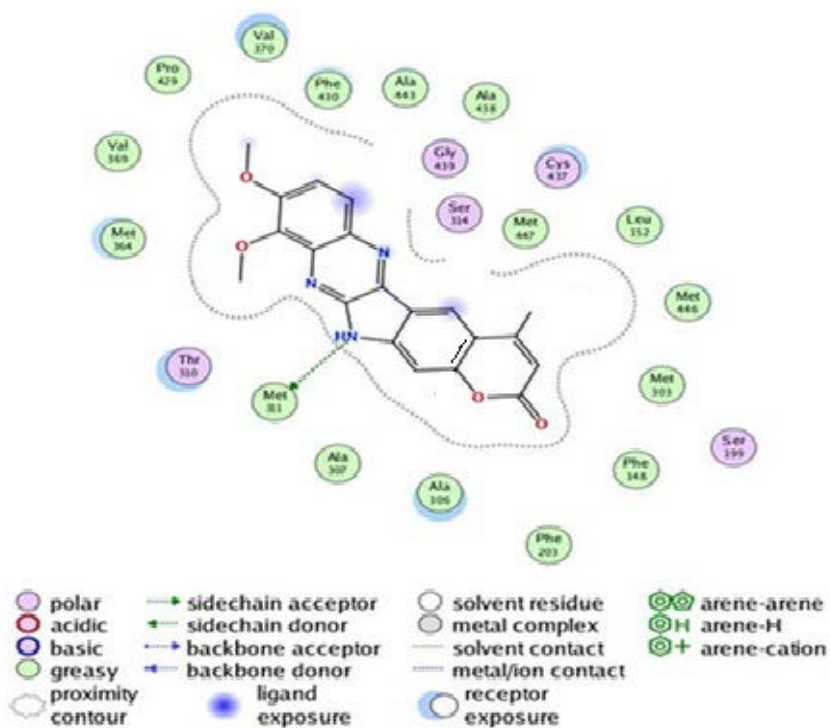
Entry: 1/5  
mol: RB16.mol



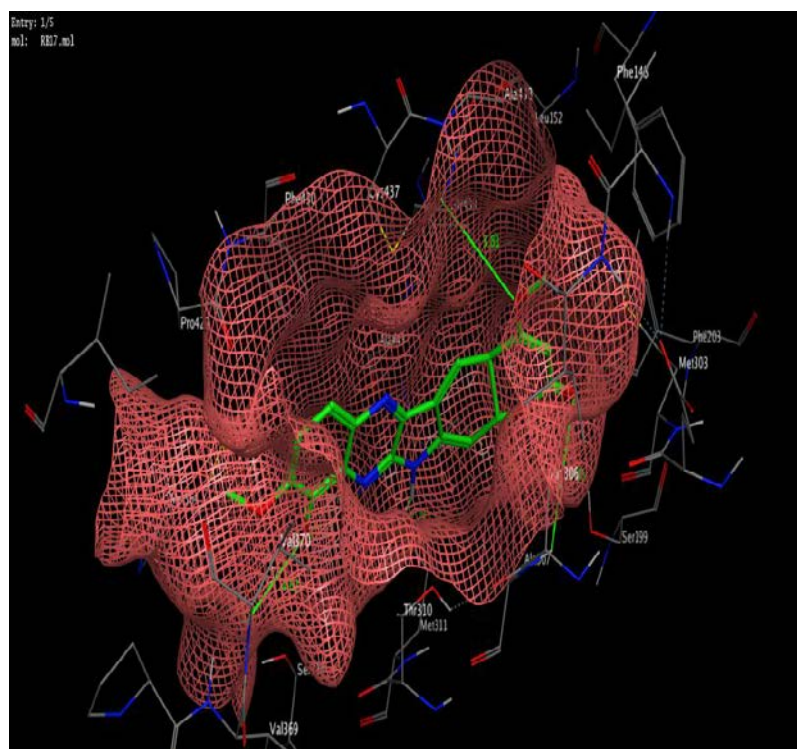
(c)

Figure 4.7: Interaction poses of compound RB16 with HER2 (a) 2D interactions (b) RB16 embedded in receptor pocket (c) Interactions along with distances

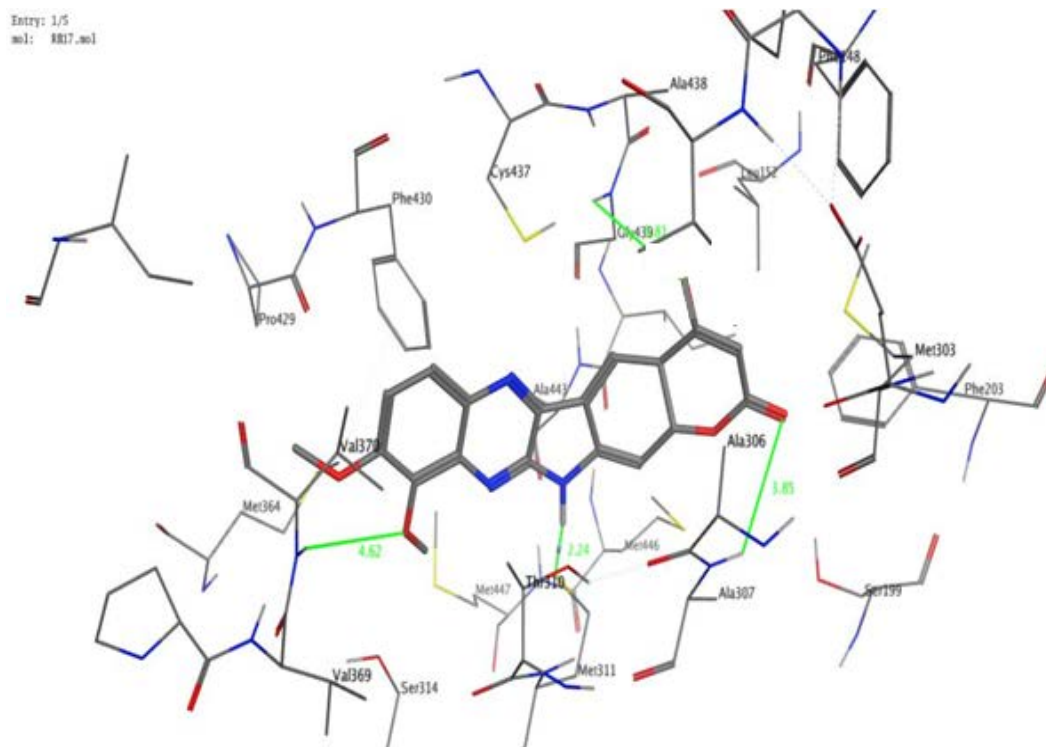
### Compound RB17



(a)

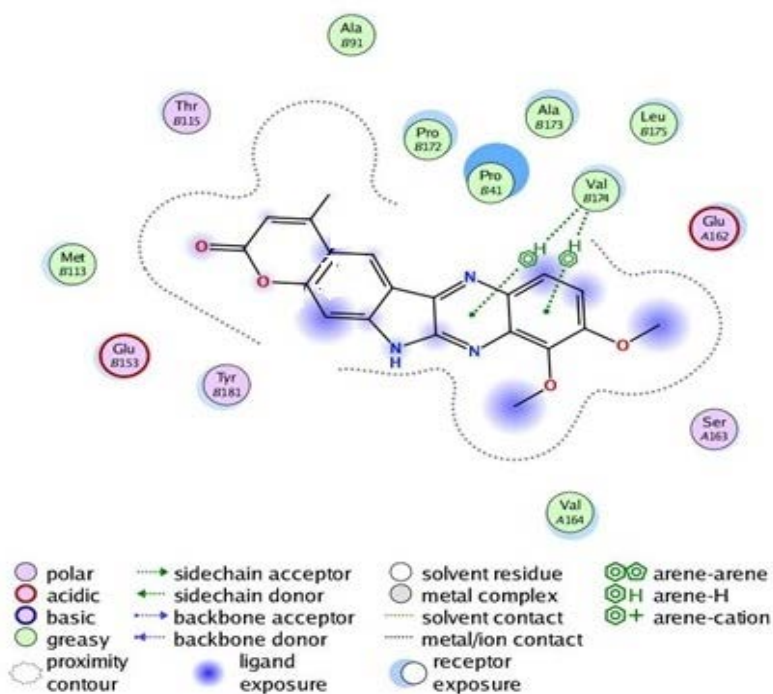


(b)

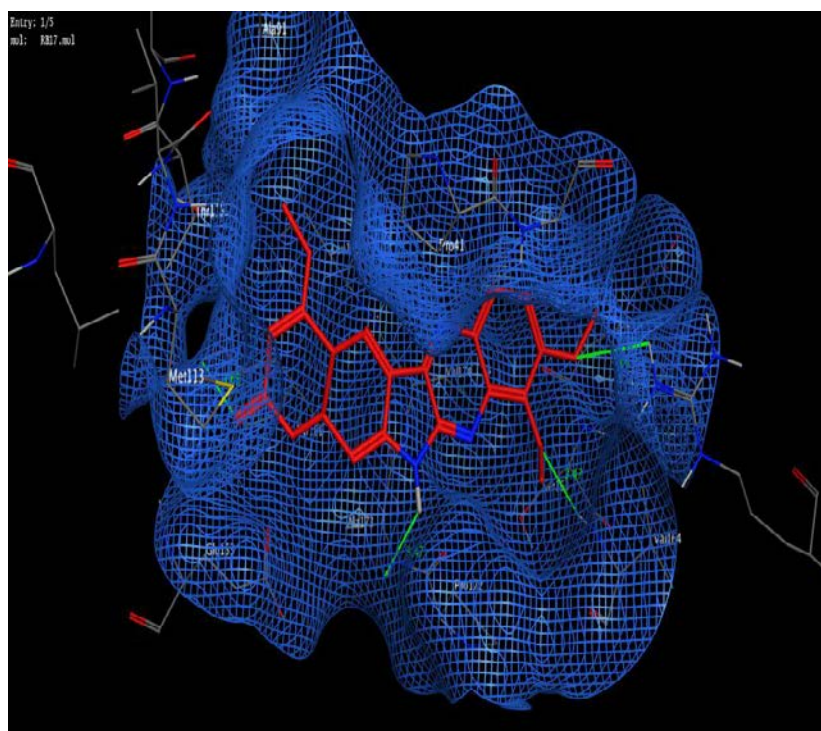


(c)

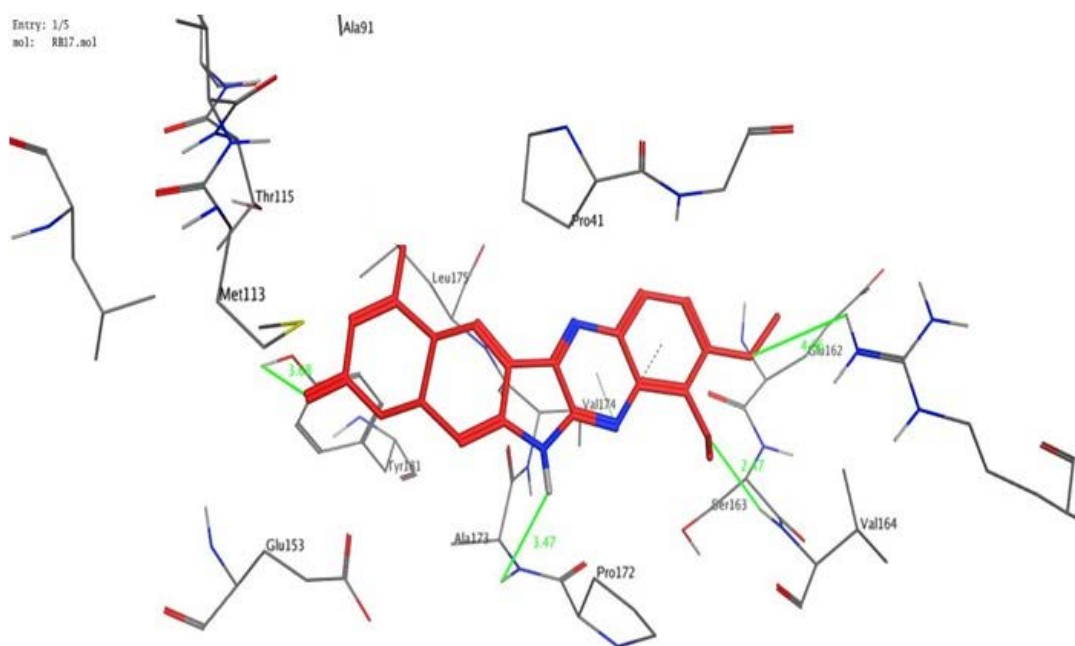
Figure 4.8: Interaction poses of compound RB17 with Aromatase (a) 2D interactions (b) RB17 embedded in receptor pocket (c) Interactions along with distances



(a)



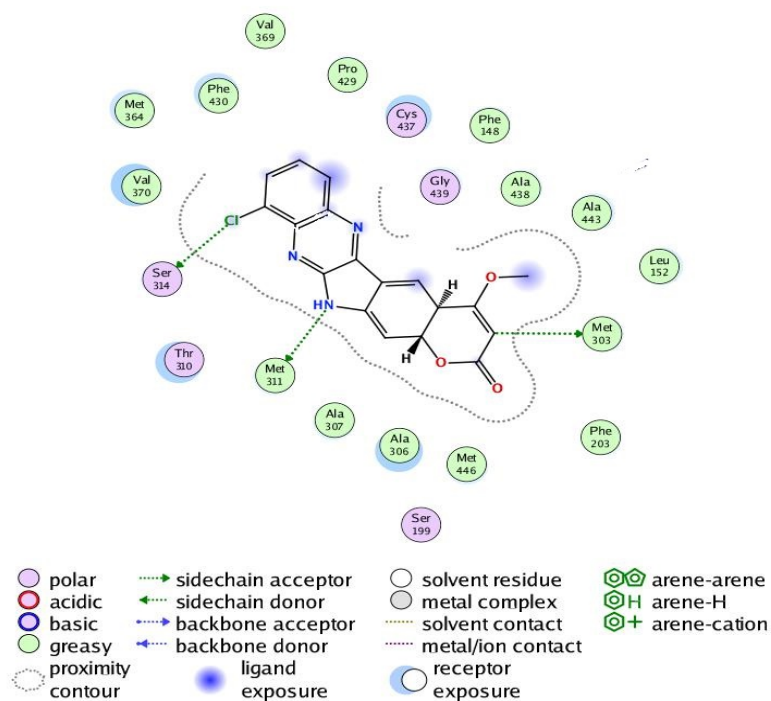
(b)



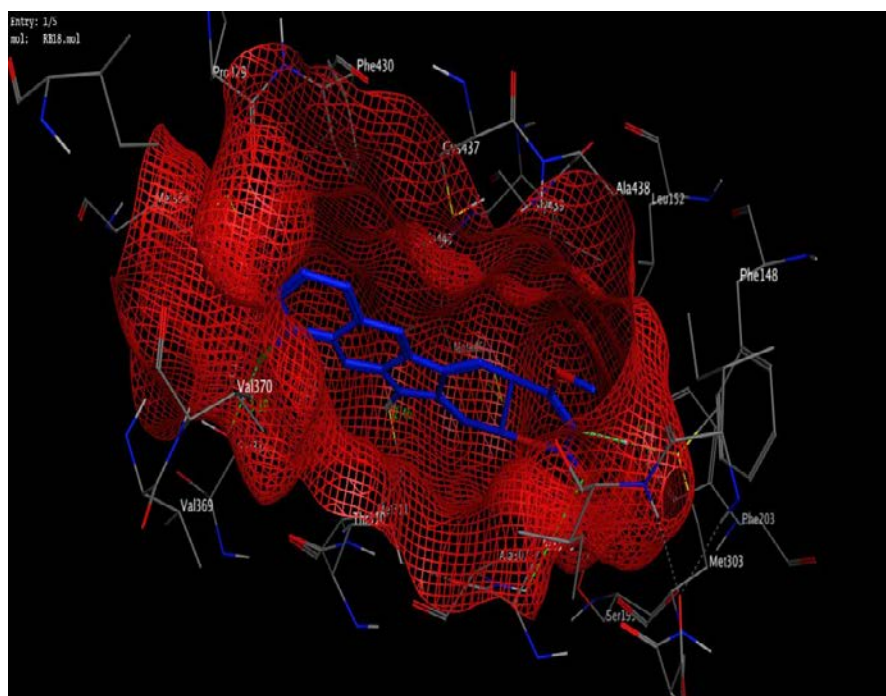
(c)

**Figure 4.9: Interaction poses of compound RB17 with HER2 (a) 2D interactions (b) RB17 embedded in receptor pocket (c) Interactions along with distances**

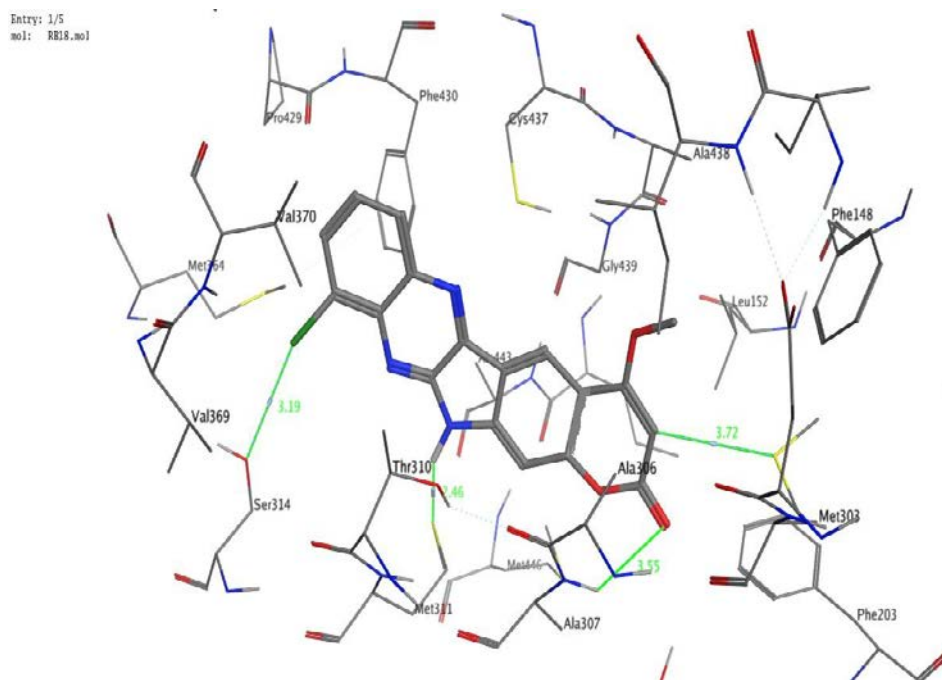
Compound RB18



(a)

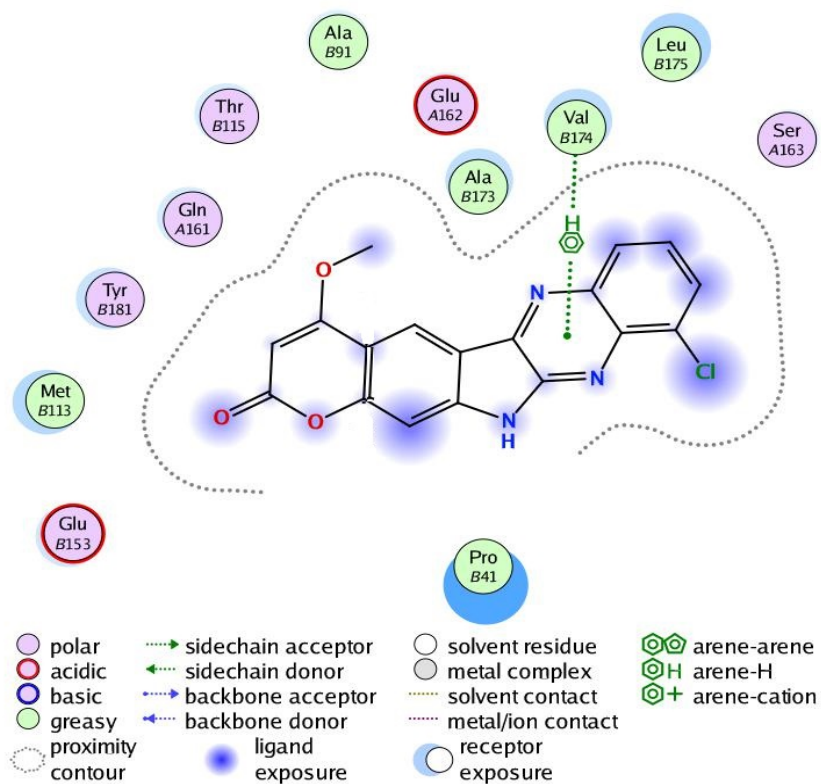


(b)

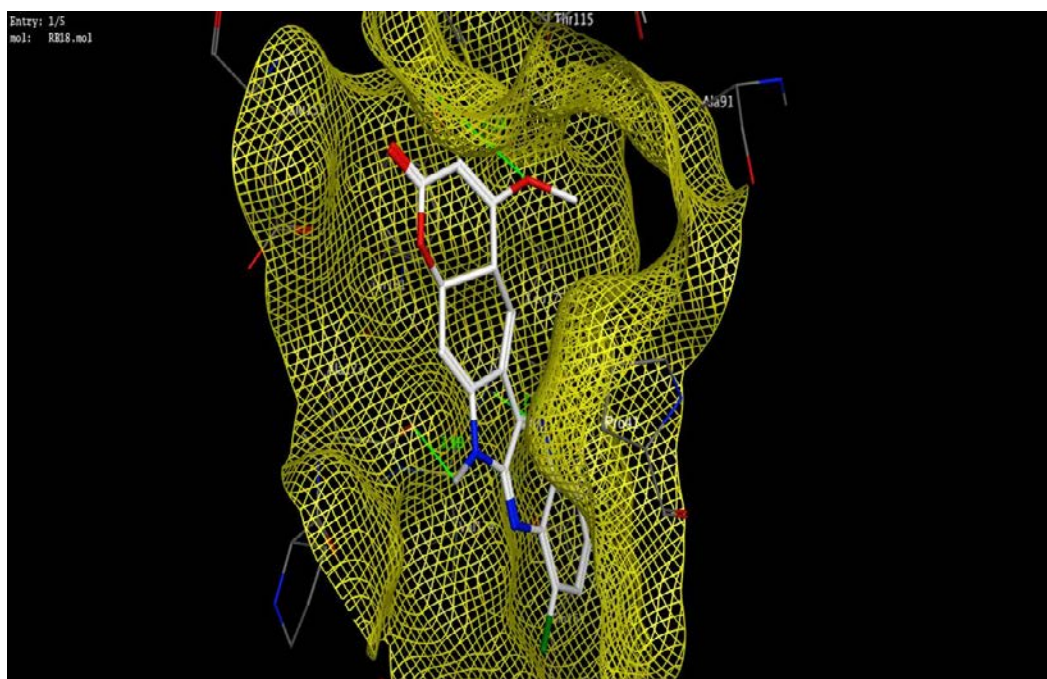


(c)

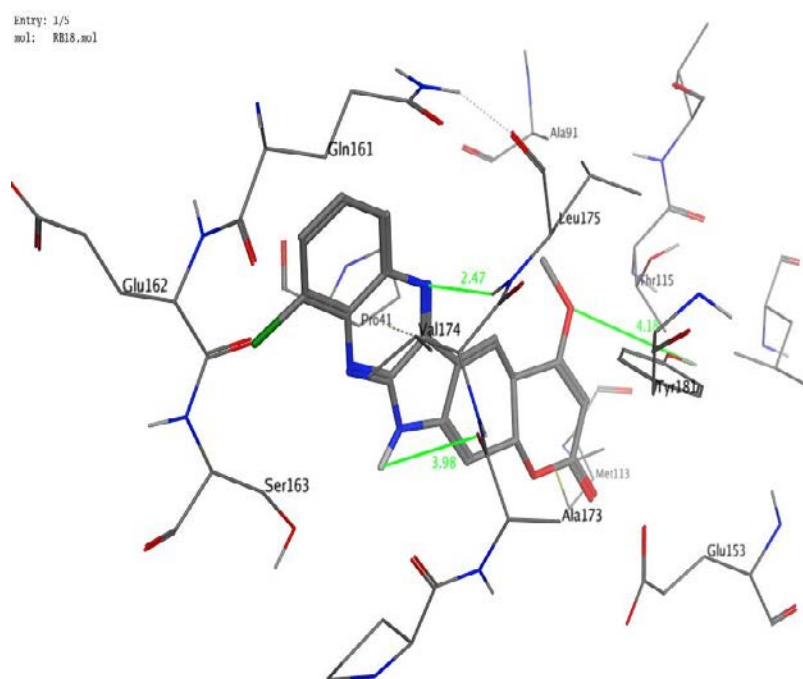
**Figure 4.10: Interaction poses of compound RB18 with Aromatase (a) 2D interactions (b) RB18 embedded in receptor pocket (c) Interactions along with distances**



(a)



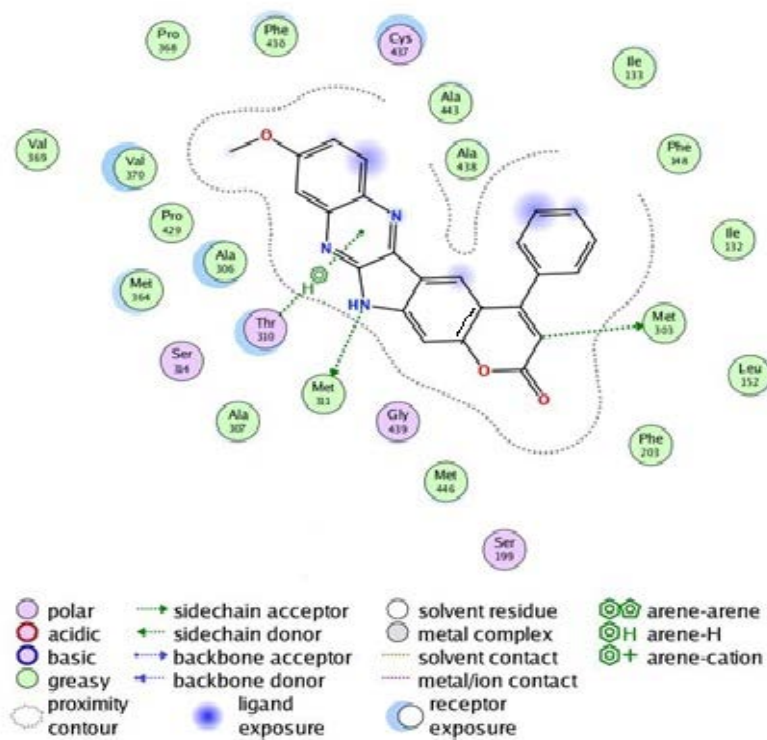
(b)



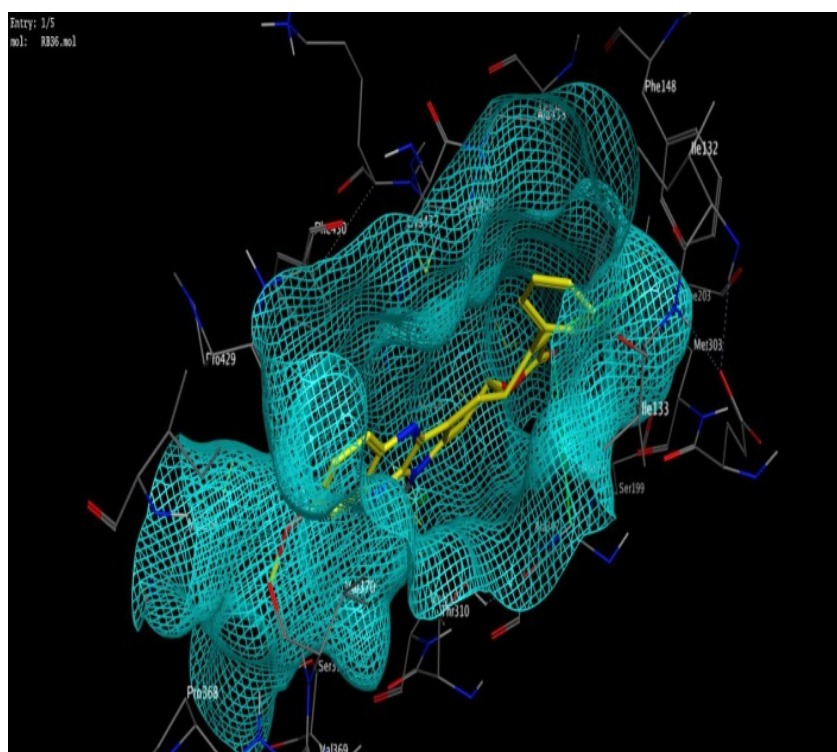
(c)

Figure 4.11: Interaction poses of compound RB18 with HER2 (a) 2D interactions (b) RB18 embedded in receptor pocket (c) Interactions along with distances

## Compound RB36

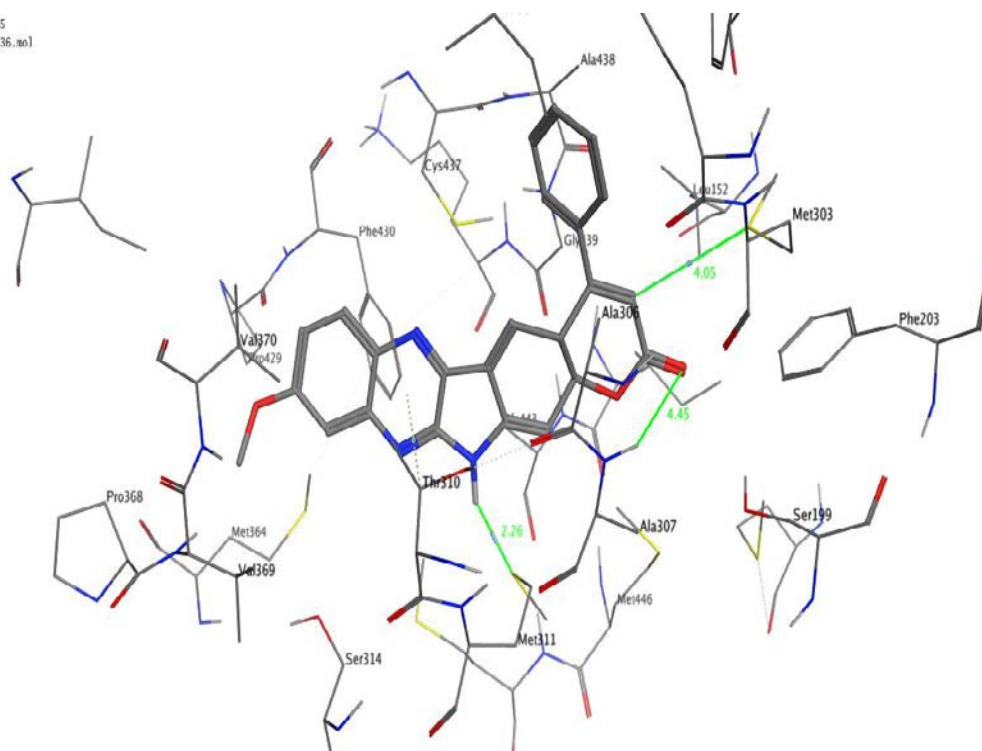


(a)



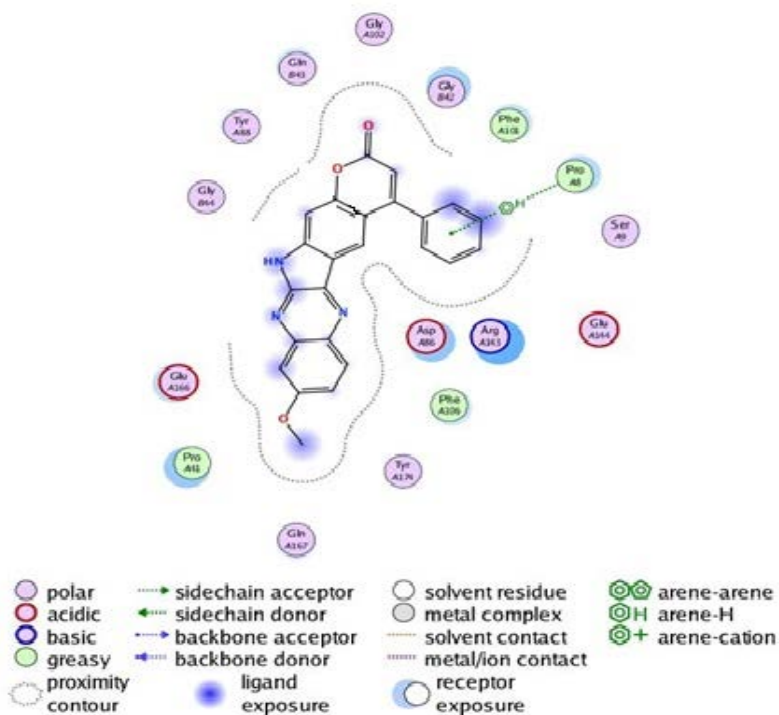
(b)

Entry: 1/5  
mol: RB36.mol

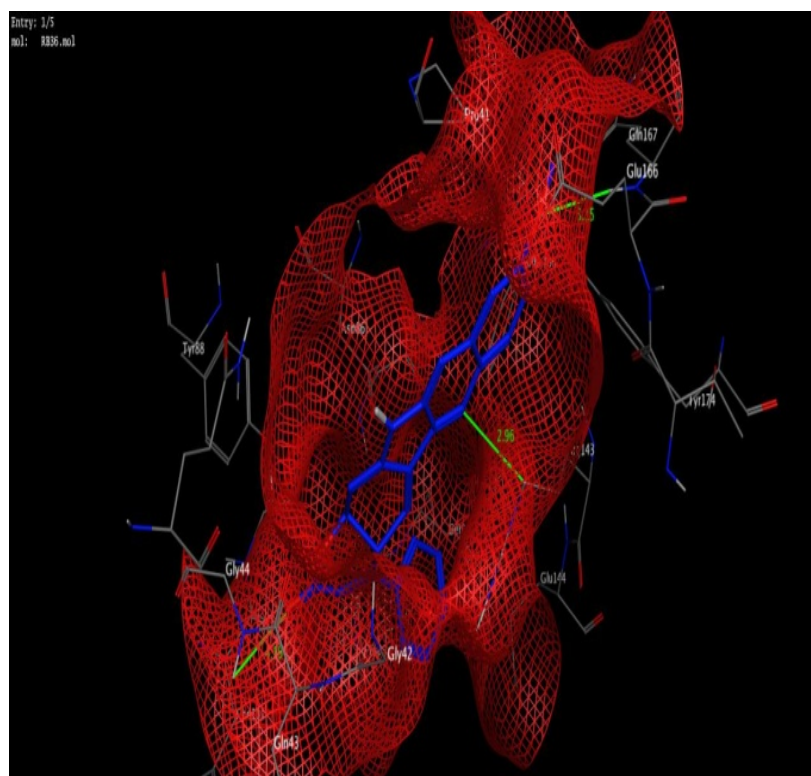


(c)

Figure 4.12: Interaction poses of compound RB36 with Aromatase (a) 2D interactions (b) RB36 embedded in receptor pocket (c) Interactions along with distances

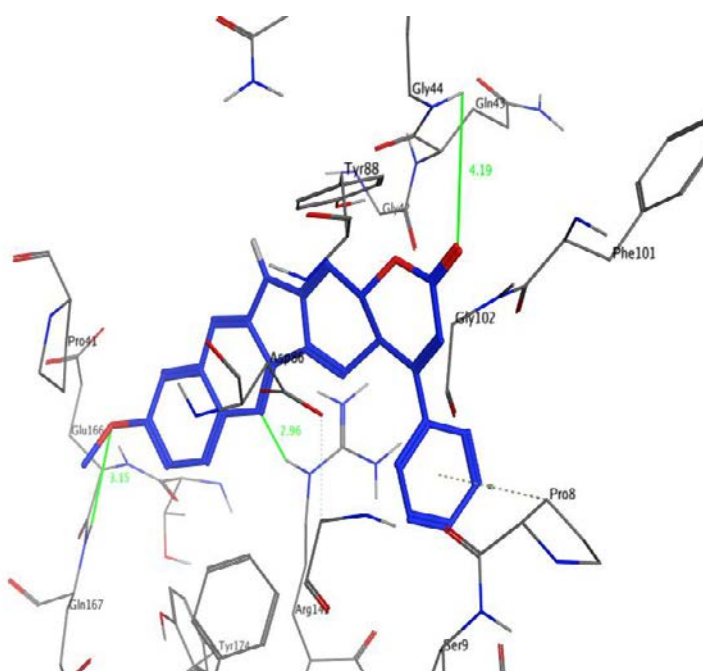


(a)



(b)

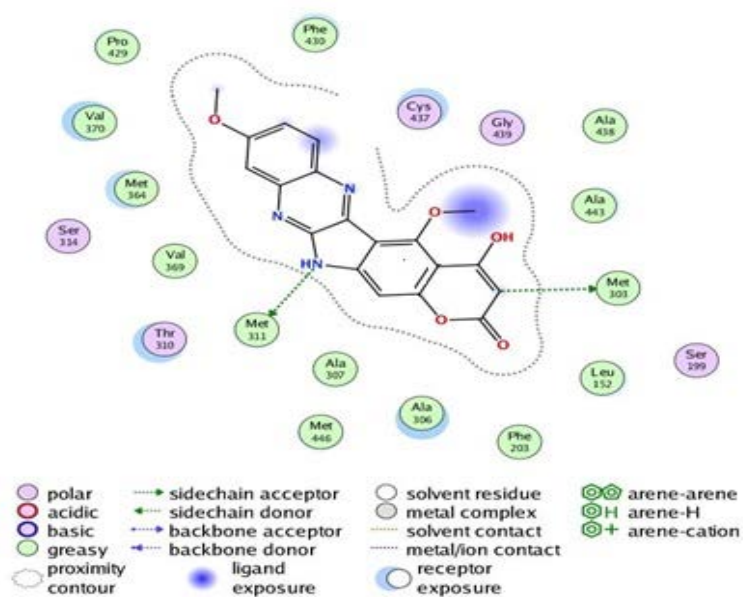
Entry: 1/5  
mol: RB36.mol



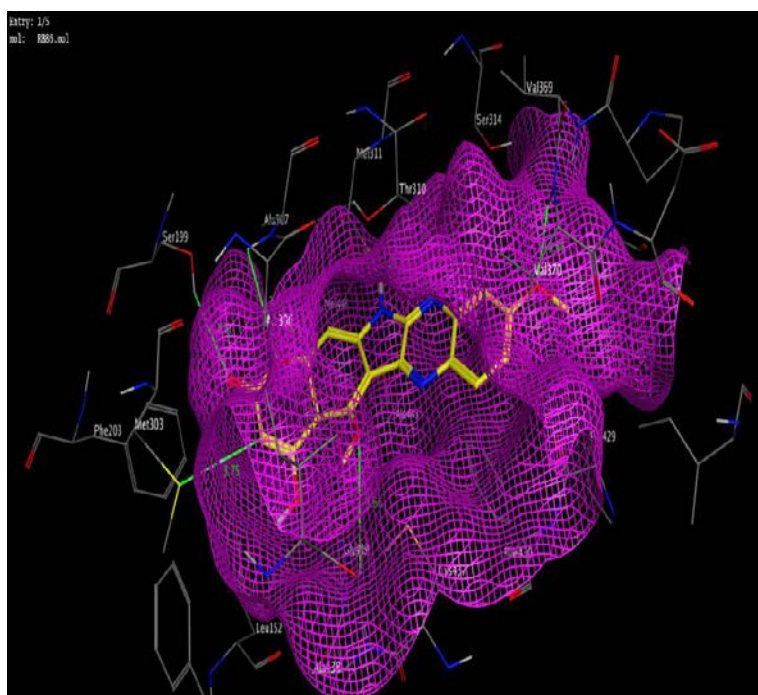
(c)

**Figure 4.13: Interaction poses of compound RB36 with HER2 (a) 2D interactions (b) RB36 embedded in receptor pocket (c) Interactions along with distances**

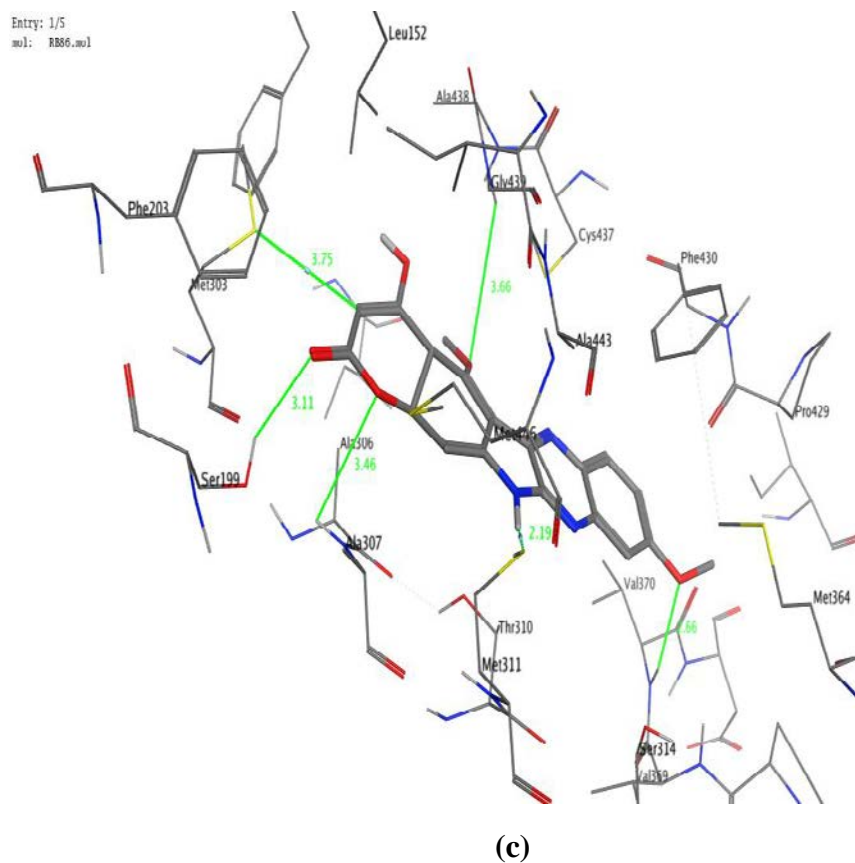
Compound RB86



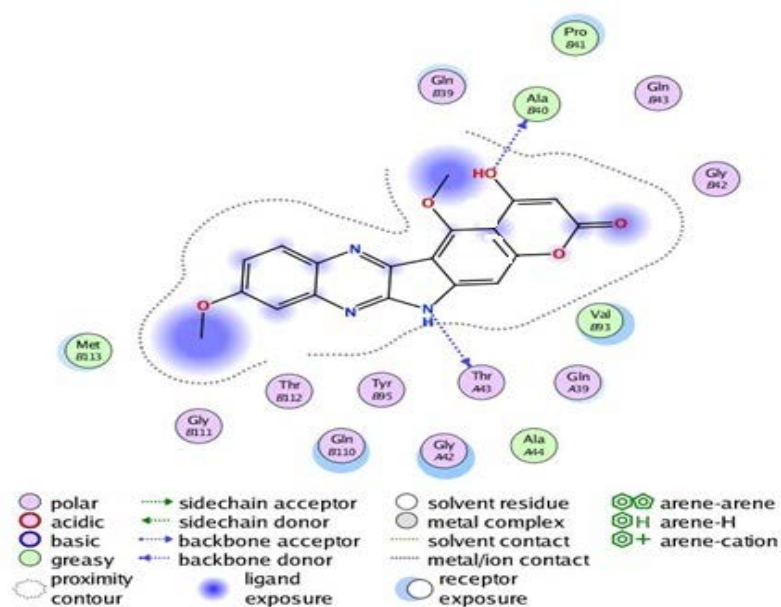
(a)

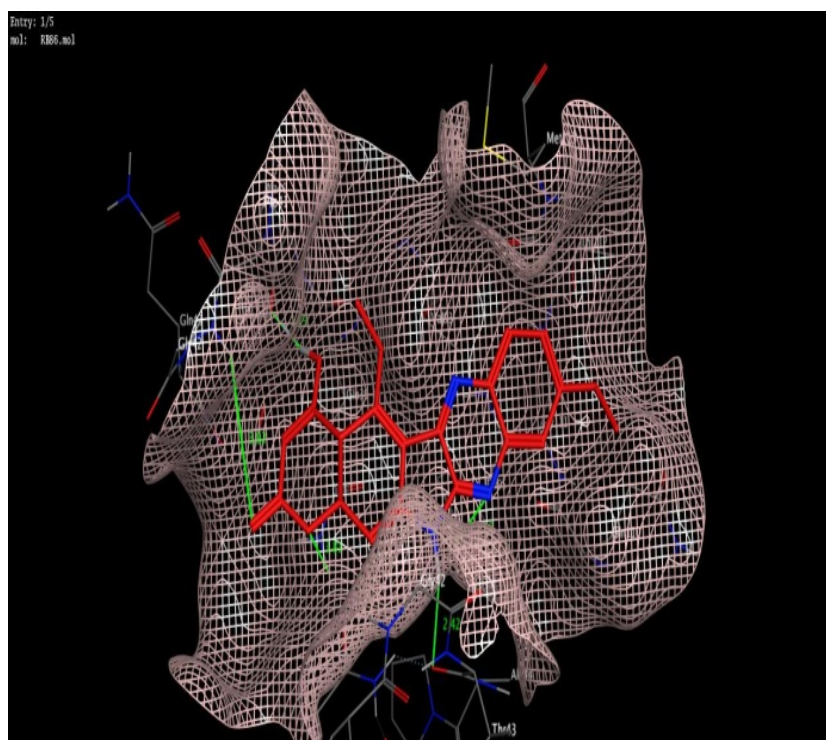


(b)

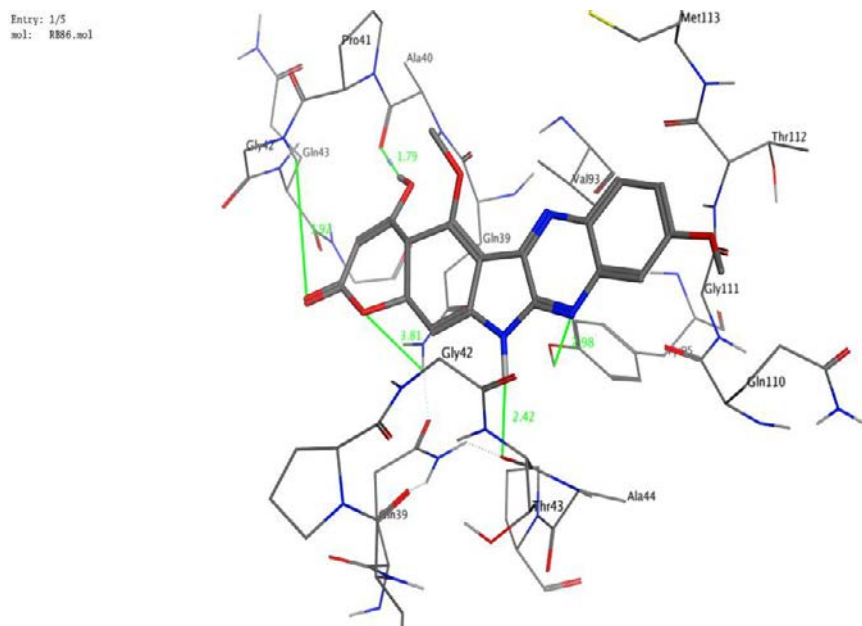


**Figure 4.14: Interaction poses of compound RB86 with Aromatase (a) 2D interactions (b) RB86 embedded in receptor pocket (c) Interactions along with distances**





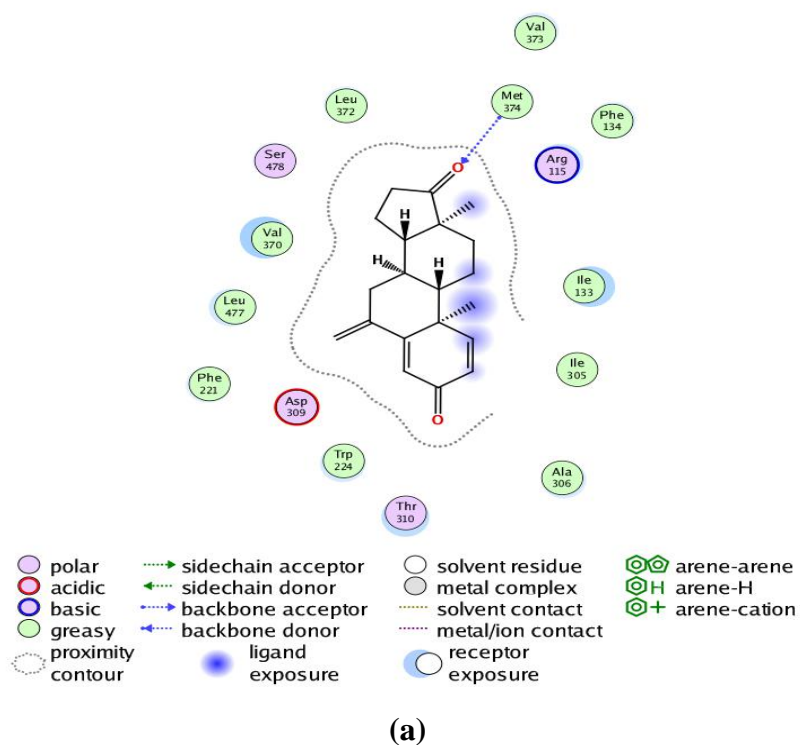
(b)



(c)

**Figure 4.15: Interaction poses of compound RB86 with HER2 (a) 2D interactions (b) RB86 embedded in receptor pocket (c) Interactions along with distances**

## Exemestane



Entry: 1/5  
mol: Exe.mol

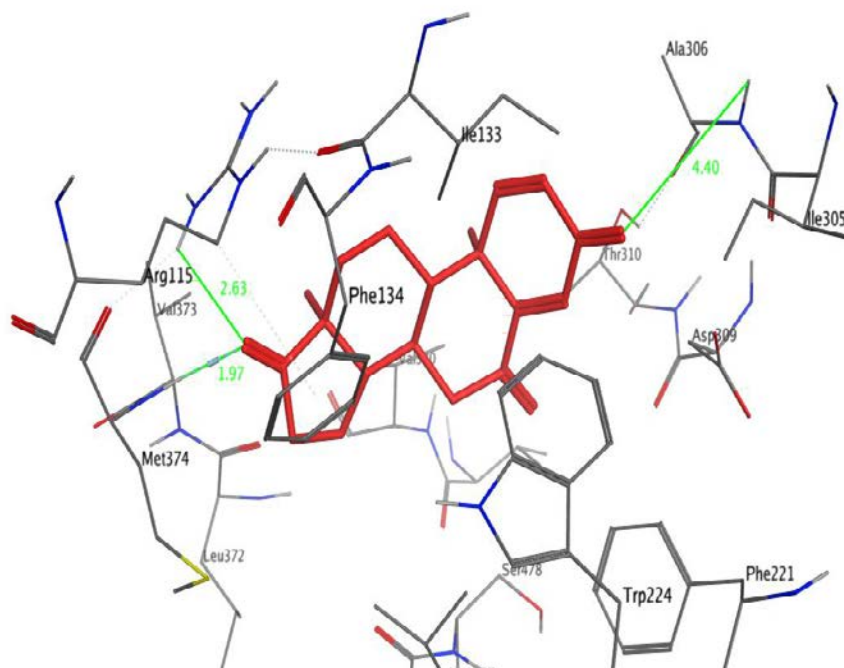
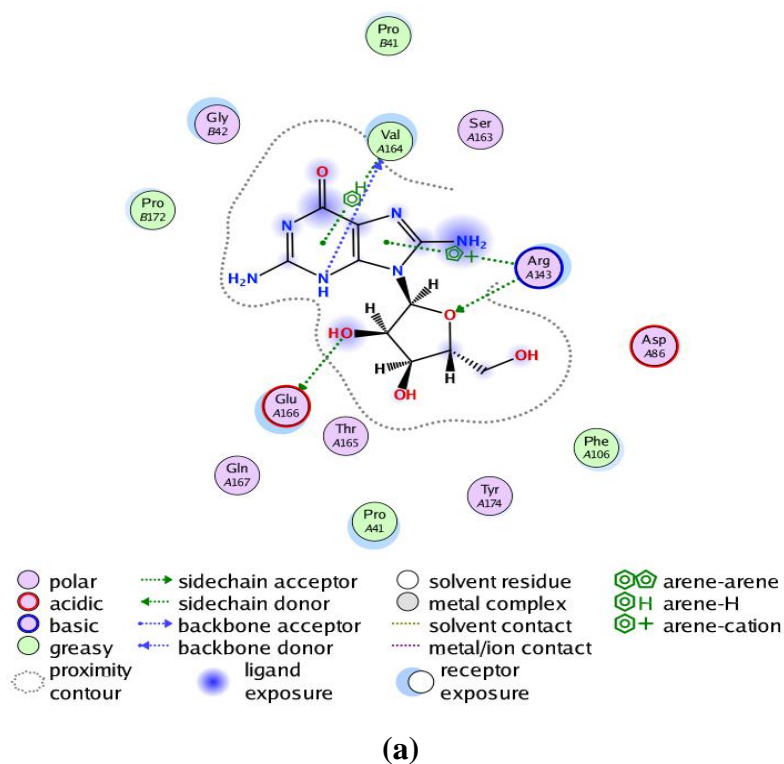


**Figure 4.16: Interaction poses of exemestane with Aromatase (a) 2D interactions (b) Interactions along with distances**

## Trastuzumab



Entry: 1/5  
mol: Trastu.mol

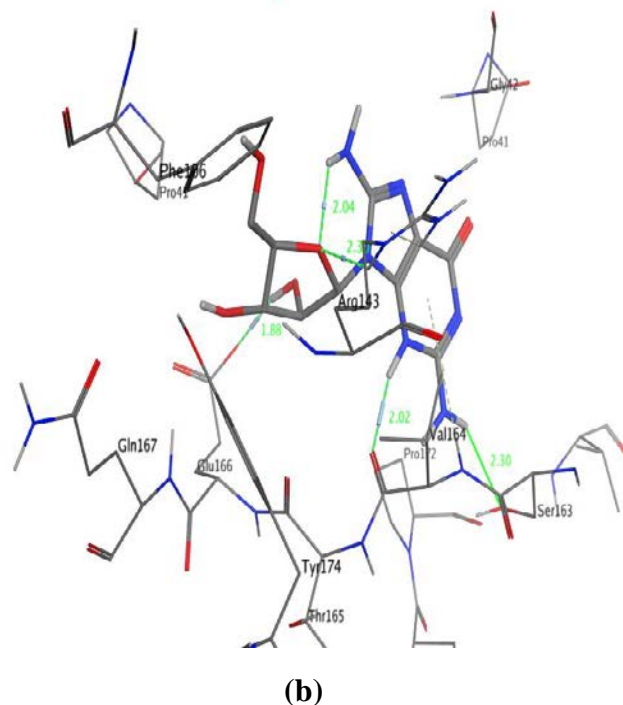
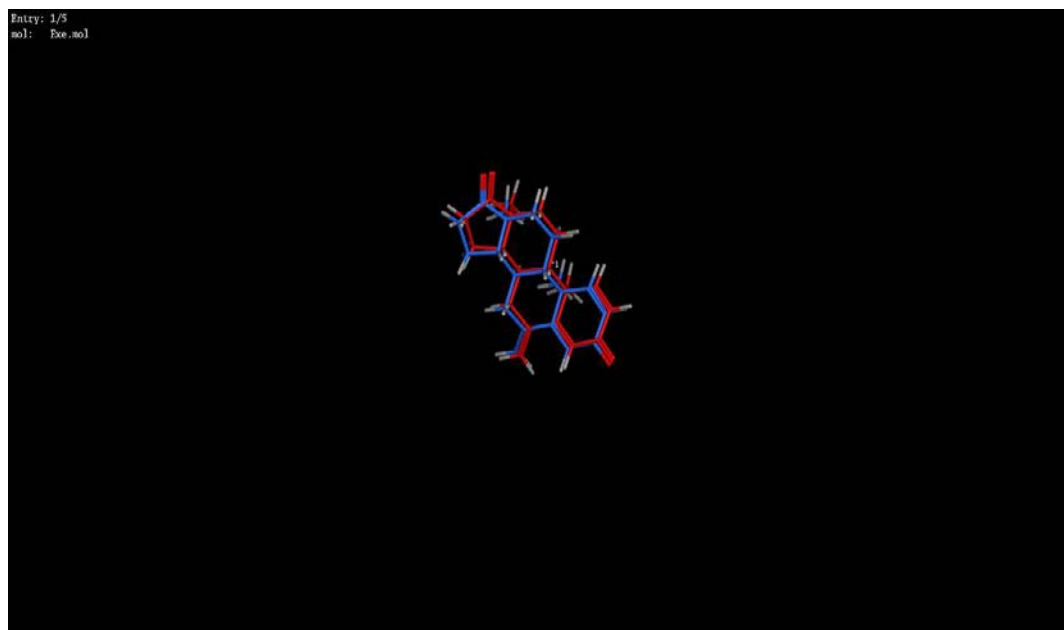


Figure 4.17: Interaction poses of trastuzumab with HER2 (a) 2D interactions (b) Interactions along with distances

## Validation of docking protocol



**Figure 4.18: Overlay of internal ligand (red) of aromatase and re-docked ligand (blue)**

### 4.1.2 Drug likeliness prediction of coumarin-quinoxaline hybrids

Drug likeliness prediction is a significant qualitative approach in drug design to predict that how “drug like” a compound is. These properties can be controlled by medicinal chemists during drug design and are directly related to characteristics of the drug like bioavailability. *In silico* drug likeliness prediction of best twelve designed molecules was carried out using Swiss ADME predictor as depicted in Table 4.4. Percentage absorption (% ABS) was calculated by using formula  $\%ABS = 109 - (0.345 \times TPSA)$ . The designed potent analogues displayed good absorption in the range of 76.5-82.77%. Results revealed that designed potent analogues showed no violation of Lipinski’s Rule of Five. These predictions suggested that designed analogues can be utilized to develop drug like candidates. The predicted drug likeliness properties of screened twelve compounds were within the acceptable ranges of all parameters and showed no-violations according to Lipinski’s rule of five (Lipinski et al., 2012). Log P is an indicator of lipophilicity and the compounds have displayed a log P value of less than 4 indicating the good penetration properties across the cell membrane. Molecular weight was below 500 which reveal good transport, diffusion and absorption properties. The number of rotatable bonds was between 1-3 describing good oral

bioavailability. The molecular polar surface area is the sum of surface of the polar atoms inside a molecule. This area is inversely proportional to the % absorption of the designed molecule indicating good bioavailability. These overall predictions suggest that the designed molecule could act as potential drug like candidates.

**Table 4.4: *In silico* drug like properties of best 12 designed molecules**

| Compound    | TPSA <sup>a</sup> | MW <sup>b</sup> | RoB <sup>c</sup> | HBD <sup>d</sup> | HBA <sup>e</sup> | IlogP<br>(MlogP) <sup>f</sup> | logS <sup>g</sup> | %<br>ABS <sup>h</sup> |
|-------------|-------------------|-----------------|------------------|------------------|------------------|-------------------------------|-------------------|-----------------------|
| <b>Rule</b> | <b>≤140</b>       | <b>≤500</b>     | <b>≤10</b>       | <b>≤5</b>        | <b>≤10</b>       | <b>≤5</b>                     | <b>&gt;-4</b>     | <b>-</b>              |
| RB13        | 77.10             | 337.30          | 1                | 1                | 6                | 2.60                          | -4.98             | 82.39                 |
| RB14        | 77.10             | 387.31          | 2                | 1                | 8                | 2.82                          | -5.55             | 82.39                 |
| RB16        | 86.33             | 349.34          | 2                | 1                | 6                | 2.91                          | -4.81             | 79.21                 |
| RB17        | 95.56             | 379.37          | 3                | 1                | 7                | 3.09                          | -4.93             | 76.03                 |
| RB18        | 77.10             | 353.76          | 1                | 1                | 5                | 2.75                          | -5.31             | 78.24                 |
| RB19        | 77.10             | 398.21          | 1                | 1                | 5                | 2.86                          | -5.51             | 82.39                 |
| RB36        | 77.10             | 395.41          | 2                | 1                | 5                | 3.26                          | -7.17             | 82.39                 |
| RB37        | 86.33             | 425.44          | 3                | 1                | 6                | 3.40                          | -7.28             | 80.28                 |
| RB86        | 95.56             | 379.37          | 3                | 1                | 7                | 2.94                          | -5.15             | 76.03                 |
| RB87        | 115.79            | 395.37          | 3                | 2                | 8                | 2.38                          | -4.56             | 78.62                 |
| RB88        | 97.33             | 369.76          | 1                | 2                | 6                | 2.25                          | -4.94             | 74.46                 |
| RB89        | 97.33             | 414.21          | 1                | 2                | 6                | 2.39                          | -5.14             | 82.14                 |

Abbreviations:<sup>a</sup>Topological polar surface area; <sup>b</sup>Molecular weight; <sup>c</sup>Number of rotatable bonds; <sup>d</sup> Number of hydrogen bond donors; <sup>e</sup>Number of hydrogen bonds acceptors; <sup>f</sup> Logarithm of compound partition coefficient between n-octanol and water; <sup>g</sup>Logarithm of water solubility; <sup>h</sup>Percentage absorption

#### 4.1.3 ADME prediction studies of coumarin-quinoxaline hybrids

Pharmacokinetic profile of a drug is of utmost significance to approve it as a suitable therapeutic candidate. Many drugs cannot fulfil the favourable pharmacokinetics and get failed in clinical trials. The preliminary screening of ADME properties of designed drugs is a useful approach in order to save time, cost as well as the risk of failure. *In silico* ADME properties of best twelve compounds were predicted using preADMET tool version 2.0 software

(preadmet.bmdrc.kr). The calculated values of absorption through various barriers were found within the standard limits for all the twelve compounds. Human intestinal absorption value greater than 80% suggests that the compound is well absorbed through intestine. Lower value of BBB from 0.14-0.90 reveals that the compound cannot cross the blood brain barrier. Caco2 value between 4 to 70 represents moderate absorption, greater than 70 suggests maximum absorption. The potent compounds with lower MDCK value indicate lower absorption towards kidney cells. Plasma protein binding greater than 85 indicates best distribution properties of potent compounds. The predicted data has been compiled in Table 4.5.

**Table 4.5: ADME properties of 12 predicted best compounds**

| <b>Compound</b> | <b>HIA%</b> | <b>Caco-2(nm/sec)</b> | <b>MDCK</b> | <b>BBB (log PS) &lt;0.4</b> | <b>Plasma protein binding (%)</b> |
|-----------------|-------------|-----------------------|-------------|-----------------------------|-----------------------------------|
| RB13            | 96.87       | 23.62                 | 2.32        | 0.19                        | 90.85                             |
| RB14            | 96.56       | 21.64                 | 1.68        | 0.07                        | 93.71                             |
| RB16            | 96.93       | 28.80                 | 2.78        | 0.16                        | 70.78                             |
| RB17            | 97.36       | 30.97                 | 3.92        | 0.10                        | 58.62                             |
| RB18            | 94.26       | 18.78                 | 3.18        | 0.10                        | 60.12                             |
| RB19            | 96.32       | 22.58                 | 0.30        | 0.23                        | 76.19                             |
| RB36            | 96.46       | 38.18                 | 3.26        | 0.16                        | 95.12                             |
| RB37            | 94.28       | 28.32                 | 2.96        | 0.16                        | 86.74                             |
| RB86            | 93.72       | 18.12                 | 4.18        | 0.10                        | 53.25                             |
| RB87            | 92.18       | 20.14                 | 4.02        | 0.12                        | 55.28                             |
| RB88            | 96.34       | 20.46                 | 3.28        | 0.10                        | 58.42                             |
| RB89            | 92.44       | 21.92                 | 3.48        | 0.10                        | 58.82                             |

#### **4.1.4 Toxicity prediction studies of coumarin-quinoxaline hybrids**

A therapeutic drug is of no use if it is toxic to other parts of the body although it is effective against particular ailment. So a preliminary idea about the toxicity of a designed molecule is highly useful to avoid failure of it during clinical stages.

Toxicity profiling of a drug directly ensures the safety profile of a particular drug. The prediction of toxicity was carried out by PreADME and PROTOX softwares. Protox predictions revealed that the designed compounds lie in Class 4 with LD50 value >900 mg/kg which is much higher dose to be toxic. Rodent toxicity tests for Carcino-Mouse and Carcino-Rat were positive which means there is no evidence of carcinogenic toxicity. Medium risk for hERG inhibition indicates that designed analogues have minimum risk on cardiac action potential. The obtained results from both the softwares have been presented in Table 4.6. From the data, it can be concluded that the designed molecules are safe to be used as a drug.

**Table 4.6: *In silico* toxicity predictions of best 12 screened compounds**

| <b>Compound</b> | <b>Carcino-Mouse</b> | <b>Carcino-Rat</b> | <b>HERG-inhibition</b> | <b>Protox Predicted LD50</b> | <b>Protox Predicted Class</b> |
|-----------------|----------------------|--------------------|------------------------|------------------------------|-------------------------------|
| RB13            | Positive             | Positive           | Medium risk            | 1050 mg/kg                   | Class 4                       |
| RB14            | Positive             | Positive           | Medium risk            | 920 mg/kg                    | Class 4                       |
| RB16            | Positive             | Positive           | Medium risk            | 920 mg/kg                    | Class 4                       |
| RB17            | Positive             | Positive           | Medium risk            | 1000 mg/kg                   | Class 4                       |
| RB18            | Positive             | Positive           | Medium risk            | 1050 mg/kg                   | Class 4                       |
| RB19            | Positive             | Positive           | Medium risk            | 1050 mg/kg                   | Class 4                       |
| RB36            | Positive             | Positive           | Medium risk            | 1000 mg/kg                   | Class 4                       |
| RB37            | Positive             | Positive           | Medium risk            | 1000mg/kg                    | Class 4                       |
| RB86            | Positive             | Positive           | Medium risk            | 1000mg/kg                    | Class 4                       |
| RB87            | Positive             | Positive           | Medium risk            | 1000mg/kg                    | Class 4                       |
| RB88            | Positive             | Positive           | Medium risk            | 920 mg/kg                    | Class 4                       |
| RB89            | Positive             | Positive           | Medium risk            | 920 mg/kg                    | Class 4                       |

#### **4.1.5 Molecular docking studies of coumarin-dihydropyrimidone hybrids**

The designed compounds (CD1-CD90) were subjected to molecular docking against human aromatase (PDB Id: 3S7S) using MOE software (Figure 4.19). Maximum compounds get fit inside the pocket of aromatase. Various docking scores displayed by the designed compounds have been displayed in Table 4.7. The docking protocol

validated and RMSD value was found to be 0.42. The docking results were compared with marketed well established aromatase inhibitor drug exemestane. Among fifty designed molecules, twelve displayed excellent docking scores among the whole library of compounds. These twelve were estimated to possess maximum aromatase inhibitory potentials among all designed molecules. These best twelve compounds were further analysed with the help of 2D and 3D binding poses to study the fitting capability inside the receptor, type of interactions involved with the receptor and distance of interactions between compounds and receptor.

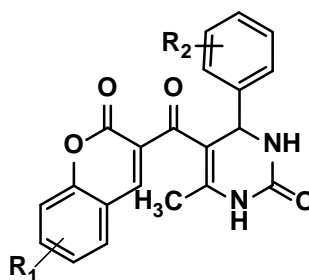


**Figure 4.19: Designed compounds (CD1-CD90)**

**Table 4.7: Docking scores of designed library of compounds**

| Compound | R <sub>1</sub>     | R <sub>2</sub>     | Docking Scores (PDB Id: 3S7S) |
|----------|--------------------|--------------------|-------------------------------|
| CD1      | H                  | H                  | -9.18                         |
| CD2      | H                  | 4-OH               | -9.32                         |
| CD3      | H                  | 4-CH <sub>3</sub>  | -8.68                         |
| CD4      | H                  | 4-OCH <sub>3</sub> | -8.23                         |
| CD5      | H                  | 4-Cl               | -8.62                         |
| CD6      | 2-OCH <sub>3</sub> | 4-OH               | -10.86                        |
| CD7      | 2-OCH <sub>3</sub> | 4-CH <sub>3</sub>  | -9.16                         |
| CD8      | 2-OCH <sub>3</sub> | 4-OCH <sub>3</sub> | -11.32                        |
| CD9      | 2-OCH <sub>3</sub> | 4-Cl               | -10.22                        |
| CD10     | 2-OCH <sub>3</sub> | 4-F                | -10.32                        |
| CD11     | 2-OH               | 4-OH               | -8.11                         |
| CD12     | 2-OH               | 4-CH <sub>3</sub>  | -8.78                         |
| CD13     | 2-OH               | 4-OCH <sub>3</sub> | -8.12                         |
| CD14     | 2-OH               | 4-Cl               | -8.46                         |
| CD15     | 2-OH               | 4-F                | -7.92                         |
| CD16     | 2-Cl               | 4-OH               | -7.36                         |
| CD17     | 2-Cl               | 4-CH <sub>3</sub>  | -7.42                         |
| CD18     | 2-Cl               | 4-OCH <sub>3</sub> | -7.88                         |
| CD19     | 2-Cl               | 4-Cl               | -10.92                        |
| CD20     | 2-Cl               | 4-F                | -11.08                        |
| CD21     | 2-Br               | 4-OH               | -7.32                         |
| CD22     | 2-Br               | 4-CH <sub>3</sub>  | -7.58                         |
| CD23     | 2-Br               | 4-OCH <sub>3</sub> | -7.12                         |

|      |                               |                                      |        |
|------|-------------------------------|--------------------------------------|--------|
| CD24 | 2-Br                          | 4-Cl                                 | -7.16  |
| CD25 | 2-Br                          | 4-F                                  | -7.62  |
| CD26 | 2-Br                          | 4-Br                                 | -7.36  |
| CD27 | 2-NO <sub>2</sub>             | 4-OH                                 | -9.27  |
| CD28 | 2-NO <sub>2</sub>             | 4-CH <sub>3</sub>                    | -11.46 |
| CD29 | 2-NO <sub>2</sub>             | 4-OCH <sub>3</sub>                   | -8.56  |
| CD30 | 2-NO <sub>2</sub>             | 4-Cl                                 | -8.14  |
| CD31 | 2-NO <sub>2</sub>             | 4-F                                  | -8.31  |
| CD32 | 2-NO <sub>2</sub>             | 4-Br                                 | -9.41  |
| CD33 | 2-NH <sub>2</sub>             | 4-OH                                 | -9.47  |
| CD34 | 2-NH <sub>2</sub>             | 4-CH <sub>3</sub>                    | -8.81  |
| CD35 | 2-NH <sub>2</sub>             | 4-OCH <sub>3</sub>                   | -8.67  |
| CD36 | 2-NH <sub>2</sub>             | 4-Cl                                 | -8.08  |
| CD37 | 2-NH <sub>2</sub>             | 4-F                                  | -8.18  |
| CD38 | 2-NH <sub>2</sub>             | 4-Br                                 | -8.38  |
| CD39 | 2-CH <sub>3</sub>             | 4-OH                                 | -8.96  |
| CD40 | 2-CH <sub>3</sub>             | 4-CH <sub>3</sub>                    | -9.08  |
| CD41 | 2-CH <sub>3</sub>             | 4-OCH <sub>3</sub>                   | -9.17  |
| CD42 | 2-CH <sub>3</sub>             | 4-Cl                                 | -9.36  |
| CD43 | 2-CH <sub>3</sub>             | 4-F                                  | -10.08 |
| CD44 | 2-CH <sub>3</sub>             | 4-NH <sub>2</sub>                    | -10.78 |
| CD45 | 2-F                           | 4-OH                                 | -9.77  |
| CD46 | 2-F                           | 4-CH <sub>3</sub>                    | -9.12  |
| CD47 | 2-F                           | 4-OCH <sub>3</sub>                   | -9.56  |
| CD48 | 2-F                           | 4-Cl                                 | -9.02  |
| CD49 | 2-F                           | 4-F                                  | -9.78  |
| CD50 | 2-F                           | 4-Br                                 | -9.24  |
| CD51 | C <sub>6</sub> H <sub>5</sub> | H                                    | -6.78  |
| CD52 | C <sub>6</sub> H <sub>5</sub> | 4-CH <sub>3</sub>                    | -6.98  |
| CD53 | C <sub>6</sub> H <sub>5</sub> | 4-F                                  | -7.42  |
| CD54 | C <sub>6</sub> H <sub>5</sub> | 4-CF <sub>3</sub>                    | -7.56  |
| CD55 | C <sub>6</sub> H <sub>5</sub> | 4,5-(CH <sub>3</sub> ) <sub>2</sub>  | -7.96  |
| CD56 | C <sub>6</sub> H <sub>5</sub> | 3-OCH <sub>3</sub>                   | -8.76  |
| CD57 | C <sub>6</sub> H <sub>5</sub> | 3,4-(OCH <sub>3</sub> ) <sub>2</sub> | -7.98  |
| CD58 | C <sub>6</sub> H <sub>5</sub> | 4-Cl                                 | -6.72  |
| CD59 | C <sub>6</sub> H <sub>5</sub> | 4-Br                                 | -6.88  |
| CD60 | C <sub>6</sub> H <sub>5</sub> | 4-NO <sub>2</sub>                    | -6.78  |
| CD61 | C <sub>6</sub> H <sub>5</sub> | H                                    | -6.78  |
| CD62 | C <sub>6</sub> H <sub>5</sub> | 4-CH <sub>3</sub>                    | -6.98  |
| CD63 | H                             | 4-Br                                 | -7.12  |
| CD64 | H                             | 4-NO <sub>2</sub>                    | -6.96  |
| CD65 | H                             | 4-F                                  | -7.08  |
| CD66 | H                             | 4-CF <sub>3</sub>                    | -7.22  |
| CD67 | H                             | 3,4-OCH <sub>3</sub>                 | -6.58  |
| CD68 | 3-Cl                          | 4-OH                                 | -7.16  |
| CD69 | 3-Cl                          | 4-CH <sub>3</sub>                    | -7.12  |

|            |                   |                      |        |
|------------|-------------------|----------------------|--------|
| CD70       | 3-Cl              | 4-OCH <sub>3</sub>   | -7.18  |
| CD71       | 3-Cl              | 4-NO <sub>2</sub>    | -6.92  |
| CD72       | 3-Cl              | 4-Br                 | -8.08  |
| CD73       | 3-OH              | 4-NO <sub>2</sub>    | -7.11  |
| CD74       | 3-OH              | 4-Cl                 | -7.78  |
| CD75       | 3-OH              | 3,4-OCH <sub>3</sub> | -6.42  |
| CD76       | 3-OH              | 4-Br                 | -6.46  |
| CD77       | 3-OH              | 4-NH <sub>2</sub>    | -6.92  |
| CD78       | 3-NH <sub>2</sub> | 4-NO <sub>2</sub>    | -9.47  |
| CD79       | 3-NH <sub>2</sub> | 4-CH <sub>3</sub>    | -6.81  |
| CD80       | 3-NH <sub>2</sub> | 3,4-OCH <sub>3</sub> | -7.67  |
| CD81       | 3-NH <sub>2</sub> | 4-Cl                 | -7.16  |
| CD82       | 3-NH <sub>2</sub> | 4-CF <sub>3</sub>    | -7.28  |
| CD83       | 3-NH <sub>2</sub> | 4-Br                 | -6.38  |
| CD84       | 3-NH <sub>2</sub> | 4-OH                 | -6.57  |
| CD85       | 3-NH <sub>2</sub> | 4-OCH <sub>3</sub>   | -6.81  |
| CD86       | 3-CH <sub>3</sub> | 4-NH <sub>2</sub>    | -6.96  |
| CD87       | 3-CH <sub>3</sub> | 4-OCH <sub>3</sub>   | -7.08  |
| CD88       | 3-CH <sub>3</sub> | 3,4-OCH <sub>3</sub> | -8.17  |
| CD89       | 3-CH <sub>3</sub> | 4-NO <sub>2</sub>    | -7.36  |
| CD90       | 3-CH <sub>3</sub> | 4-Cl                 | -8.08  |
| Exemestane |                   |                      | -11.28 |

Various interactions displayed by the best twelve hybrid molecules have been displayed in Table 4.8 along with the distances. Among these, 2D and 3D binding patterns of these six hybrid compounds have been depicted in Figures 4.20 to 4.25 whereas binding patterns of exemestane have been depicted in Figure 4.26. Compounds CD8, CD20 and CD28 revealed comparable scores to exemestane with excellent interactions at very short distances. The main amino acid residue involved in interactions were CYS437, Ala306, Val370, Thr310, Met310, Pro429, Trp341, Arg435 and 411. It was evident that the best compounds revealed almost similar binding patterns as the standard drug exemestane. The main types of interactions involved in binding were hydrogen bonding, Arene-H and side chain acceptor interactions.

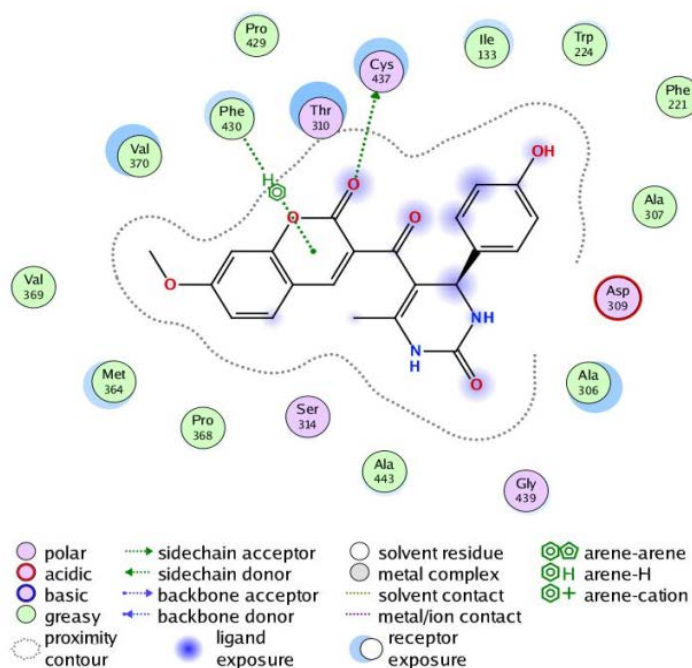
**Table 4.8: Various interactions revealed by best twelve designed compounds**

| Compound | Docking Score<br>(PDB Id: 3S7S) | Type of Interactions & Distances  |
|----------|---------------------------------|---|
| CD6      | -10.86                          | Phe430(Arene-H interaction), Cys435(H-bond with =O; 3.95Å), Val370(H-bond with O; 2.63Å), Pro368(H-bond with O; 2.36Å), Ala306(H-bond |

|      |        |  |
|------|--------|--|
|      |        | with =O; 4.51Å)  |
| CD8  | -11.32 | Ala306(Arene-H interaction), Cys437(H-bond with =O; 3.34Å), Thr310(H-bond with N; 3.17Å), Val370(H-bond with O; 2.83Å), Ala306(H-bond with -NH; 2.23Å)   |
| CD9  | -10.22 | Phe430(Arene-H interaction), Cys435(H-bond with =O; 3.75Å), Thr310(H-bond with N; 3.47Å), Val370(H-bond with O; 2.37Å), Cys437(H-bond with =O; 3.14Å),   |
| CD10 | -10.32 | Ala306(Arene-H interaction), Cys437(H-bond with =O; 3.44Å), Cys437(Side chain acceptor interaction with H; 3.95Å), Arg115(H-bond with O; 3.65Å)  |
| CD19 | -10.92 | Thr310(Arene-H interaction), Cys437(Side chain acceptor interaction with H; 3.65Å), Pro429(H-bond with -NH; 2.07Å), Trp341(H-bond with Cl; 2.27Å), Arg115(H-bond with O; 3.65Å), Arg115(H-bond with =O; 3.20Å), Val370(H-bond with -NH; 4.19Å) |
| CD20 | -11.08 | Met303(Side chain acceptor interaction with H; 3.65Å), Cys437(Side chain acceptor interaction with H; 3.75Å), Cys437(Side chain acceptor interaction with H; 4.15Å), Arg435(H-bond with -NH; 2.74Å), Arg435(H-bond with =O; 3.55Å)             |
| CD28 | -11.46 | Arg435(H-bond with =O; 2.08Å), Arg145(H-bond with O; 2.21Å), Pro429(H-bond with -NH; 2.14Å), Trp141(H-bond with O; 1.57Å), Val373(H-bond with -NH; 4.66Å)  |
| CD32 | -9.41  | Arg145(H-bond with O; 2.29Å), Pro429(H-bond with -NH; 2.37Å), Trp141(H-bond with O; 1.77Å)   |
| CD42 | -9.36  | Cys437(H-bond with =O; 3.58Å), Ala438(Arene-H interaction), Arg155(H-bond with -NH; 3.88Å)   |
| CD43 | -10.08 | Cys437(Side chain acceptor interaction with H; 4.33Å), Cys437(H-bond with =O; 3.51Å), Arg155(H-bond with -NH; 3.81Å)   |

|            |        |  |
|------------|--------|--|
| CD44       | -10.78 | Cys437(Side chain acceptor interaction with H; 4.27Å), Cys437(H-bond with =O; 3.59Å), Ala438(Arene-H interaction), Arg155(H-bond with -NH; 3.38Å), Cys437(H-bond with -NH; 3.88Å)                  |
| CD49       | -9.78  | Arg435(H-bond with -NH; 2.74Å), Met303(Side chain receptor interaction with H; 3.65Å), Cys437(Side chain receptor interaction with H; 4.15Å),Cys437(Side chain receptor interaction with H; 3.75Å) |
| Exemestane | -11.28 | Met374(H bond with =O; 1.97Å), Arg115(H bond with =O; 2.63Å), Ala306(H bond with =O; 4.40Å)  |

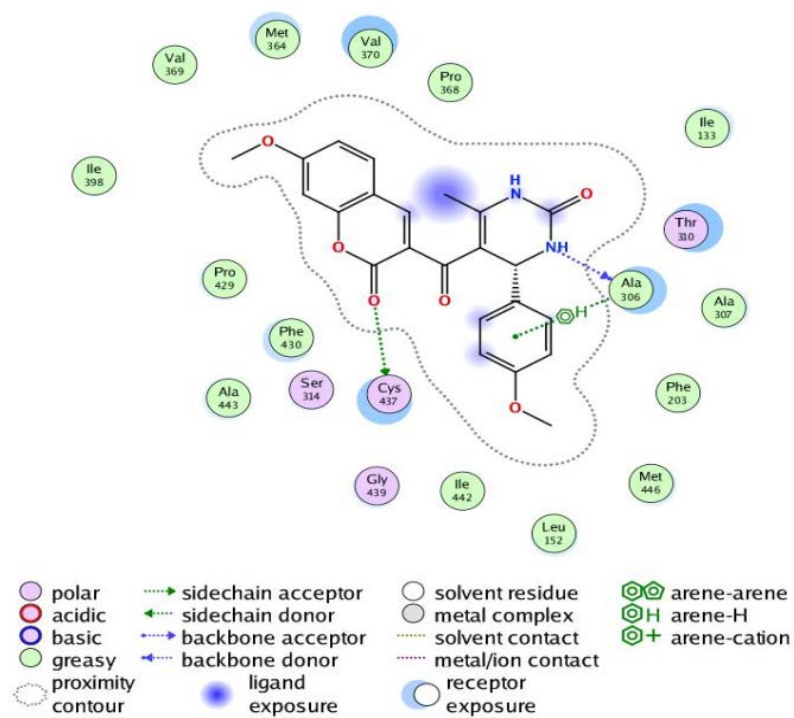
Compound CD6



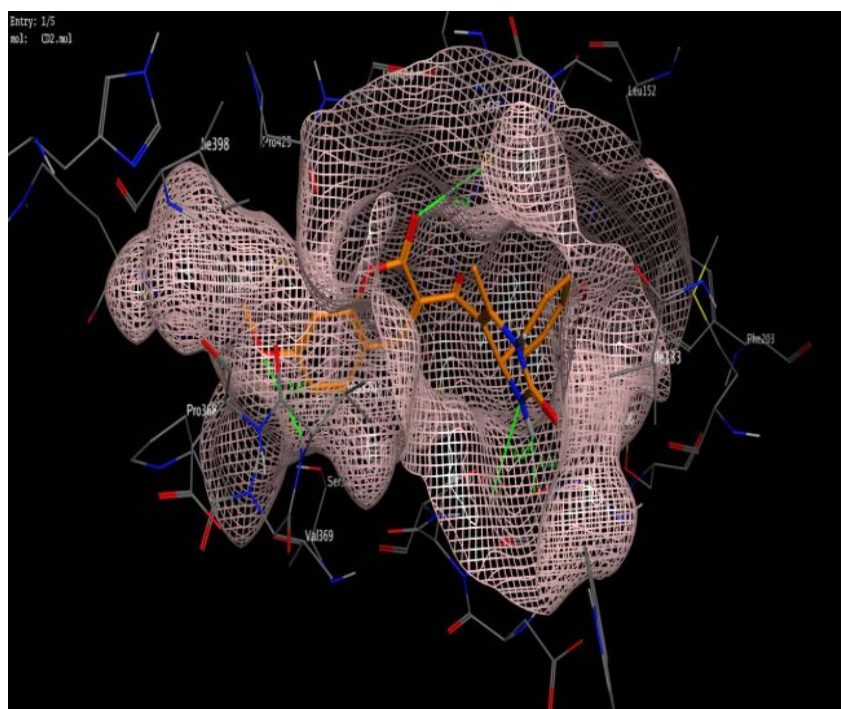
(a)



## Compound CD8

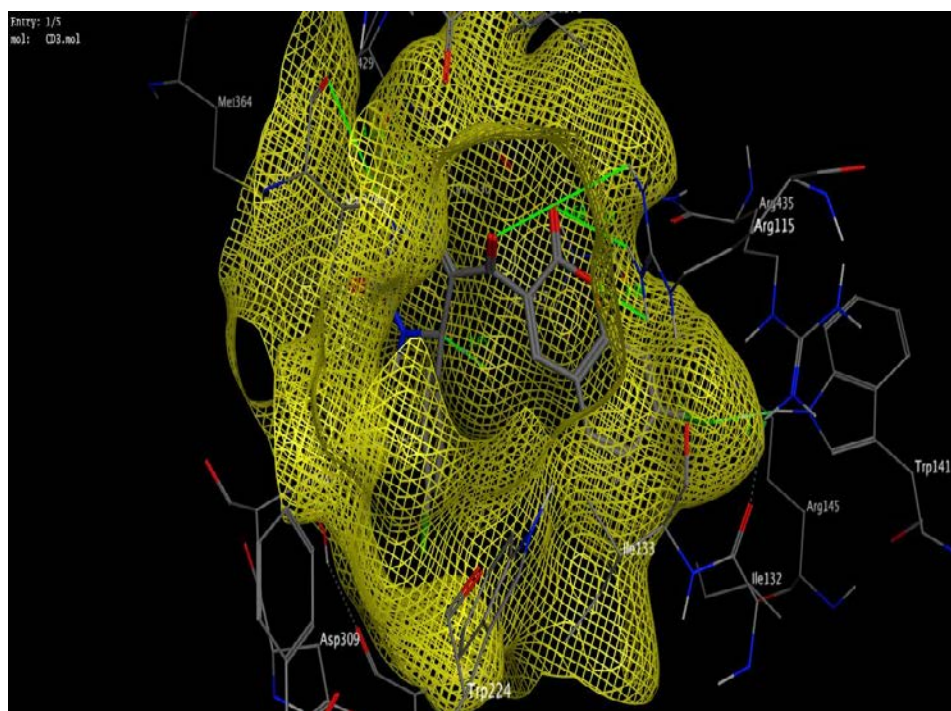


(a)

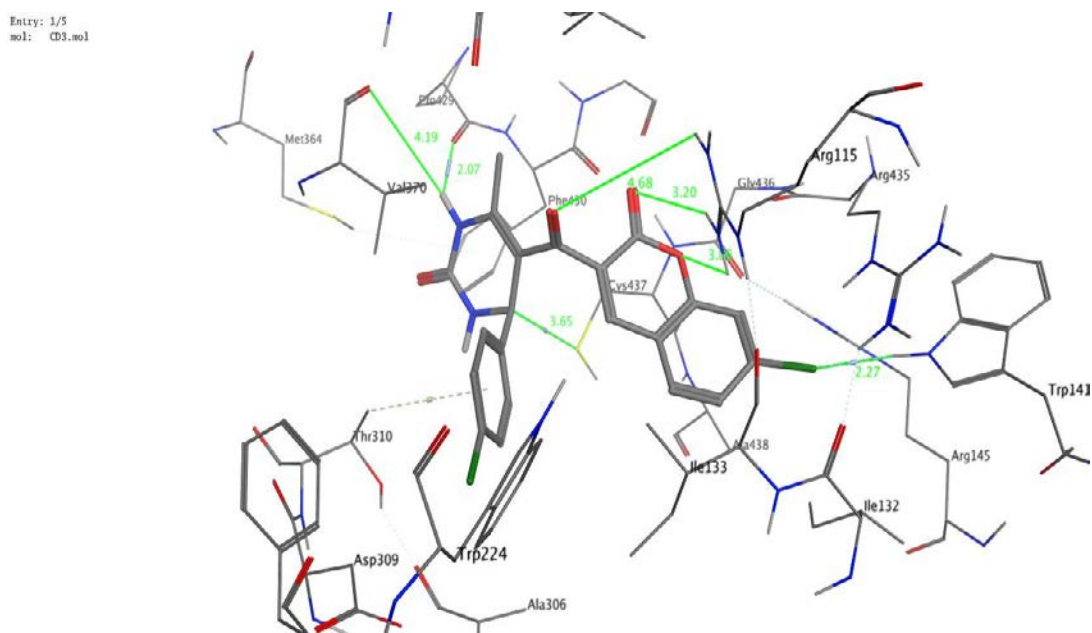


(b)





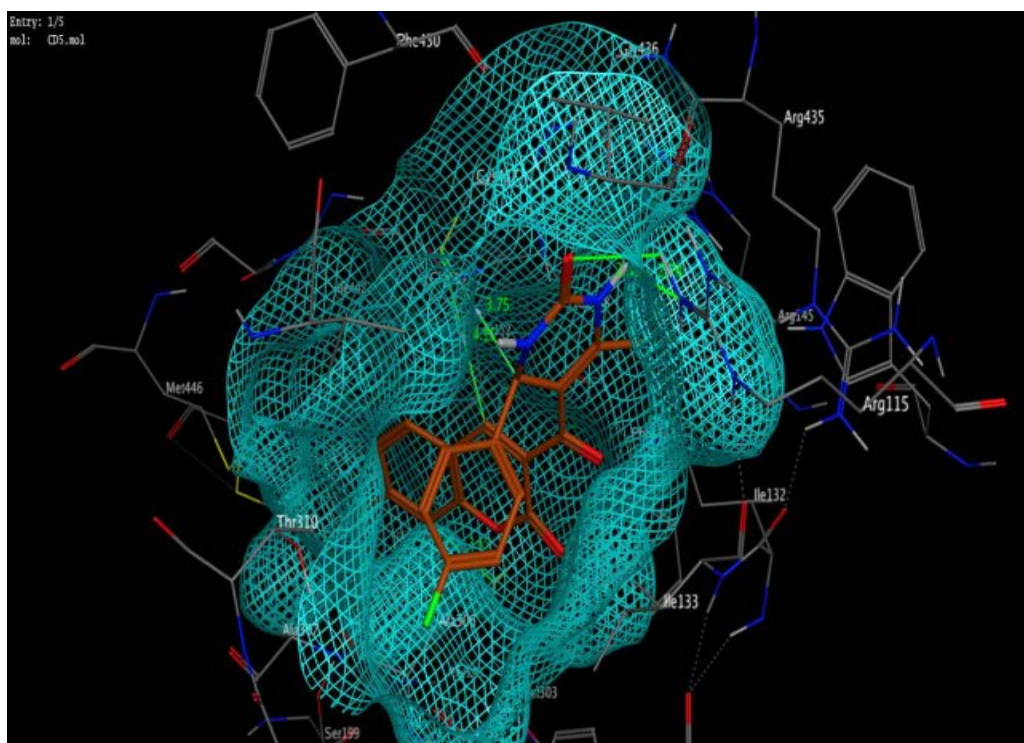
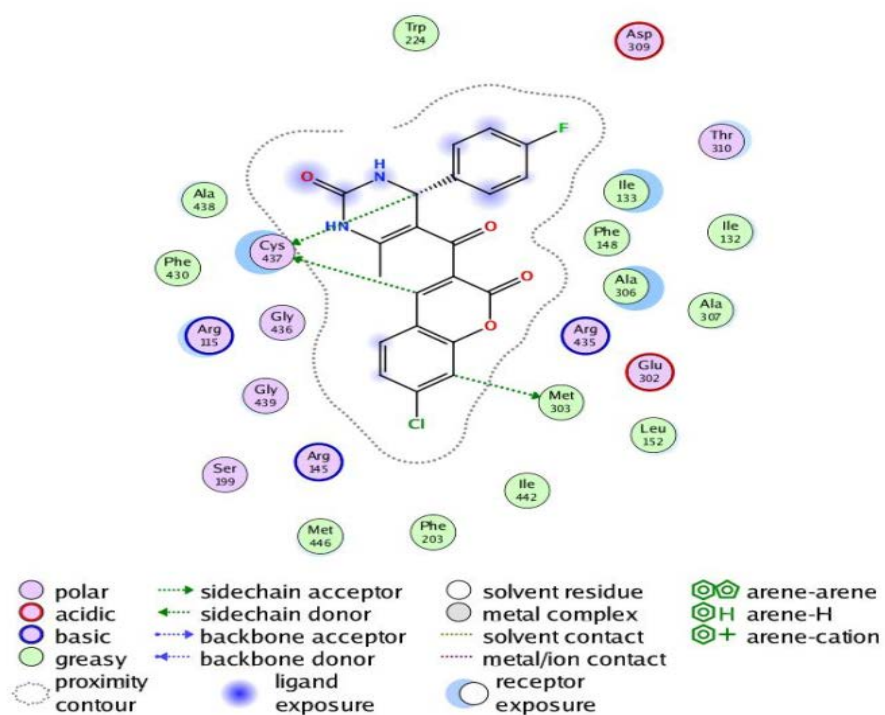
(b)



(c)

**Figure 4.22: Interaction poses of CD19 with aromatase (a) 2D interactions (b) CD19 embedded in receptor pocket (c) Interactions along with distances**

## Compound CD20



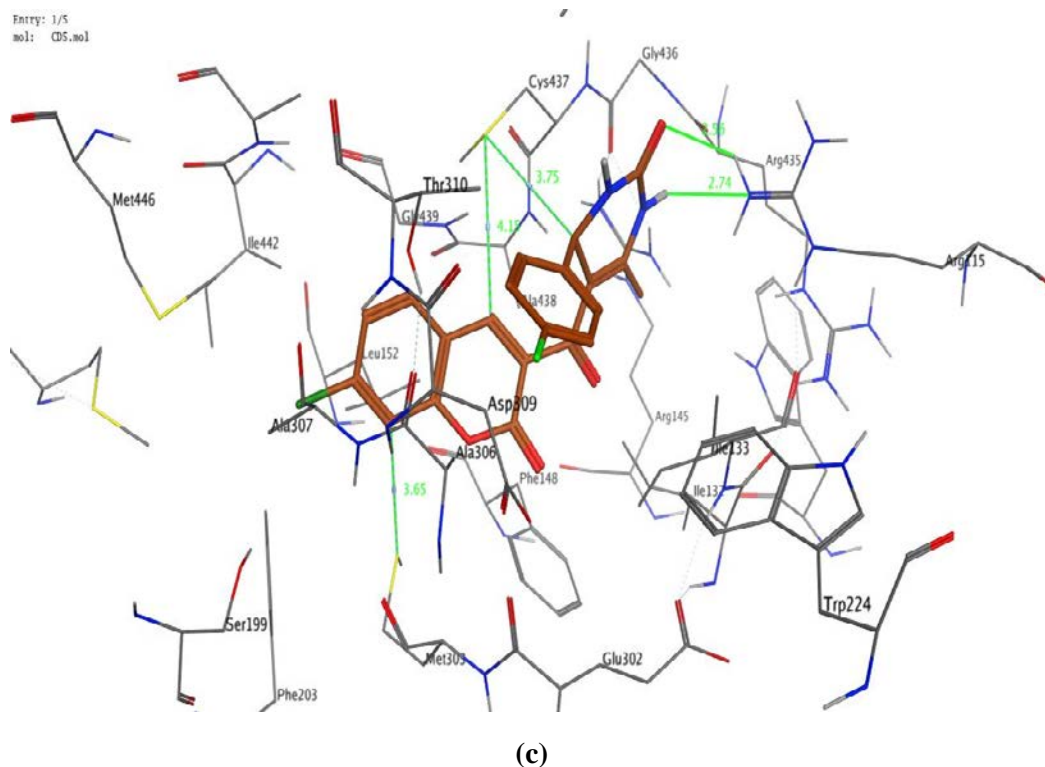
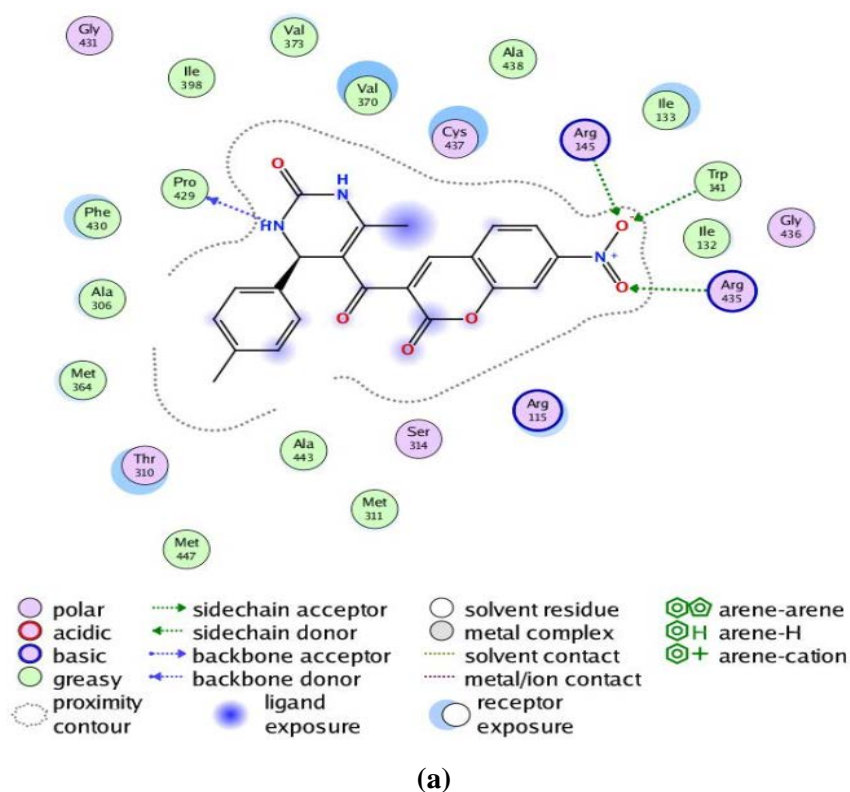
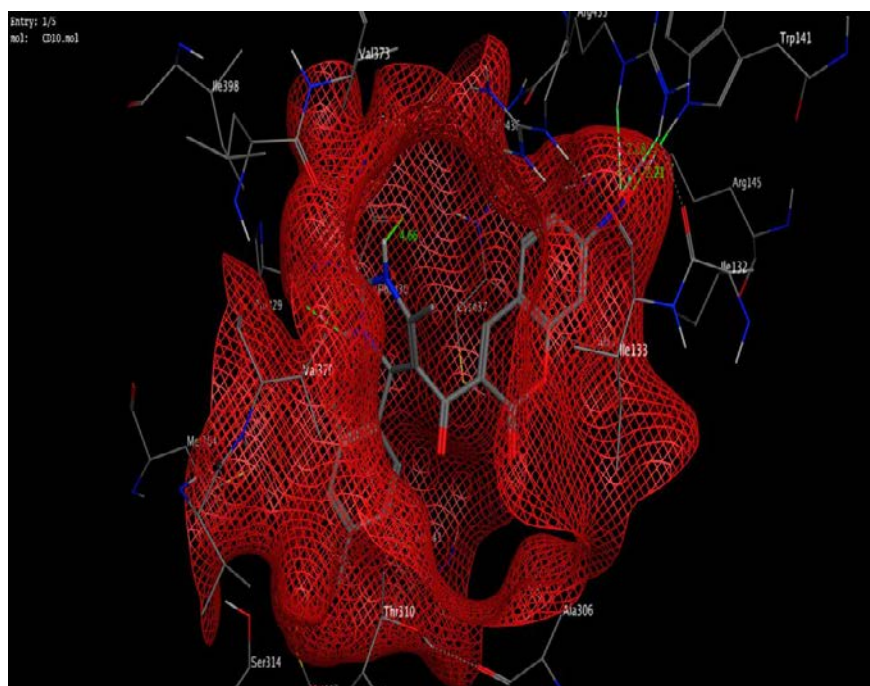


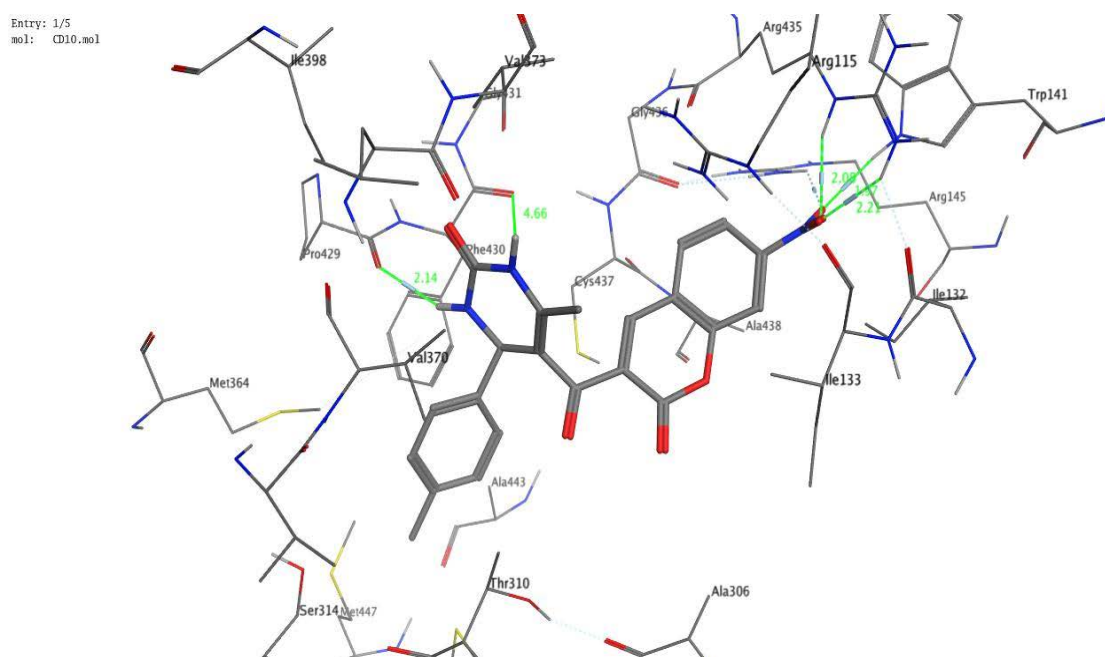
Figure 4.23: Interaction poses of CD20 with aromatase (a) 2D interactions (b) CD20 embedded in receptor pocket (c) Interactions along with distances

### Compound CD28





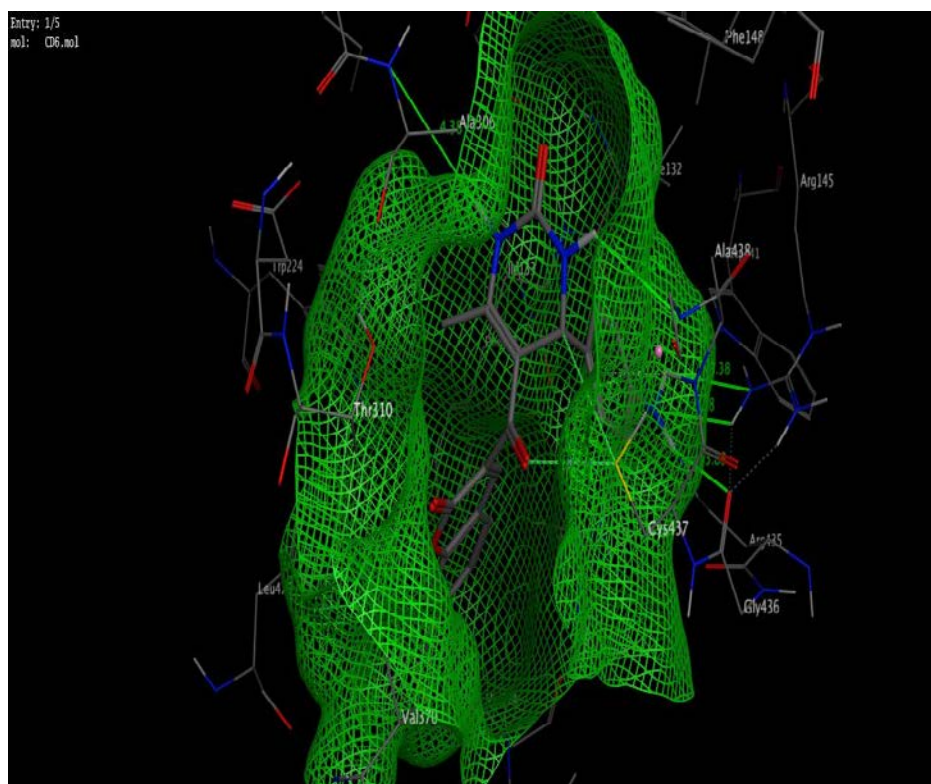
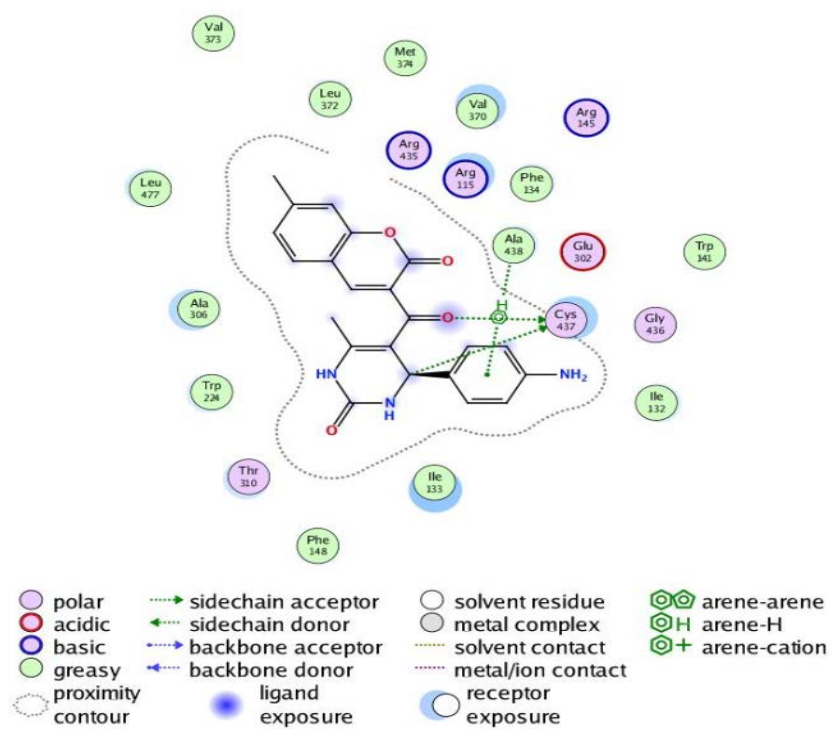
(b)



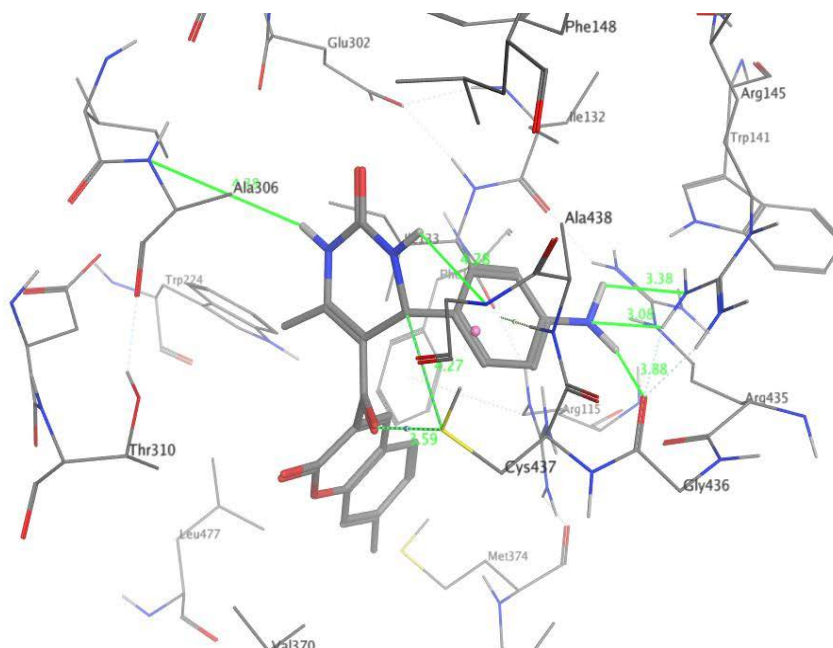
(c)

Figure 4.24: Interaction poses of CD28 with aromatase (a) 2D interactions (b) CD28 embedded in receptor pocket (c) Interactions along with distances

## Compound CD44



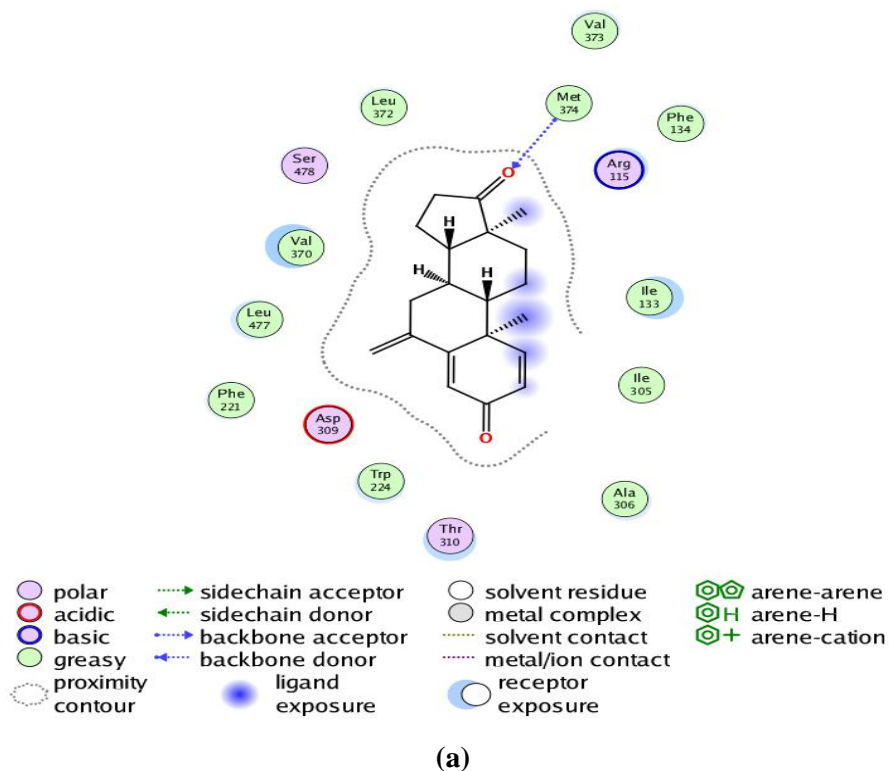
Entry: 1/5  
mol: CD6.mol



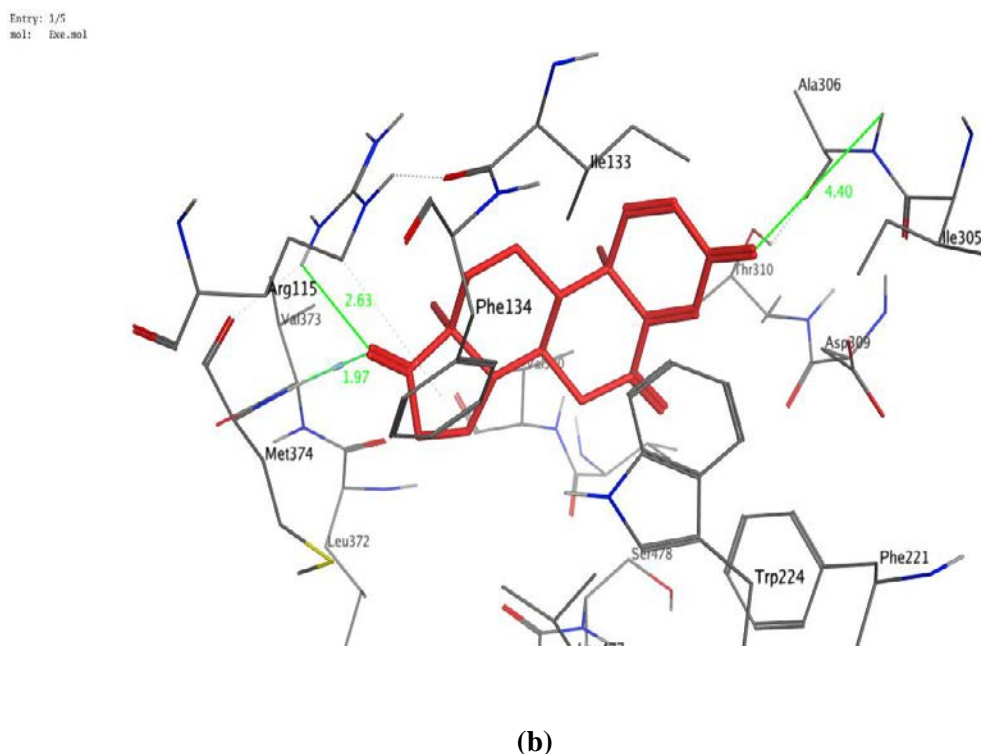
(c)

Figure 4.25: Interaction poses of CD44 with aromatase (a) 2D interactions (b) CD44 embedded in receptor pocket (c) Interactions along with distances

### Exemestane



(a)



**Figure 4.26: Interaction poses of Exemestane with aromatase (a) 2D interactions (b) Interactions along with distances**

#### 4.1.6 Drug likeliness prediction of coumarin-dihydropyrimidone hybrids

Drug likeliness prediction is a promising approach to get an idea about drug like properties of designed molecules. These properties are important to predict the bioavailability of drugs and medicinal chemist can modify the factors affecting it accordingly. Drug likeliness features of best twelve compounds were predicted by using Swiss ADME predictor. Percentage absorption (% ABS) was calculated by using formula  $\% \text{ABS} = 109 - (0.345 \times \text{TPSA})$ . The designed potent analogues displayed good absorption in the range of 76.5-82.77%. Results evidenced that designed potent analogues showed no violation of Lipinski's Rule of Five as represented in Table 4.9. Hence it can be postulated that the designed molecules may serve as drug like candidates.

**Table 4.9: *In silico* drug like properties of best twelve designed hybrids**

| Compound    | TPSA <sup>a</sup> | MW <sup>b</sup> | RoB <sup>c</sup> | HBD <sup>d</sup> | HBA <sup>e</sup> | IlogP (MlogP) <sup>f</sup> | logS <sup>g</sup> | % ABS <sup>h</sup> |
|-------------|-------------------|-----------------|------------------|------------------|------------------|----------------------------|-------------------|--------------------|
| <b>Rule</b> | ≤140              | ≤500            | ≤10              | ≤5               | ≤10              | ≤5                         | >-4               | -                  |
| CD6         | 117.87            | 406.39          | 4                | 3                | 6                | 1.30                       | -4.43             | 82.39              |

|      |        |        |   |   |   |      |       |       |
|------|--------|--------|---|---|---|------|-------|-------|
| CD8  | 106.87 | 420.41 | 5 | 2 | 6 | 1.51 | -4.53 | 82.39 |
| CD9  | 97.64  | 424.83 | 4 | 2 | 5 | 2.45 | -4.68 | 75.41 |
| CD10 | 97.64  | 408.67 | 4 | 2 | 6 | 2.31 | -4.25 | 75.41 |
| CD19 | 88.41  | 429.25 | 3 | 2 | 4 | 3.10 | -5.52 | 79.21 |
| CD20 | 88.41  | 412.80 | 3 | 2 | 5 | 2.99 | -4.97 | 76.03 |
| CD28 | 134.23 | 419.39 | 4 | 2 | 6 | 1.47 | -5.37 | 82.39 |
| CD32 | 134.23 | 484.26 | 4 | 2 | 6 | 1.64 | -4.99 | 82.39 |
| CD42 | 88.41  | 408.83 | 3 | 2 | 4 | 2.54 | -4.91 | 78.49 |
| CD43 | 88.41  | 392.28 | 3 | 2 | 5 | 2.41 | -4.47 | 78.49 |
| CD44 | 114.43 | 389.40 | 3 | 3 | 4 | 1.82 | -4.42 | 82.39 |
| CD49 | 88.41  | 396.34 | 3 | 2 | 6 | 2.05 | -4.33 | 78.49 |

Abbreviations:<sup>a</sup>Topological polar surface area; <sup>b</sup>Molecular weight; <sup>c</sup>Number of rotatable bonds; <sup>d</sup> Number of hydrogen bond donors; <sup>e</sup>Number of hydrogen bonds acceptors; <sup>f</sup> Logarithm of compound partition coefficient between n-octanol and water; <sup>g</sup>Logarithm of water solubility; <sup>h</sup>Percentage absorption

#### 4.1.7 ADME prediction studies of coumarin-dihydropyrimidinone hybrids

*In silico* ADME properties of best twelve compounds were predict using preADMET tool version 2.0 software (preadmet.bmdrc.kr). The calculated values of absorption through various barriers were found within the standard limits for all the twelve compounds. Human intestinal absorption value greater than 80% suggests that the compound is well absorbed through intestine. Lower value of BBB from 0.14-0.90 reveals that the compound cannot cross the blood brain barrier. Caco2 value between 4 to 70 represents moderate absorption, greater than 70 suggests maximum absorption. The potent compounds with lower MDCK value indicate lower absorption towards kidney cells. Plasma protein binding greater than 85 indicates best distribution properties of potent compounds. The predicted data has been compiled in Table 4.10.

Table 4.10: ADME properties of 12 predicted best compounds

| Compound | HIA%  | Caco-2(nm/sec) | MDCK  | BBB (log PS) <0.4 | Plasma protein binding (%) |
|----------|-------|----------------|-------|-------------------|----------------------------|
| CD6      | 94.43 | 20.08          | 1.53  | 0.019             | 92.22                      |
| CD8      | 94.27 | 22.11          | 1.58  | 0.022             | 91.43                      |
| CD9      | 95.23 | 21.58          | 0.42  | 0.073             | 77.78                      |
| CD10     | 94.36 | 21.88          | 1.15  | 0.042             | 90.58                      |
| CD19     | 94.26 | 18.78          | 0.25  | 0.53              | 91.32                      |
| CD20     | 95.32 | 20.91          | 0.55  | 0.28              | 86.19                      |
| CD28     | 92.46 | 20.18          | 0.22  | 0.019             | 99.12                      |
| CD32     | 95.28 | 18.32          | 0.028 | 0.02              | 92.74                      |
| CD42     | 95.72 | 21.56          | 0.31  | 0.47              | 90.25                      |
| CD43     | 92.18 | 20.14          | 4.02  | 0.12              | 90.28                      |
| CD44     | 92.55 | 21.06          | 7.91  | 0.09              | 88.73                      |
| CD49     | 93.26 | 21.32          | 0.83  | 0.14              | 90.11                      |

#### 4.1.8 *In silico* toxicity studies of coumarin-dihydropyrimidone hybrids

A preliminary idea about the toxicity of a designed molecule is of utmost importance as it may be helpful to prevent the failure of it during clinical stages. The *in silico* toxicity prediction was carried out by PreADME and PROTOX softwares. Prottox suggested that designed compounds lie in Class 4 and 5 with LD50 value >900 mg/kg which is much higher dose to be toxic. Carcino-Mouse and Carcino-Rat toxicity test were found positive suggesting that there is no evidence of carcinogenic toxicity. Medium risk for hERG inhibition evidenced that designed analogues have minimum risk on cardiac action potential. The predicted data have been presented in Table 4.11. From the data, it can be concluded that the designed molecules are safe to be used as a drug.

**Table 4.11: *In silico* toxicity results for best 12 hybrid compounds**

| <b>Compound</b> | <b>Carcino-Mouse</b> | <b>Carcino-Rat</b> | <b>HERG-inhibition</b> | <b>Protox Predicted LD50</b> | <b>Protox Predicted Class</b> |
|-----------------|----------------------|--------------------|------------------------|------------------------------|-------------------------------|
| CD6             | Positive             | Positive           | Medium risk            | 1350 mg/kg                   | Class 4                       |
| CD8             | Positive             | Positive           | Medium risk            | 1350 mg/kg                   | Class 4                       |
| CD9             | Positive             | Positive           | Medium risk            | 3200 mg/kg                   | Class 5                       |
| CD10            | Positive             | Positive           | Medium risk            | 2500 mg/kg                   | Class 5                       |
| CD19            | Positive             | Positive           | Medium risk            | 1120 mg/kg                   | Class 4                       |
| CD20            | Positive             | Positive           | Medium risk            | 1120 mg/kg                   | Class 4                       |
| CD28            | Positive             | Positive           | Medium risk            | 1350 mg/kg                   | Class 4                       |
| CD32            | Positive             | Positive           | Medium risk            | 1000 mg/kg                   | Class 4                       |
| CD42            | Positive             | Positive           | Medium risk            | 1000 mg/kg                   | Class 4                       |
| CD43            | Positive             | Positive           | Medium risk            | 1000 mg/kg                   | Class 4                       |
| CD44            | Positive             | Positive           | Medium risk            | 1350 mg/kg                   | Class 4                       |
| CD49            | Positive             | Positive           | Medium risk            | 1000 mg/kg                   | Class 4                       |

#### **4.1.9 Molecular docking studies of coumarin-dihydropyridine hybrids**

The designed compounds (DP1-DP75) (Figure 4.27) were subjected to molecular docking against human aromatase (PDB Id: 3S7S) using MOE software. Maximum compounds get fit inside the pocket of aromatase. Various docking scores displayed by the designed compounds have been displayed in Table 4.12. The docking protocol validated and RMSD value was found to be 0.28. The docking results were compared with marketed well established aromatase inhibitor drug exemestane. Among seventy five designed molecules, twelve (DP12, DP18-20, DP26-28, DP32, DP56, DP58, DP61, DP63) displayed excellent docking scores among the whole library of compounds. These twelve were estimated to possess maximum aromatase inhibitory potentials among all designed molecules. These best twelve compounds were further analysed with the help of 2D and 3D binding poses to study the fitting capability inside the receptor, type of interactions involved with the receptor and distance of interactions between compounds and receptor.

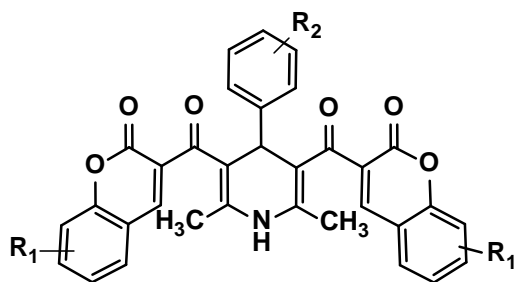


Figure 4.27: Designed coumarin-dihydropyridine hybrids (DP1-DP75)

Table 4.12: Docking scores of designed library of compounds

| Compound | R <sub>1</sub>     | R <sub>2</sub>     | Docking Scores (PDB Id: 3S7S) |
|----------|--------------------|--------------------|-------------------------------|
| DP1      | 2-OCH <sub>3</sub> | H                  | -9.18                         |
| DP2      | 2-OCH <sub>3</sub> | 4-OH               | -9.32                         |
| DP3      | 2-OCH <sub>3</sub> | 4-CH <sub>3</sub>  | -8.68                         |
| DP4      | 2-OCH <sub>3</sub> | 4-OCH <sub>3</sub> | -8.23                         |
| DP5      | 2-OCH <sub>3</sub> | 4-Cl               | -8.62                         |
| DP6      | 2-OCH <sub>3</sub> | 4-Br               | -8.86                         |
| DP7      | 2-OCH <sub>3</sub> | 4-CF <sub>3</sub>  | -9.16                         |
| DP8      | 2-OCH <sub>3</sub> | 4-NH <sub>2</sub>  | -9.32                         |
| DP9      | 2-OCH <sub>3</sub> | 4-Cl               | -8.22                         |
| DP10     | 2-OCH <sub>3</sub> | 4-F                | -9.32                         |
| DP11     | H                  | H                  | -8.11                         |
| DP12     | H                  | 4-OCH <sub>3</sub> | -9.78                         |
| DP13     | H                  | 4-Br               | -8.12                         |
| DP14     | H                  | 4-CH <sub>3</sub>  | -8.46                         |
| DP15     | H                  | 4-Cl               | -7.92                         |
| DP16     | H                  | 4-F                | -7.36                         |
| DP17     | H                  | 4-CF <sub>3</sub>  | -7.42                         |
| DP18     | H                  | 4-Cl               | -10.78                        |
| DP19     | H                  | 4-OH               | -9.98                         |
| DP20     | H                  | 4-NO <sub>2</sub>  | -11.08                        |
| DP21     | 2-F                | 4-OH               | -7.32                         |
| DP22     | 2-F                | 4-CH <sub>3</sub>  | -7.58                         |
| DP23     | 2-F                | 4-OCH <sub>3</sub> | -7.12                         |
| DP24     | 2-F                | 4-Cl               | -7.16                         |
| DP25     | 2-F                | 4-NH <sub>2</sub>  | -7.62                         |
| DP26     | 2-F                | 4-F                | -10.28                        |
| DP27     | 2-Cl               | 4-Cl               | -10.86                        |
| DP28     | 2-Cl               | 4-NO <sub>2</sub>  | -11.54                        |
| DP29     | 2-Cl               | 4-OCH <sub>3</sub> | -8.56                         |
| DP 30    | 2-Cl               | 4-CH <sub>3</sub>  | -8.14                         |
| DP 31    | 2-Cl               | 4-F                | -8.31                         |
| DP32     | 2-OH               | 4-CH <sub>3</sub>  | -12.68                        |
| DP33     | 2-OH               | 4-OH               | -9.47                         |
| DP34     | 2-OH               | 4-CH <sub>3</sub>  | -8.81                         |

|            |                               |                                      |        |
|------------|-------------------------------|--------------------------------------|--------|
| DP35       | 2-OH                          | 4-OCH <sub>3</sub>                   | -8.67  |
| DP36       | 2-OH                          | 4-Cl                                 | -8.08  |
| DP37       | 2-OH                          | 4-F                                  | -8.18  |
| DP38       | 2-OH                          | 4-Br                                 | -8.38  |
| DP39       | 2-NO <sub>2</sub>             | 4-OH                                 | -8.96  |
| DP40       | 2-NO <sub>2</sub>             | 4-CH <sub>3</sub>                    | -9.08  |
| DP41       | 2-NO <sub>2</sub>             | 4-OCH <sub>3</sub>                   | -9.17  |
| DP42       | 2-NO <sub>2</sub>             | 4-Cl                                 | -9.36  |
| DP43       | 2-NO <sub>2</sub>             | 4-F                                  | -8.08  |
| DP44       | 2-NO <sub>2</sub>             | 4-NH <sub>2</sub>                    | -8.78  |
| DP45       | 2-Br                          | 4-OH                                 | -8.77  |
| DP46       | 2-Br                          | 4-CH <sub>3</sub>                    | -8.12  |
| DP47       | 2-Br                          | 4-OCH <sub>3</sub>                   | -8.56  |
| DP48       | 2-Br                          | 4-Cl                                 | -9.02  |
| DP49       | 2-Br                          | 4-F                                  | -8.78  |
| DP50       | 2-Br                          | 4-Br                                 | -8.24  |
| DP51       | C <sub>6</sub> H <sub>5</sub> | H                                    | -6.78  |
| DP52       | C <sub>6</sub> H <sub>5</sub> | 4-CH <sub>3</sub>                    | -6.98  |
| DP53       | C <sub>6</sub> H <sub>5</sub> | 4-F                                  | -7.42  |
| DP54       | C <sub>6</sub> H <sub>5</sub> | 4-CF <sub>3</sub>                    | -7.56  |
| DP55       | C <sub>6</sub> H <sub>5</sub> | 4,5-(CH <sub>3</sub> ) <sub>2</sub>  | -7.96  |
| DP56       | 2-NH <sub>2</sub>             | 4-NH <sub>2</sub>                    | -9.68  |
| DP57       | 2-NH <sub>2</sub>             | 3,4-(OCH <sub>3</sub> ) <sub>2</sub> | -7.98  |
| DP58       | 2-NH <sub>2</sub>             | 4-Cl                                 | -9.92  |
| DP59       | 2-NH <sub>2</sub>             | 4-Br                                 | -6.88  |
| DP60       | 2-NH <sub>2</sub>             | 4-NO <sub>2</sub>                    | -6.78  |
| DP61       | 2-CH <sub>3</sub>             | 4-CH <sub>3</sub>                    | -9.76  |
| DP62       | 2-CH <sub>3</sub>             | 4-CF <sub>3</sub>                    | -6.98  |
| DP63       | 2-CH <sub>3</sub>             | 4-NH <sub>2</sub>                    | -10.64 |
| DP64       | 2-CH <sub>3</sub>             | 4-NO <sub>2</sub>                    | -6.96  |
| DP65       | 2-CH <sub>3</sub>             | 4-F                                  | -7.08  |
| DP66       | 2-CH <sub>3</sub>             | 4-OH                                 | -7.22  |
| DP67       | 2-CH <sub>3</sub>             | 3,4-OCH <sub>3</sub>                 | -6.58  |
| DP68       | 2-Cl                          | 4-Br                                 | -7.16  |
| DP69       | 2-Cl                          | 4-CF <sub>3</sub>                    | -7.12  |
| DP70       | 2-Cl                          | 4-NH <sub>2</sub>                    | -7.18  |
| DP71       | 2-NH <sub>2</sub>             | 4-F                                  | -6.92  |
| DP72       | 2-NH <sub>2</sub>             | 4-CF <sub>3</sub>                    | -8.08  |
| DP73       | 2-NH <sub>2</sub>             | 4-CH <sub>3</sub>                    | -7.11  |
| DP74       | 2-NH <sub>2</sub>             | 4-Br                                 | -7.78  |
| DP75       | 2-NH <sub>2</sub>             | 4-OCH <sub>3</sub>                   | -6.42  |
| Exemestane |                               |                                      | -11.24 |

Various interactions displayed by the best twelve hybrid molecules have been displayed in Table 4.13 along with the distances. Among these, 2D and 3D binding

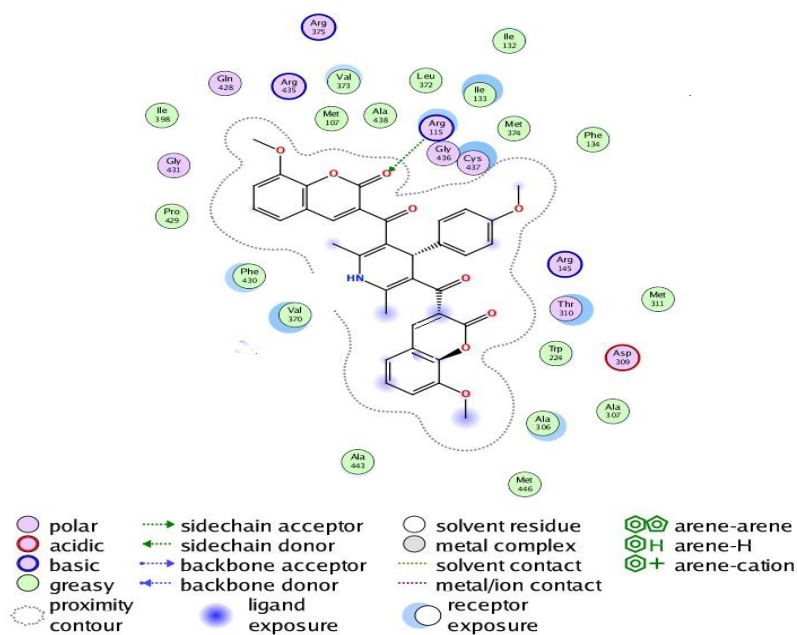
patterns of six hybrid compounds have been depicted in Figures 4.28 to 4.34 whereas binding patterns of exemestane have been depicted in Figure 4.35. The main amino acid residue involved in interactions were CYS437, Ala438, Arg115, Gly439, Thr310, Met311, Pro429, Trp141, and Arg435. It was evident that the best compounds revealed almost similar binding patterns as the standard drug exemestane. The main types of interactions involved in binding were hydrogen bonding, Arene-H and side chain acceptor interactions.

**Table 4.13: Interactions of best twelve screened Compounds**

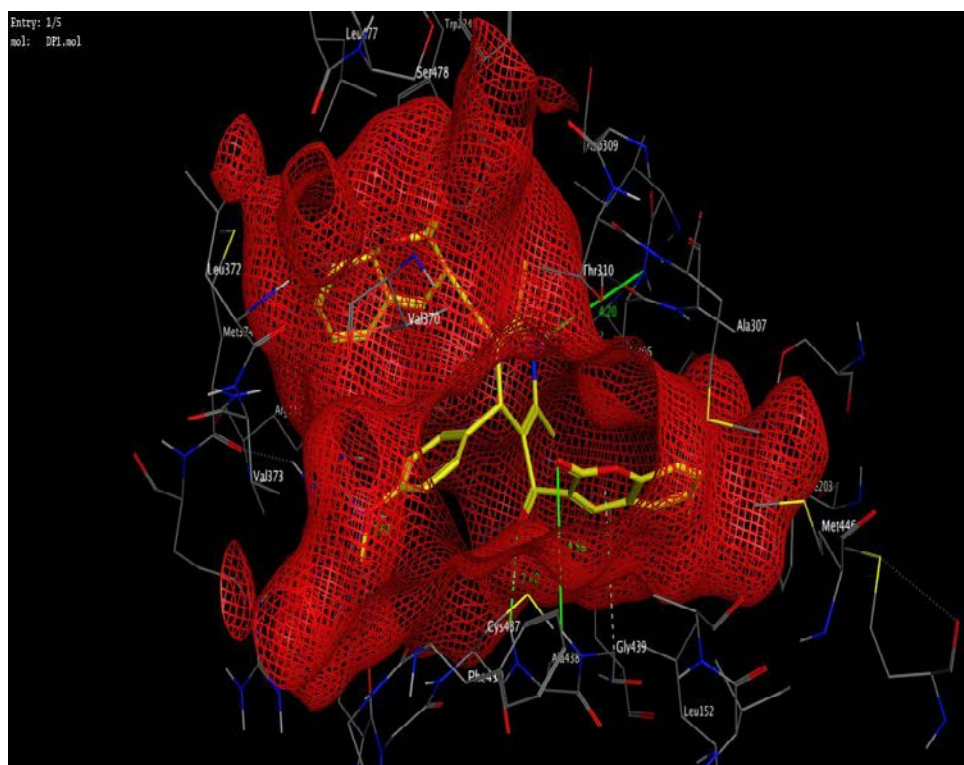
| Compound | Docking Scores | Type of interactions and distances  |
|----------|----------------|---|
| DP12     | -9.78          | Gly439(Arene-H interaction), Ala438(H-bond with =O; 2.48Å), Gly439(H-bond with =O; 4.98Å), Ala306(H-bond with =O; 4.20Å), Arg115(H-bond with -O; 2.48Å) |
| DP18     | -10.78         | Trp141(Cl-H interaction; 2.40Å), Ala438(H-bond with =O; 2.43Å), Gly439(H-bond with =O; 2.78Å), Thr210(H-bond with -O; 4.15Å)                            |
| DP19     | -9.98          | Cys437( Side chain interactions at 4.32Å), Cys 4357(H-bond with -N; 3.77Å), Thr310(H-bond with =O; 2.52Å)   |
| DP20     | -11.08         | Trp141(H-bond with =O; 2.60Å), Ala436(H-bond with =O; 3.57Å), Arg115(H-bond with -O; 1.90Å), Arg435(H-bond with -O; 2.26Å)                              |
| DP26     | -10.26         | Cys437( Side chain interactions at 3.55Å), Met107( Side chain interactions at 4.26Å), Thr310(H-bond with -NH; 4.64Å), Ala443(H-bond with =O; 4.14Å),    |
| DP27     | -10.86         | Met 311(H-bond with =O; 3.93Å), Met303 & Cys437(Two Side chain interactions at 3.41Å and 3.53Å), Ala 307(H-bond with -O; 3.88Å)                         |
| DP28     | -11.54         | Met 311(H-bond with =O; 3.28Å), Cys437(Two Side chain interactions at 3.50Å and 3.93Å), Pro 429(H-bond with -N; 1.97Å)                                  |

|            |        |  |
|------------|--------|--|
| DP32       | -12.68 | Ile 133(H-bond with =O; 3.66Å), Arg 435(H-bond with -N; 2.24Å), Ala438(H-bond with =O; 1.93Å), Phe 430(Arene-H interaction)                |
| DP56       | -9.68  | Leu372(H bond with -NH; 2.26Å), Leu477(H bond with -NH; 2.16Å), Thr310(H bond with =O; 3.16Å), Arg115(H bond with =O; 3.67Å)               |
| DP58       | -9.92  | Thr310(H bond with =O; 3.26Å), Arg115(H bond with =O; 3.61Å), Pro 429(H-bond with -N; 2.97Å)   |
| DP61       | -9.76  | Gly439(Arene-H interaction), Pro429(H bond with -NH; 2.47Å), Met311(Side chain acceptor interaction, 3.65Å), Gly436(H bond with =O, 3.62Å) |
| DP63       | -10.64 | Ala438(H bond with =O, 2.06Å), Gly439(H bond with =O, 2.74Å), , Leu477(H bond with -NH; 2.76Å),  |
| Exemestane | -11.28 | Met374(H bond with =O; 1.97Å), Arg115(H bond with =O; 2.63Å), Ala306(H bond with =O; 4.40Å)  |

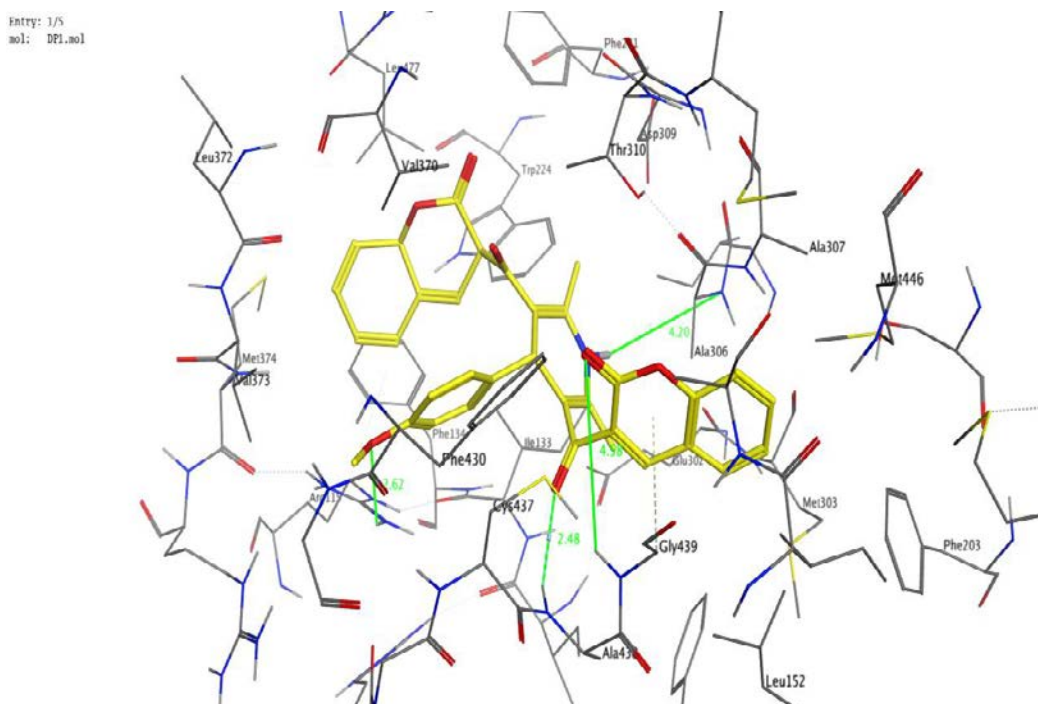
### Compound DP12



(a)



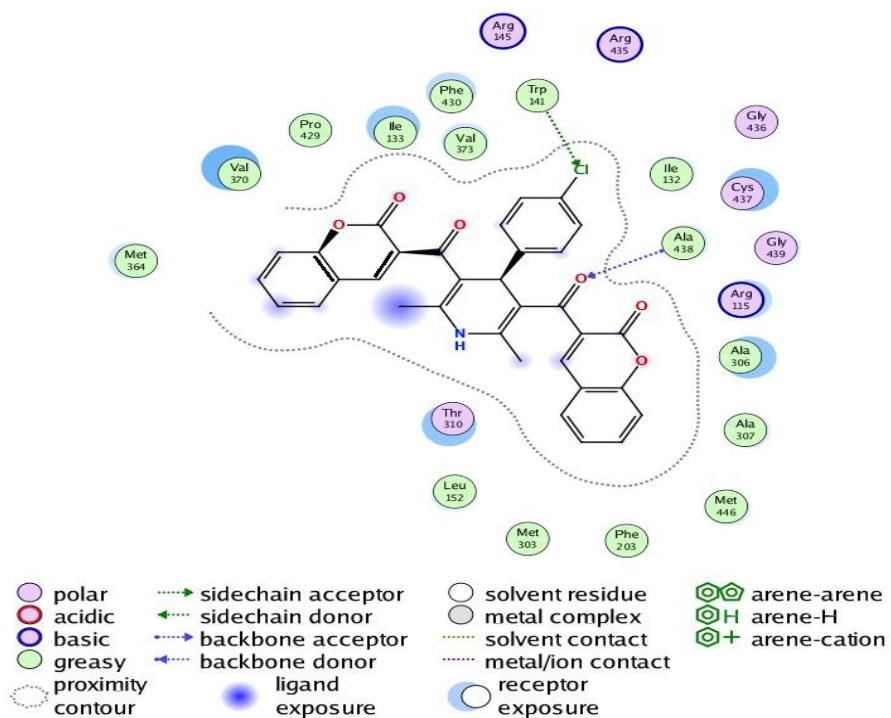
(b)



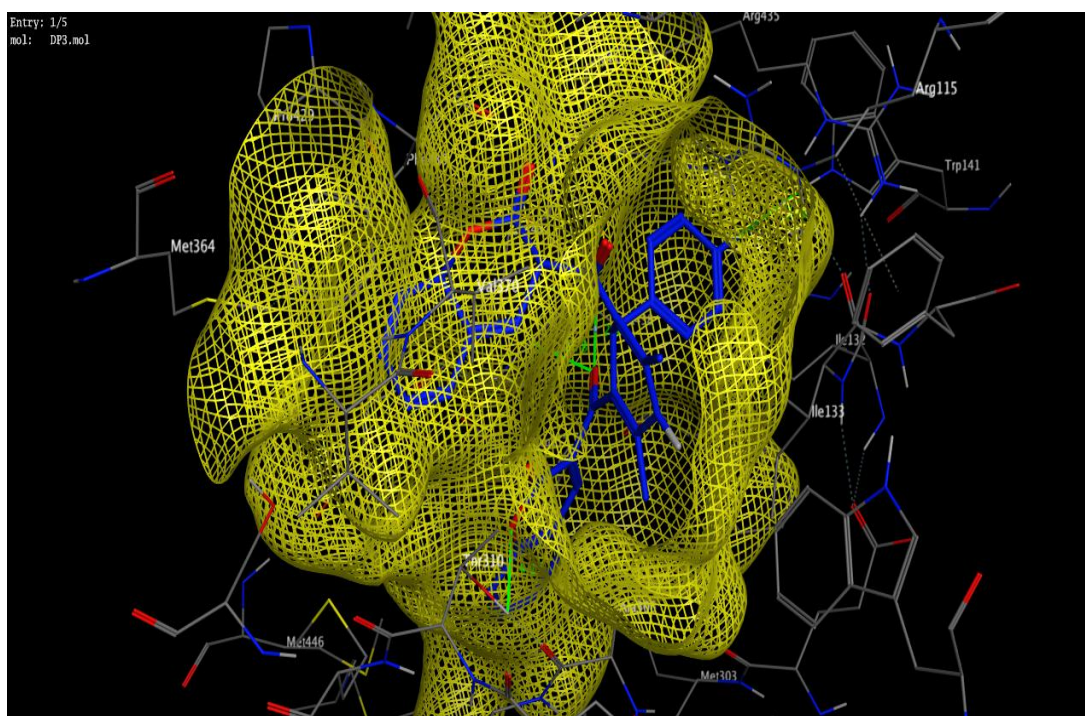
(c)

**Figure 4.28: Interaction poses of DP12 with aromatase (a) 2D interactions (b) DP12 embedded in receptor pocket (c) Interactions along with distances**

## Compound DP18

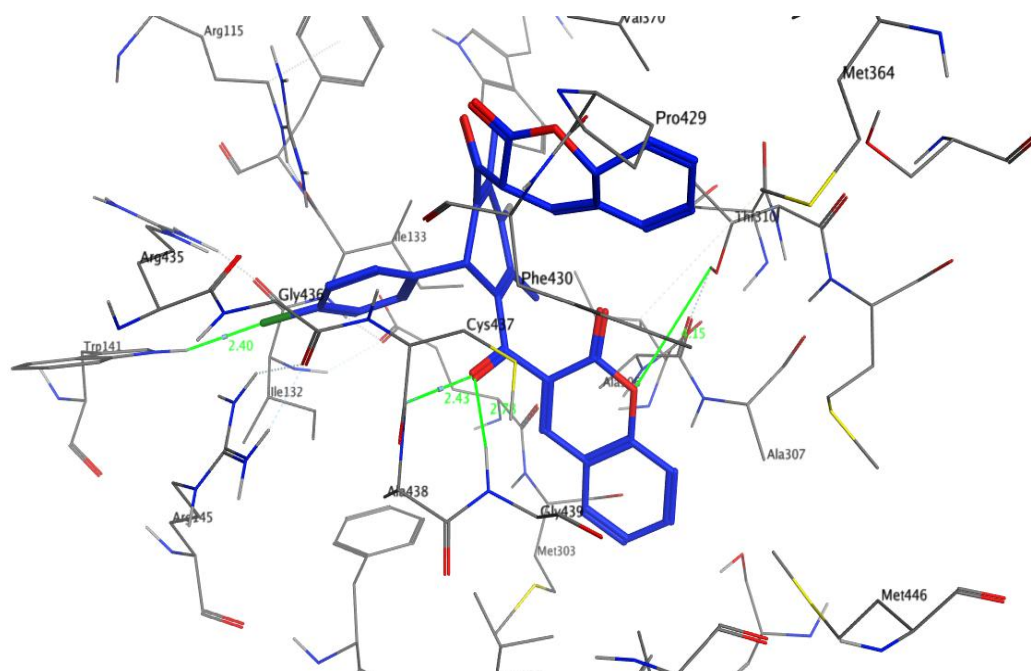


(a)



(b)

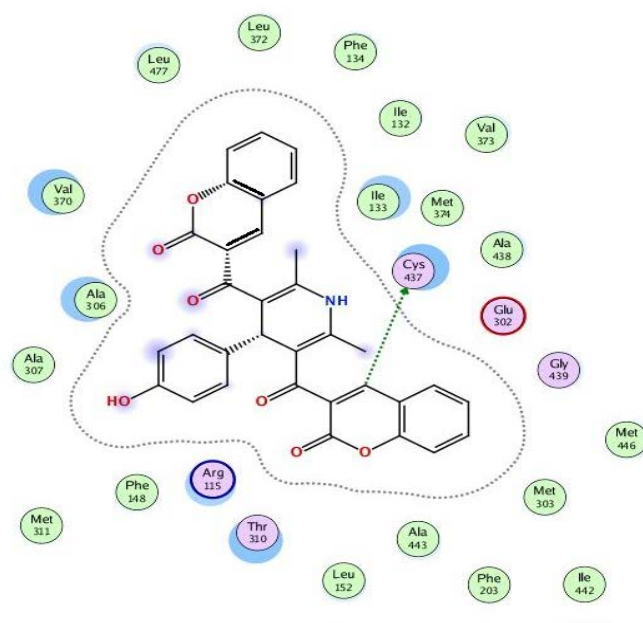
Entry: 1/5  
mol: DP3.mol



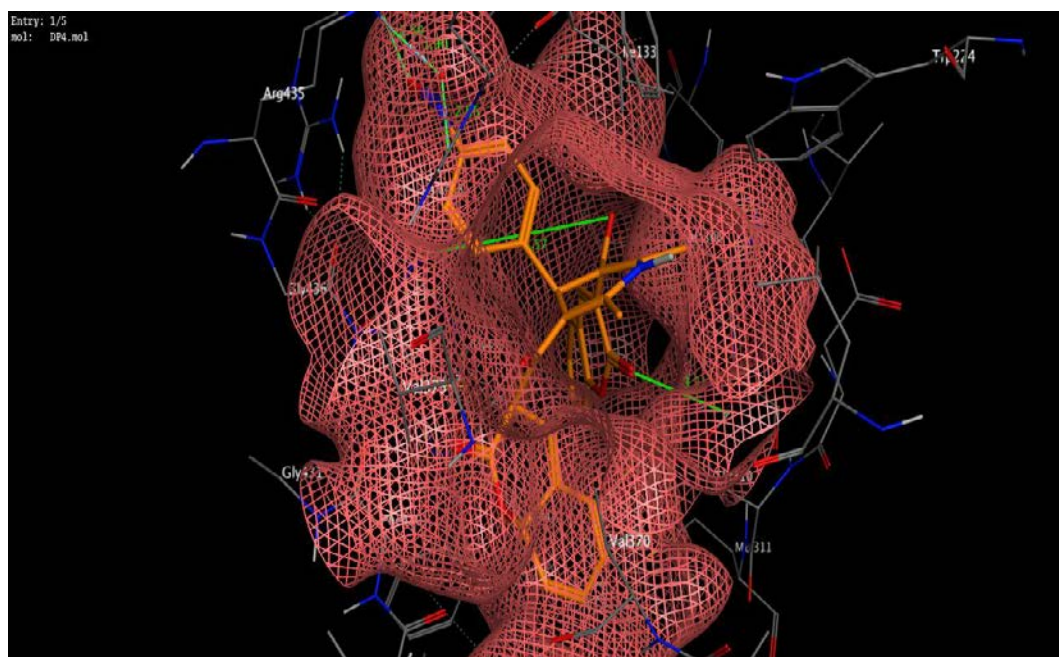
(c)

**Figure 4.29:** Interaction poses of DP18 with aromatase (a) 2D interactions (b) DP18 embedded in receptor pocket (c) Interactions along with distances

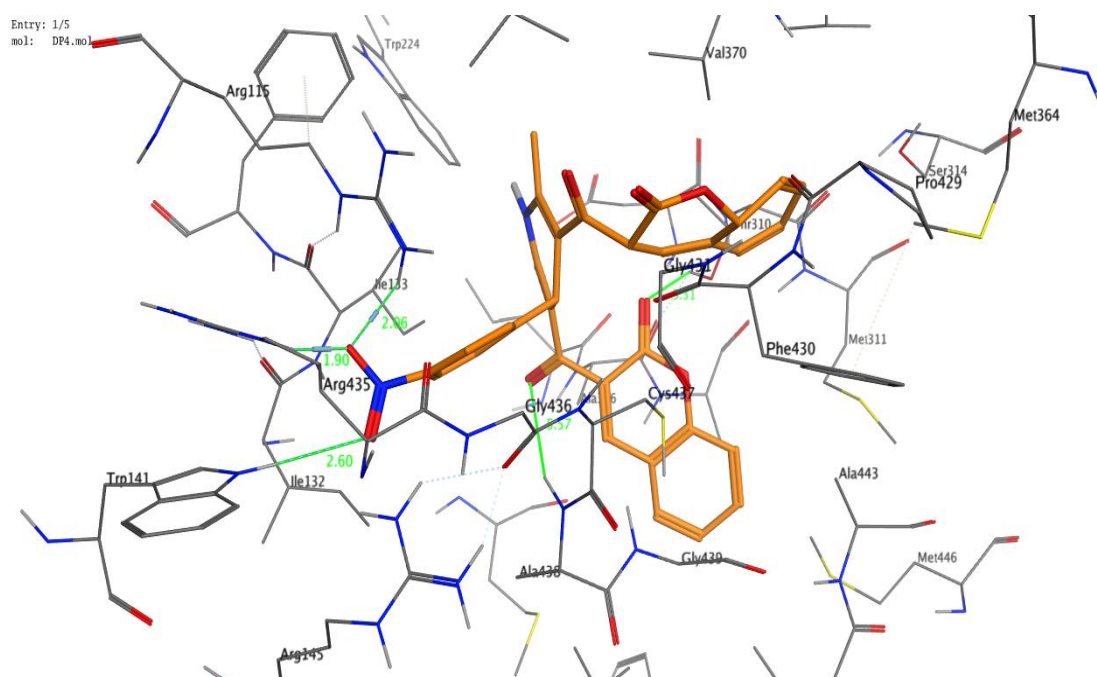
### Compound DP20



(a)



(b)

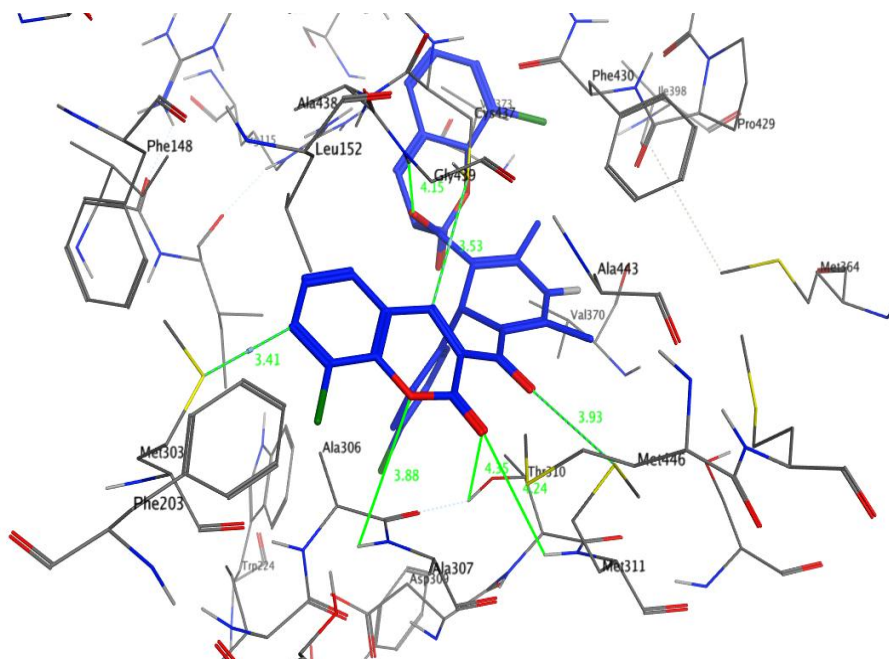


(c)

**Figure 4.30: Interaction poses of DP20 with aromatase (a) 2D interactions (b) DP20 embedded in receptor pocket (c) Interactions along with distances**



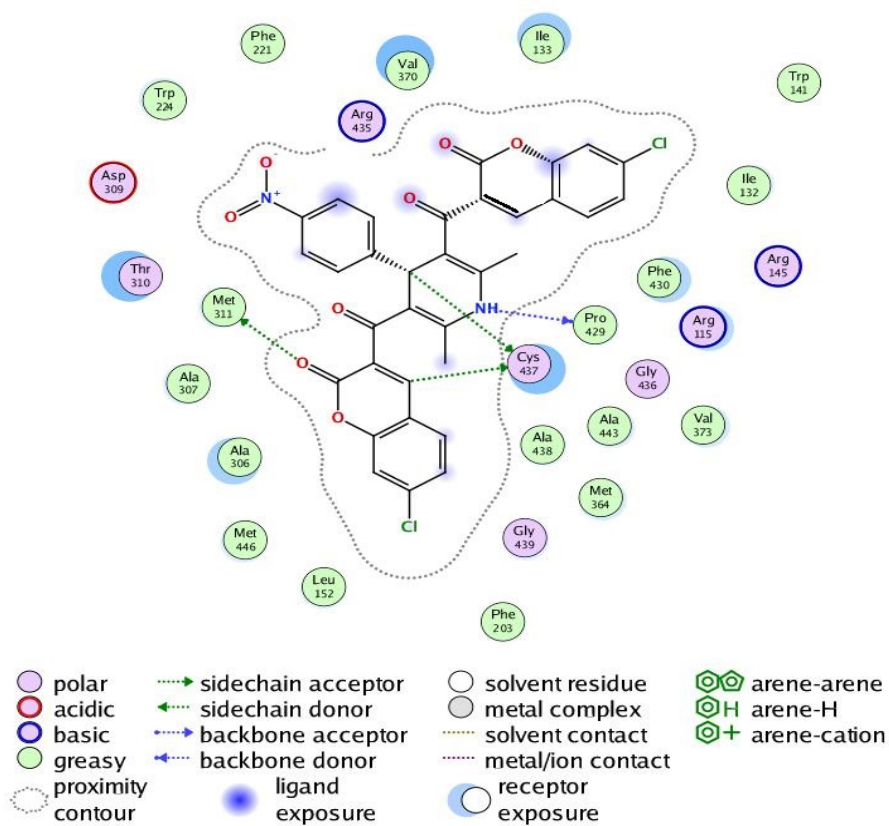
Entry: 1/5  
mol: DP6.mol



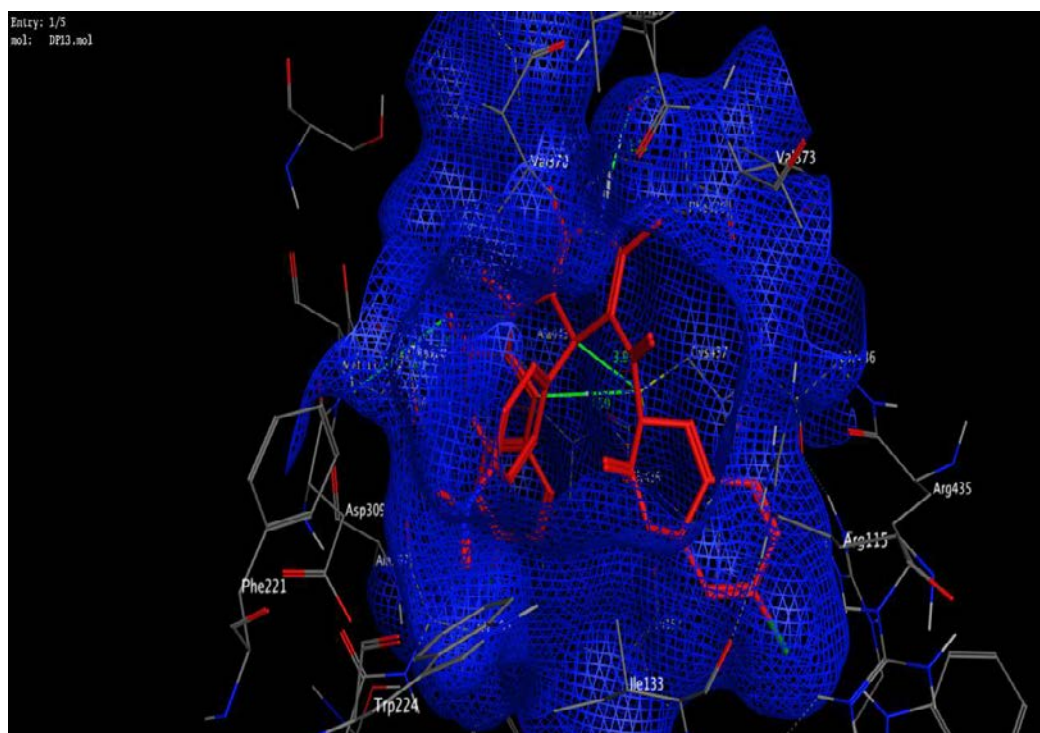
(c)

Figure 4.31: Interaction poses of DP27 with aromatase (a) 2D interactions (b) DP27 embedded in receptor pocket (c) Interactions along with distances

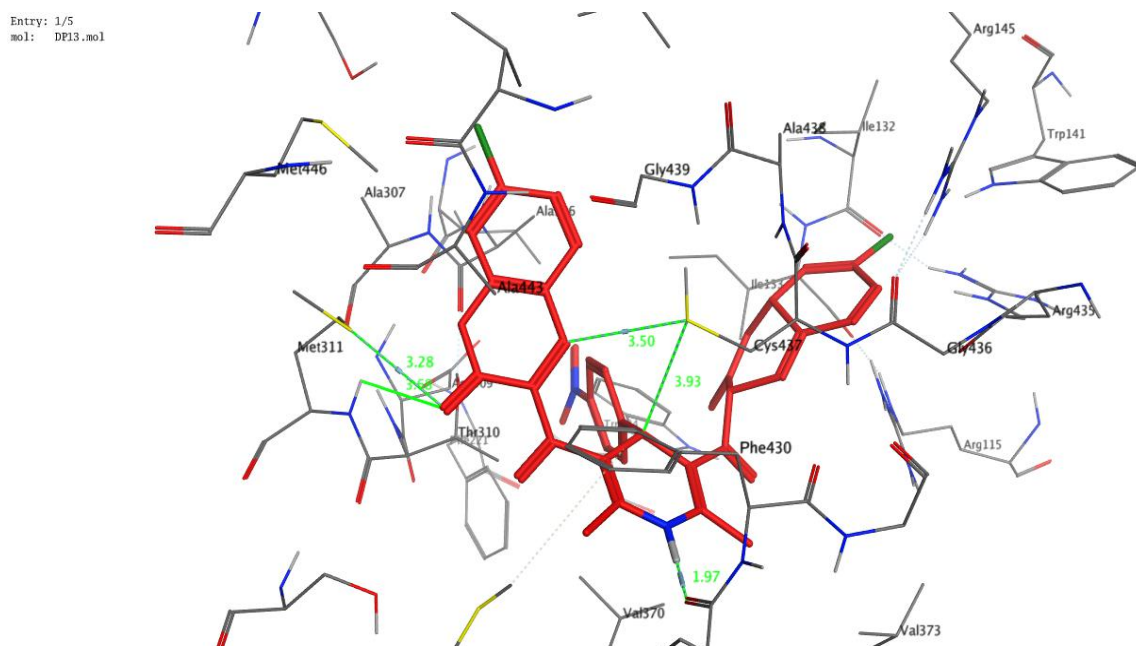
Compound DP28



(a)



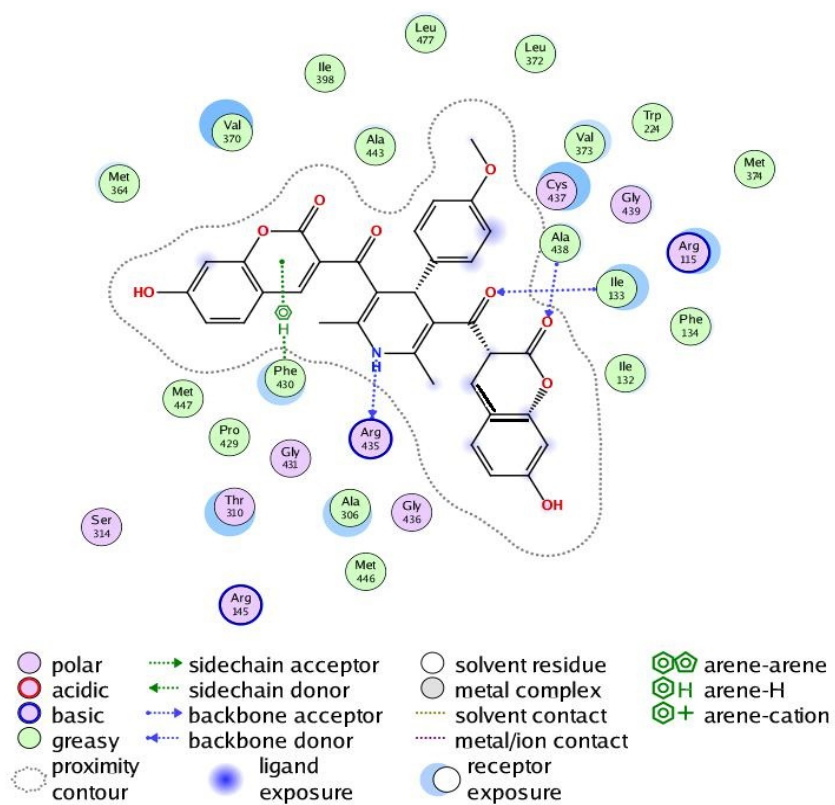
(b)



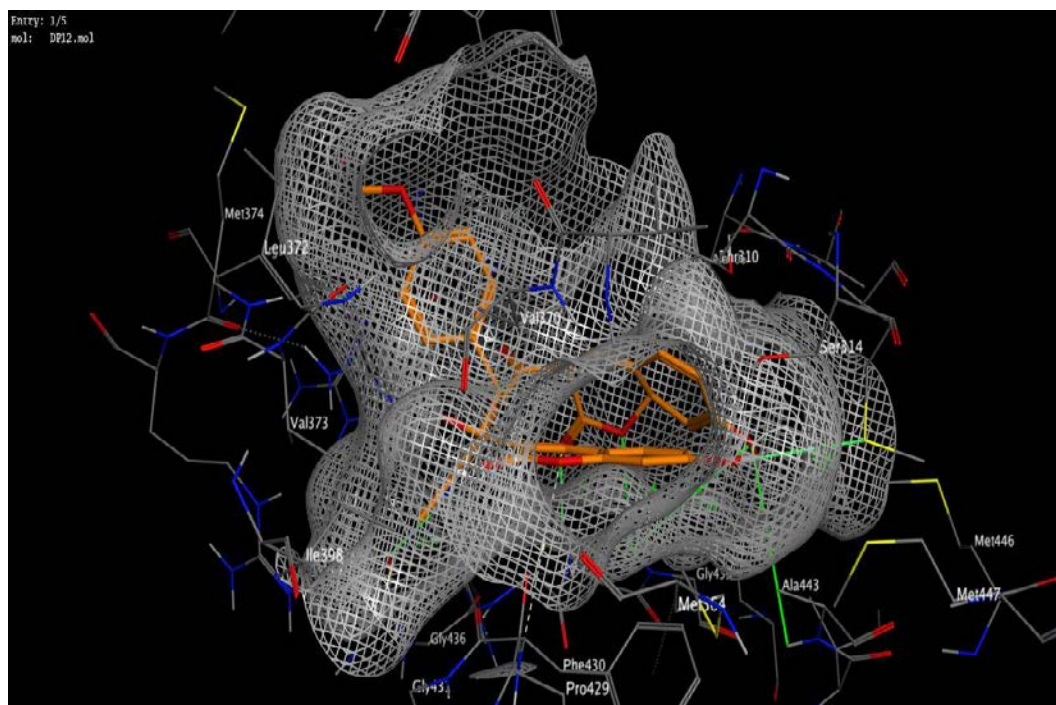
(c)

**Figure 4.32:** Interaction poses of DP28 with aromatase (a) 2D interactions (b) DP28 embedded in receptor pocket (c) Interactions along with distances

## Compound DP32

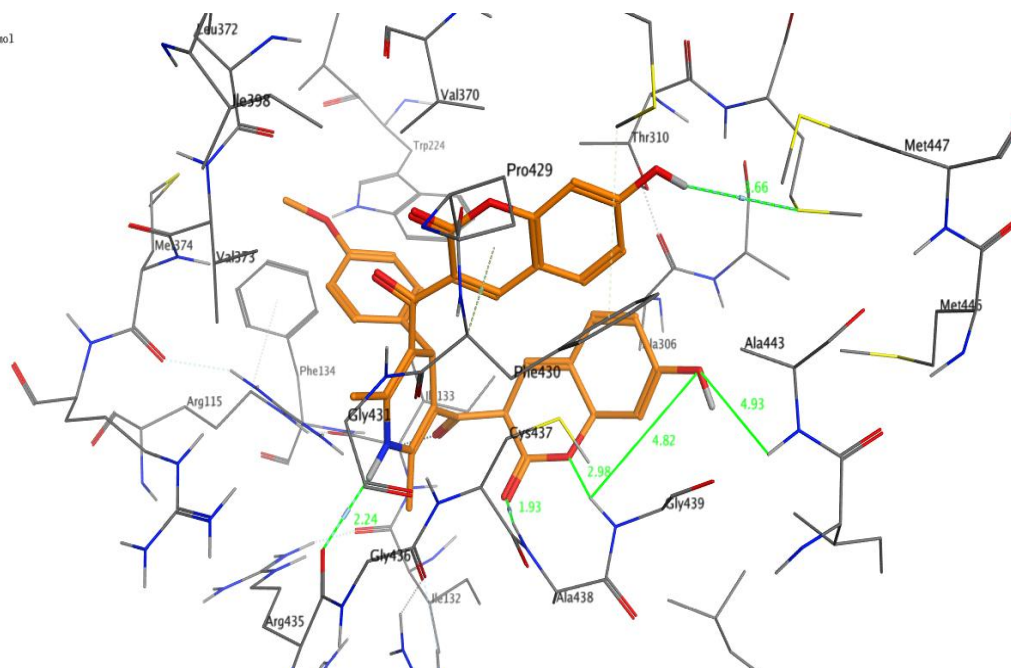


(a)



(b)

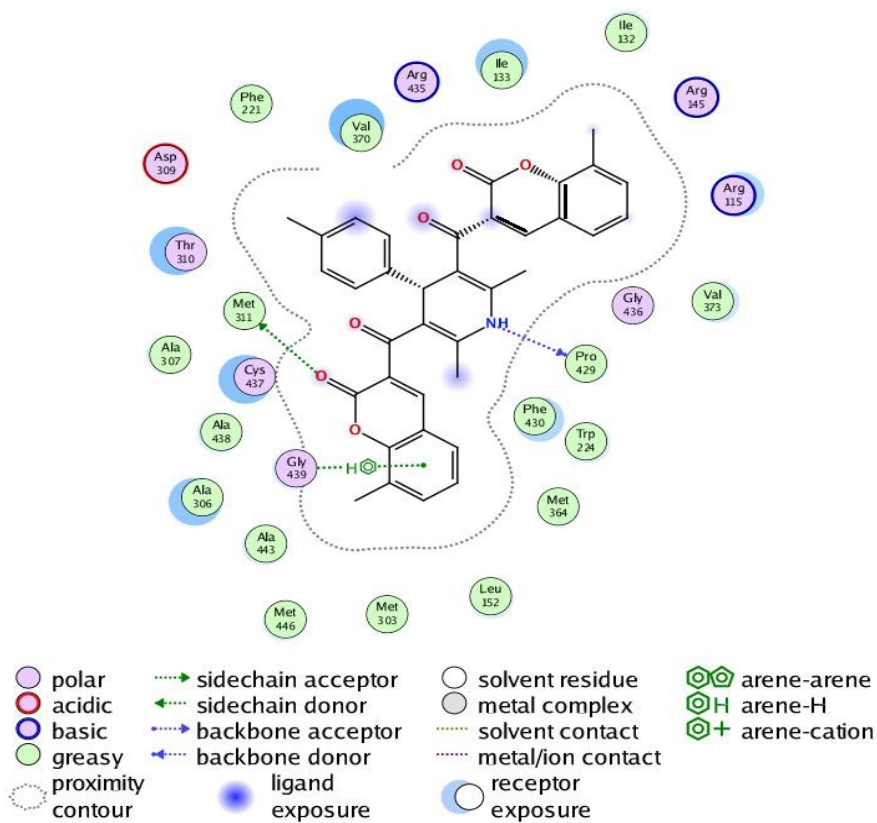
Entry: 1/5  
mol: DP12.mol



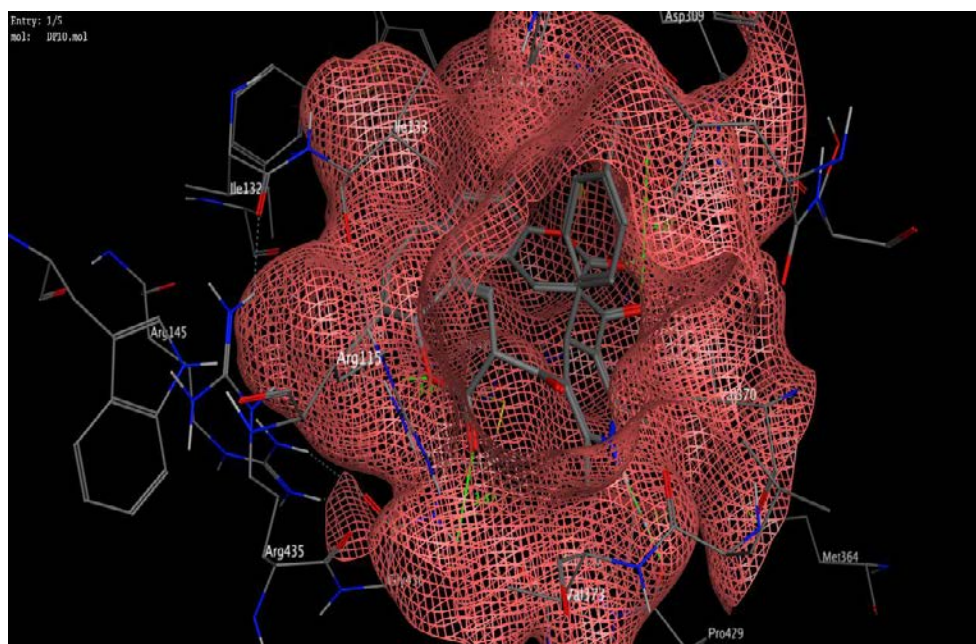
(c)

Figure 4.33: Interaction poses of DP32 with aromatase (a) 2D interactions (b) DP32 embedded in receptor pocket (c) Interactions along with distances

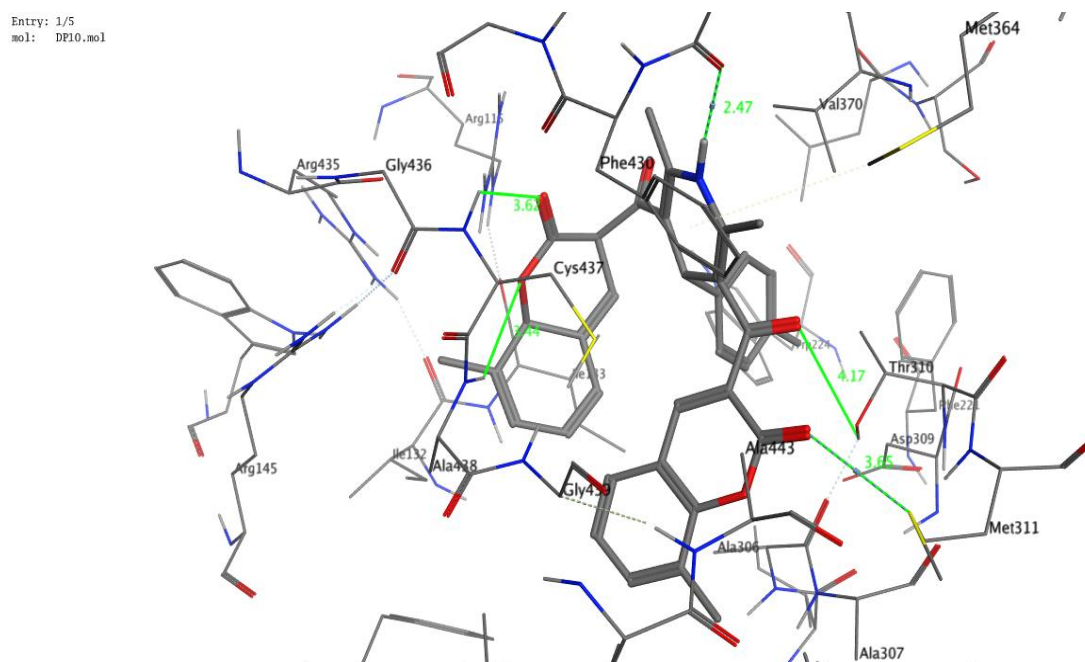
### Compound DP61



(a)



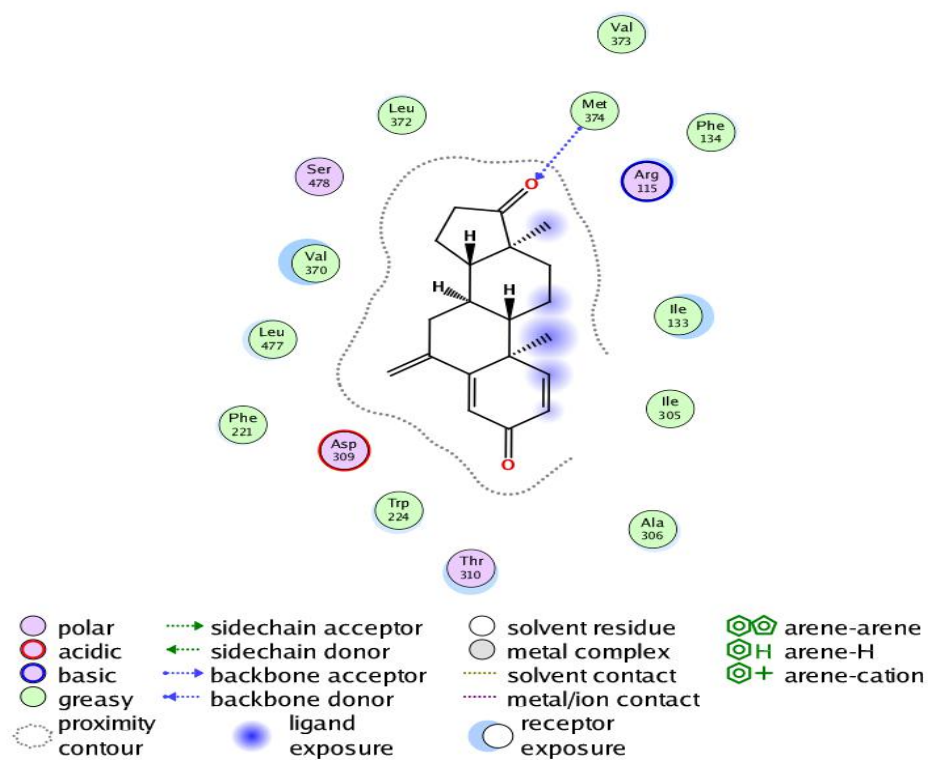
(b)



(c)

**Figure 4.34: Interaction poses of DP61 with aromatase (a) 2D interactions (b) DP61 embedded in receptor pocket (c) Interactions along with distances**

## Exemestane



Entry: 1/5  
mol: Exe.mol

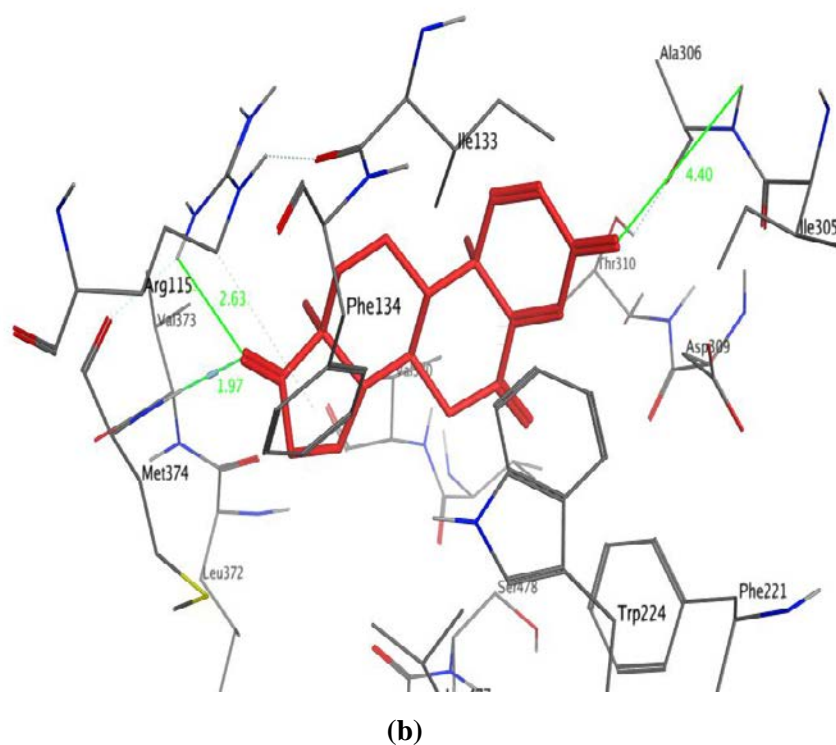


**Figure 4.35: Interaction poses of Exemestane with aromatase (a) 2D interactions (b) Interactions along with distances**

#### 4.1.10 Drug likeliness prediction of coumarin-dihydropyridine hybrids

Drug likeliness prediction is a promising approach to get an idea about drug like properties of designed molecules. These properties are important to predict the bioavailability of drugs and medicinal chemist can modify the factors affecting it accordingly. Drug likeliness features of best twelve compounds were predicting by using Swiss ADME predictor. Percentage absorption (% ABS) was calculated by using formula  $\%ABS = 109 - (0.345 \times TPSA)$ . The designed potent analogues displayed good absorption in the range of 58.5-72.8%. Results evidenced that designed potent analogues showed only one violation of Lipinski's Rule of Five as represented in Table 4.14. The molecular weights of the designed hybrid molecules were found higher than 500. But, violation of molecular weight does not makes any commitment about the fact that the molecules will not behave like drug. There several antibiotic drugs and compounds from natural origins whose molecular weights are greater than 500. Hence it can be postulated that the designed molecules may serve as drug like candidates.

**Table 4.14: *In silico* drug like properties of best twelve designed hybrids**

| Compound    | TPSA <sup>a</sup> | MW <sup>b</sup> | RoB <sup>c</sup> | HBD <sup>d</sup> | HBA <sup>e</sup> | IlogP (MlogP) <sup>f</sup> | logS <sup>g</sup> | % ABS <sup>h</sup> |
|-------------|-------------------|-----------------|------------------|------------------|------------------|----------------------------|-------------------|--------------------|
| <b>Rule</b> | <b>≤140</b>       | <b>≤500</b>     | <b>≤10</b>       | <b>≤5</b>        | <b>≤10</b>       | <b>≤5</b>                  | <b>&gt;-4</b>     | <b>-</b>           |
| DP12        | 115.82            | 559.56          | 6                | 1                | 7                | 3.16                       | -7.09             | 69.39              |
| DP18        | 106.59            | 563.98          | 5                | 1                | 6                | 3.15                       | -7.60             | 72.22              |
| DP19        | 126.46            | 545.54          | 5                | 2                | 7                | 2.62                       | -6.87             | 65.41              |
| DP20        | 138.64            | 574.54          | 6                | 1                | 8                | 2.63                       | -7.08             | 61.41              |
| DP26        | 106.59            | 583.62          | 5                | 1                | 9                | 3.16                       | -7.34             | 72.22              |
| DP27        | 106.59            | 632.26          | 5                | 1                | 6                | 3.09                       | -8.07             | 72.22              |
| DP28        | 139.23            | 643.59          | 6                | 1                | 8                | 3.26                       | -7.68             | 60.39              |
| DP32        | 144.23            | 591.26          | 6                | 3                | 9                | 2.68                       | -6.82             | 59.24              |
| DP56        | 146.41            | 574.83          | 5                | 4                | 6                | 2.44                       | -5.96             | 58.48              |
| DP58        | 142.23            | 594.01          | 5                | 3                | 6                | 2.46                       | -6.91             | 59.93              |
| DP61        | 106.59            | 571.62          | 5                | 1                | 6                | 3.93                       | -7.92             | 72.22              |
| DP63        | 132.61            | 572.61          | 5                | 2                | 6                | 3.65                       | -7.27             | 63.24              |

Abbreviations:<sup>a</sup>Topological polar surface area; <sup>b</sup>Molecular weight; <sup>c</sup>Number of rotatable bonds; <sup>d</sup> Number of hydrogen bond donors; <sup>e</sup>Number of hydrogen bonds acceptors; <sup>f</sup>

Logarithm of compound partition coefficient between n-octanol and water; <sup>§</sup>Logarithm of water solubility; <sup>h</sup>Percentage absorption

#### 4.1.11 ADME prediction studies of coumarin-dihydropyrimidinone hybrids

*In silico* ADME properties of best twelve compounds were predict using preADMET tool version 2.0 software (preadmet.bmdrc.kr). The calculated values of absorption through various barriers were found within the standard limits for all the twelve compounds. Human intestinal absorption value greater than 80% suggests that the compound is well absorbed through intestine. Lower value of BBB from 0.14-0.90 reveals that the compound cannot cross the blood brain barrier. Caco2 value between 4 to 70 represents moderate absorption, greater than 70 suggests maximum absorption. The potent compounds with lower MDCK value indicate lower absorption towards kidney cells. Plasma protein binding greater than 85 indicates best distribution properties of potent compounds. The predicted data has been compiled in Table 4.15.

**Table 4.15: ADME properties of 12 predicted best compounds**

| Compound | HIA % | Caco-2(nm/sec) | MDCK  | BBB (log PS) <0.4 | Plasma protein binding (%) |
|----------|-------|----------------|-------|-------------------|----------------------------|
| DP12     | 96.43 | 25.77          | 0.044 | 0.36              | 96.43                      |
| DP18     | 96.27 | 22.95          | 0.044 | 0.17              | 94.43                      |
| DP19     | 95.12 | 23.58          | 0.042 | 0.034             | 87.78                      |
| DP20     | 98.36 | 18.88          | 0.043 | 0.032             | 93.99                      |
| DP26     | 96.26 | 25.00          | 0.043 | 0.11              | 95.32                      |
| DP27     | 97.32 | 24.19          | 0.55  | 0.16              | 100.00                     |
| DP28     | 97.46 | 18.11          | 0.042 | 0.03              | 99.12                      |
| DP32     | 94.11 | 20.77          | 0.043 | 0.069             | 89.14                      |
| DP56     | 95.72 | 21.56          | 0.31  | 0.47              | 90.25                      |
| DP58     | 95.21 | 20.84          | 0.043 | 0.062             | 95.69                      |
| DP61     | 92.55 | 21.06          | 0.091 | 0.09              | 88.73                      |
| DP63     | 96.43 | 21.61          | 1.53  | 0.043             | 88.72                      |

#### 4.1.12 *In silico* toxicity studies of coumarin-dihydropyrimidone hybrids

A preliminary idea about the toxicity of a designed molecule is of utmost importance as it may be helpful to prevent the failure of it during clinical stages. The *in silico* toxicity prediction was carried out by PreADME and PROTOX softwares. Prottox suggested that designed compounds lie in Class 4 and 5 with LD50 value >900 mg/kg which is much higher dose to be toxic. Carcino-Mouse and Carcino-Rat toxicity test were found positive suggesting that there is no evidence of carcinogenic toxicity. Medium risk for hERG inhibition evidenced that designed analogues have minimum risk on cardiac action potential. The predicted data have been presented in Table 4.16. From the data, it can be concluded that the designed molecules are safe to be used as a drug.

**Table 4.16: *In silico* toxicity results for best 12 hybrid compounds**

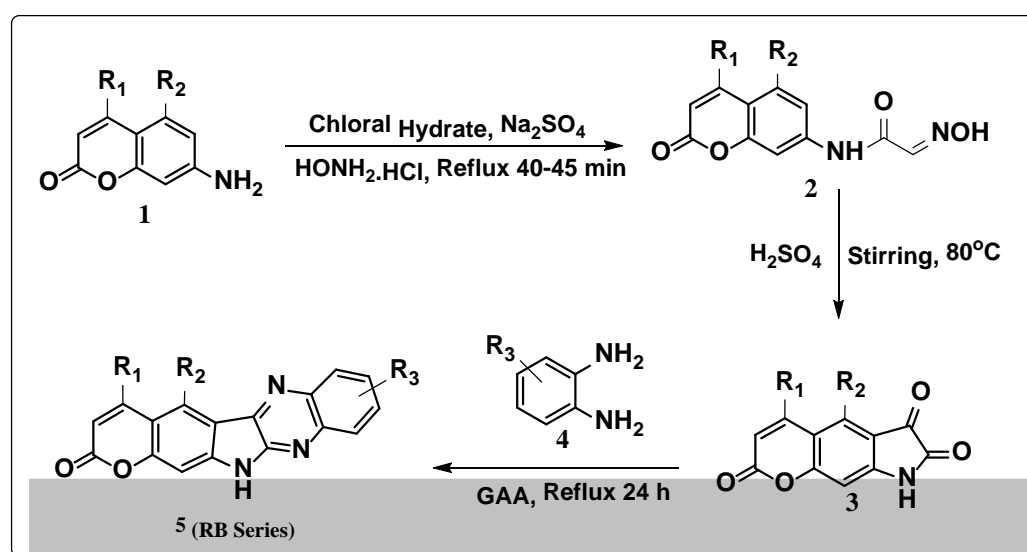
| Compound | Carcino-Mouse | Carcino-Rat | HERG-inhibition | Prottox Predicted LD50 | Prottox Predicted Class |
|----------|---------------|-------------|-----------------|------------------------|-------------------------|
| DP12     | Positive      | Positive    | Medium risk     | 3000 mg/kg             | Class 5                 |
| DP18     | Positive      | Positive    | Medium risk     | 1350 mg/kg             | Class 4                 |
| DP19     | Positive      | Positive    | Medium risk     | 3200 mg/kg             | Class 5                 |
| DP20     | Positive      | Positive    | Medium risk     | 1150 mg/kg             | Class 4                 |
| DP26     | Positive      | Positive    | Medium risk     | 1120 mg/kg             | Class 4                 |
| DP27     | Positive      | Positive    | Medium risk     | 1350 mg/kg             | Class 4                 |
| DP28     | Positive      | Positive    | Medium risk     | 1920 mg/kg             | Class 5                 |
| DP32     | Positive      | Positive    | Medium risk     | 3000 mg/kg             | Class 5                 |
| DP56     | Positive      | Positive    | Medium risk     | 1200 mg/kg             | Class 4                 |
| DP58     | Positive      | Positive    | Medium risk     | 1350 mg/kg             | Class 4                 |
| DP61     | Positive      | Positive    | Medium risk     | 2050 mg/kg             | Class 5                 |
| DP63     | Positive      | Positive    | Medium risk     | 3000 mg/kg             | Class 5                 |

## 4.2 Synthesis

### 4.2.1 Synthesis of coumarin-quinoxaline hybrids

The synthesis of coumarin-quinoxaline hybrids involved a three steps process. The first step was formation of an isonitroso acetanilide intermediate **2** which was formed

by reaction of substituted 7-amino coumarin **1** with chloral hydrate in the presence of hydroxylamine hydrate. This intermediate was then cyclised to isatin **3** derivatives by following the classic Sandmeyer cyclization (Silva *et al.*, 2013). These isatin derivatives were further made to react with various substituted ethylene diamine derivatives **4** in the presence of glacial acetic acid to yield coumarin-quinoxaline derivatives **5** (**RB13-14**, **RB16-19**, **RB36-37**, **RB86-89**) (Avula *et al.*, 2013). The whole synthetic process has been outlined in Scheme 1 and physical characterization is given in Table 4.17. All the synthesized compounds were purified by recrystallization and characterized spectroscopically by modern analytical techniques.



Scheme 1. Synthetic route for coumarin-quinoxaline hybrids

Table 4.17: Physical characterization of coumarin-quinoxaline hybrid molecules

| Compound | R <sub>1</sub>                | R <sub>2</sub> | R <sub>3</sub>                       | % Yield | Melting Point |
|----------|-------------------------------|----------------|--------------------------------------|---------|---------------|
| RB13     | CH <sub>3</sub>               | H              | 4-F                                  | 78      | 288-290 °C    |
| RB14     | CH <sub>3</sub>               | H              | 4-CF <sub>3</sub>                    | 66      | 268-270 °C    |
| RB16     | CH <sub>3</sub>               | H              | 3-OCH <sub>3</sub>                   | 72      | 298-301 °C    |
| RB17     | CH <sub>3</sub>               | H              | 3,4-(OCH <sub>3</sub> ) <sub>2</sub> | 66      | 298-301 °C    |
| RB18     | CH <sub>3</sub>               | H              | 4-Cl                                 | 78      | 278-280 °C    |
| RB19     | CH <sub>3</sub>               | H              | 4-Br                                 | 76      | 271-273 °C    |
| RB36     | C <sub>6</sub> H <sub>5</sub> | H              | 3-OCH <sub>3</sub>                   | 56      | 281-283 °C    |
| RB37     | C <sub>6</sub> H <sub>5</sub> | H              | 3,4-(OCH <sub>3</sub> ) <sub>2</sub> | 58      | 278-281 °C    |

|      |    |                  |                                      |    |            |
|------|----|------------------|--------------------------------------|----|------------|
| RB86 | OH | OCH <sub>3</sub> | 3-OCH <sub>3</sub>                   | 62 | 308-310 °C |
| RB87 | OH | OCH <sub>3</sub> | 3,4-(OCH <sub>3</sub> ) <sub>2</sub> | 65 | 308-310 °C |
| RB88 | OH | OCH <sub>3</sub> | 4-Cl                                 | 68 | 265-267 °C |
| RB89 | OH | OCH <sub>3</sub> | 4-Br                                 | 72 | 266-268 °C |

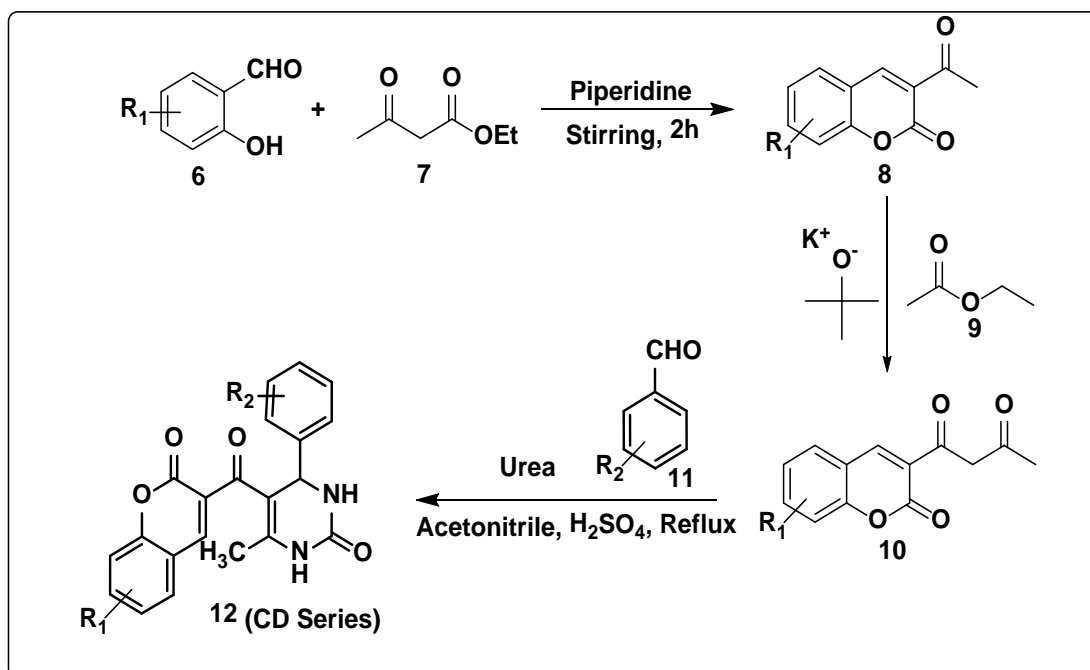
The structures of coumarin-quinoxaline hybrids were found to be novel and were determined by 2D NMR, IR and HRMS experiments. IR spectrum of the synthesized compounds showed bond at 3340-3367 for NH and 1020-1098 cm<sup>-1</sup> corresponds to C=N and C-O stretch respectively in the synthesized compounds. In <sup>1</sup>H-NMR spectra of compounds, appearance of singlet peak at  $\delta$  12.09-13.05 ppm, corresponds to the presence of NH group of pyrrolidine bridging coumarin and quinoxaline moieties, whereas the peak of proton in pyrone appeared as 6.17. In <sup>13</sup>C NMR spectra peak at 155.20-162.64 ppm confirmed the presence of C=O and C=N in the hybrid molecules. The mass peak of RB17 with m/z 332.0990 (calcd. m/z 332.0927 [M+H]<sup>+</sup>) was observed in high resolution mass spectra (HRMS) represents the given structures.

#### 4.2.2 Synthesis of coumarin-dihydropyrimidinone hybrids

The synthesis of coumarin-dihydropyrimidinone hybrids involved a three steps process. The first step was formation of 3-acetyl coumarin **8** which was formed by reaction of substituted salicylaldehydes **6** with ethyl acetoacetate **7** in the presence of piperdine (Vekariya *et al.*, 2017). This intermediate was then converted to 3-acetoacetyl coumarin derivative **10** by reacting with ethyl acetate **9** in the presence of potassium tertiary butoxide. In the final step this 3-acetoacetyl coumarin was condensed with various aromatic aldehydes **11** in the presence of urea and acetonitrile under acidic environment to yield the title compounds **12** (**CD6**, **CD8-10**, **CD19-20**, **CD28**, **CD32**, **CD42-44**, **CD49**) (Elmagharby *et al.*, 2013). The whole synthetic process has been outlined in Scheme 1. The mechanistic path to formulate this series of compounds is explained in Figure 4.36 and physical characterization is given in Table 4.18. All the synthesized compounds were purified by recrystallization and characterized spectroscopically by modern analytical techniques.

The structures of coumarin-dihydropyrimidinone hybrids were found to be novel and were determined by 2D NMR, IR and HRMS experiments. IR spectrum of the synthesized compounds showed prominent peaks at 3371(-NH), 3026(-CH), 1671(-

CN), 1758(-C=O), 1677(C=N), 1250(-CO) in the synthesized compounds. In  $^1\text{H}$ -NMR spectra of compounds, appearance of singlet peaks at  $\delta$  8.50-10.00 ppm, corresponds to the presence of two NH groups of dihydropyrimidinone moiety, whereas the peak of proton in pyrone appeared as 8.30-8.70. In  $^{13}\text{C}$  NMR spectra peak at 199.0 ppm confirmed the presence of C=O bridging the two moieties and at 150.0 ppm was confirming the C=O in the dihydropyrimidinone moiety. The mass peak of CD28 with  $m/z$  420.1088 (calcd.  $m/z$  488.1062  $[\text{M}+\text{H}]^+$ ) was observed in high resolution mass spectra (HRMS) represents the given structures.



### Scheme 2. Synthetic pathway for coumarin-dihydropyrimidinone hybrids

The plausible mechanism is supposed to be started with condensation between the aromatic aldehyde **a** and urea **b** to form a hydroxyl phenyl urea intermediate **c** which upon removal of a water molecule get converted to an iminium **d** intermediate. This iminium intermediate acted as an electrophile which provides platform for nucleophilic addition of di-enol derivative **e** to form another intermediate **f**. This intermediate upon release of water molecule gets cyclized into dihydropyrimidinone derivative **g** (Figure 4.36).

Table 4.18: Physical characterization of coumarin-dihydropyrimidinone hybrids

| Compound | R <sub>1</sub>     | R <sub>2</sub>     | % Yield | Melting point |
|----------|--------------------|--------------------|---------|---------------|
| CD6      | 2-OCH <sub>3</sub> | 4-OH               | 66      | 268-270 °C    |
| CD8      | 2-OCH <sub>3</sub> | 4-OCH <sub>3</sub> | 72      | 286-288 °C    |
| CD9      | 2-OCH <sub>3</sub> | 4-Cl               | 78      | 258-261 °C    |
| CD10     | 2-OCH <sub>3</sub> | 4-F                | 80      | 242-244 °C    |
| CD19     | 2-Cl               | 4-Cl               | 56      | 229-233 °C    |
| CD20     | 2-Cl               | 4-F                | 62      | 226-228 °C    |
| CD28     | 2-NO <sub>2</sub>  | 4-CH <sub>3</sub>  | 58      | 245-246 °C    |
| CD32     | 2-NO <sub>2</sub>  | 4-Br               | 76      | 263-265 °C    |
| CD42     | 2-CH <sub>3</sub>  | 4-Cl               | 74      | 265-267 °C    |
| CD43     | 2-CH <sub>3</sub>  | 4-F                | 78      | 241-243 °C    |
| CD44     | 2-CH <sub>3</sub>  | 4-NH <sub>2</sub>  | 62      | 230-232 °C    |
| CD49     | 2-F                | 4-F                | 63      | 252-254 °C    |

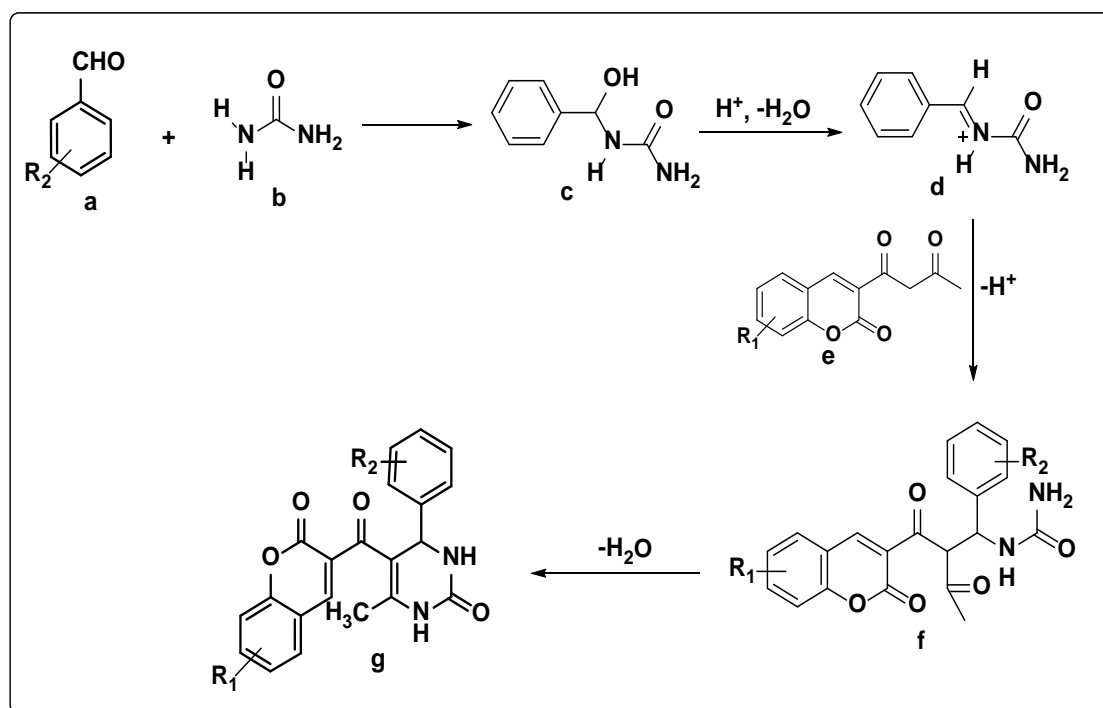
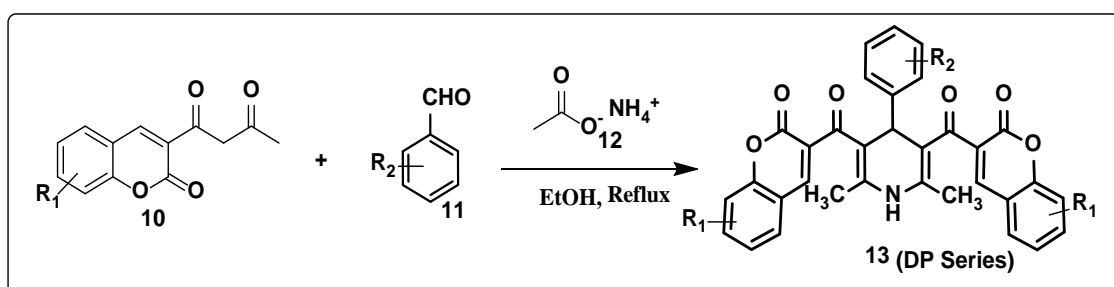


Figure 4.36: Plausible mechanism of dihydropyrimidinones

### 4.2.3 Synthesis of Coumarin-Dihydropyridine Hybrids

The first two steps in synthesis of coumarin-dihydropyridine hybrids were common as in case of coumarin-dihydropyrimidinone hybrids. The first step in the synthesis was formation of 3-acetyl coumarin which was formed by reaction of substituted salicylaldehydes with ethyl acetoacetate in the presence of piperidine (Vekariya *et al.*, 2017). This intermediate was then converted to 3-acetoacetyl coumarin derivative by reacting with ethyl acetate in the presence of potassium tertiary butoxide. Further, preparation of coumarin-dihydropyridine hybrids **13** (DP12, DP18-20, DP26-28, DP32, DP56, DP58, DP61, DP63) involved one pot synthesis in which 3-acetoacetyl coumarin **10** was refluxed with benzaldehydes **11** in the presence of ammonium acetate **12** and ethanol (Sohal *et al.*, 2014). The synthetic process has been outlined in Scheme 3. The products were symmetrical dihydropyridine derivatives which were prepared by classic Hantzsch method. The mechanistic path to formulate this series of compounds is explained in Figure 4.37 and physical characterization is given in Table 4.19. All the synthesized compounds were purified by recrystallization and characterized spectroscopically by modern analytical techniques. The plausible mechanism showed that synthesis of symmetrical dihydropyridines involved addition of compound **h** and **j** to form compound **l** accompanied by loss of an acetic acid molecule. At the same time, Knoevenegal condensation between **h** and **i** to give compound **m**, which follows Michael addition with compound **l** produces compound **n**. In the last step cyclization occurs to produce compound **8** and rearrange to yield 1,4-dihydropyridine molecules **o** (Figure 4.37).



Scheme 3. Synthetic process for coumarin-dihydropyridine hybrids

Table 4.19: Physical characterization of coumarin-dihydropyridine hybrids

| Compound | R <sub>1</sub>    | R <sub>2</sub>     | Percentage yield | Melting point |
|----------|-------------------|--------------------|------------------|---------------|
| DP12     | H                 | 4-OCH <sub>3</sub> | 66               | 286-288 °C    |
| DP18     | H                 | 4-Cl               | 82               | 292-294 °C    |
| DP19     | H                 | 4-OH               | 45               | 268-271 °C    |
| DP20     | H                 | 4-NO <sub>2</sub>  | 56               | 256-258 °C    |
| DP26     | 2-F               | 4-F                | 66               | 246-249 °C    |
| DP27     | 2-Cl              | 4-Cl               | 72               | 236-238 °C    |
| DP28     | 2-Cl              | 4-NO <sub>2</sub>  | 78               | 255-257 °C    |
| DP32     | 2-OH              | 4-OCH <sub>3</sub> | 66               | 273-275 °C    |
| DP56     | 2-NH <sub>2</sub> | 4-NH <sub>2</sub>  | 70               | 275-277 °C    |
| DP58     | 2-NH <sub>2</sub> | 4-Cl               | 71               | 251-253 °C    |
| DP61     | 2-CH <sub>3</sub> | 4-CH <sub>3</sub>  | 87               | 240-242 °C    |
| DP63     | 2-CH <sub>3</sub> | 4-NH <sub>2</sub>  | 74               | 262-264 °C    |

The structures of coumarin-dihydropyridine hybrids were found to be novel and were determined by 2D NMR, IR and HRMS experiments. IR spectrum of the synthesized compounds showed prominent peaks at 3371(-NH), 3026(-CH), 1643(-CN), 1748(-C=O), 1671(C=N), 1256(-CO) in the synthesized compounds. In <sup>1</sup>H-NMR spectra of compounds, appearance of singlet peaks at  $\delta$  8.70-8.71 ppm, corresponds to the presence of two NH groups of dihydropyridine moiety, whereas the peak of proton in pyrone appeared as 8.30-8.70. In <sup>13</sup>C NMR spectra peak at 199.0 ppm confirmed the presence of C=O bridging the two moieties and at 159.0 ppm was corresponding to the C=O groups of pyrone ring. The mass peak of DP28 with m/z 643.0597 (calcd. m/z 643.0630 [M+H]<sup>+</sup>) was observed in high resolution mass spectra (HRMS) represents the given structures.

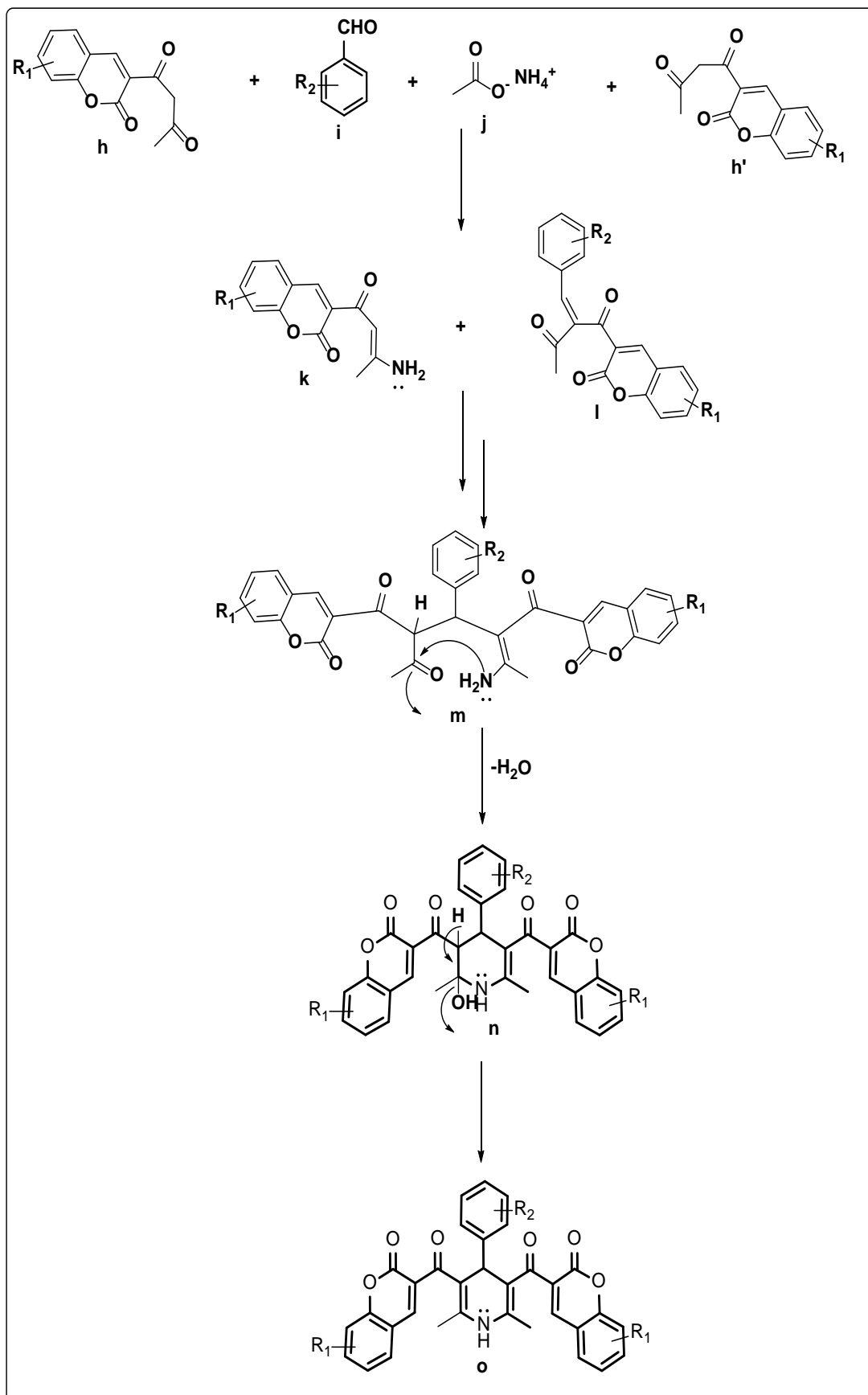


Figure 4.37: Plausible mechanism for formation of symmetrical dihydropyridines

### **4.3 *In vitro* antiproliferative activity**

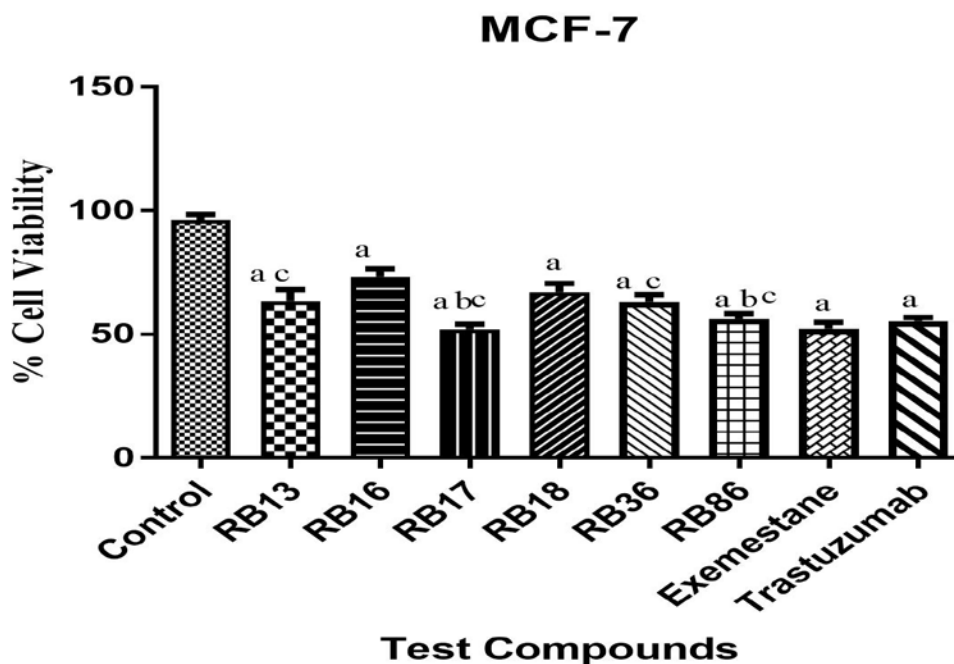
#### **4.3.1 *In vitro* antiproliferative evaluation of the synthesized coumarin-quinoxaline hybrids**

Twelve synthesized coumarin-quinoxaline hybrid molecules were evaluated for anticancer activity against breast cancer (MCF7, T47D), liver cancer (HepG2) and lung cancer (A549) cell lines. The compounds exhibited the  $IC_{50}$  values at micromolar ranges (Table 4.20). Exemestane and trastuzumab were used as reference drugs against breast cancer cell lines whereas doxorubicin was used against liver and lung cancer cell lines. Compound RB17 (3.8-5.12  $\mu$ M) and RB86 (6.86-18.6  $\mu$ M) displayed maximum potency against all the cell lines which was almost comparable to reference drugs Exemestane;  $IC_{50}$ = 2.16 and 8.32  $\mu$ M, Trastuzumab;  $IC_{50}$ = 9.18  $\mu$ M and 11.26  $\mu$ M against breast cancer cell lines and Doxorubicin;  $IC_{50}$ = 1.38  $\mu$ M and 3.56  $\mu$ M against liver and lung cancer cell lines. Rest of the compounds revealed good to moderate activity against breast cancer cell lines and moderate to poor activity against lung and liver cancer cell lines. The most potent compounds RB17 and RB86 were also evaluated for normal cell toxicity against human lung fibroblast cell lines WI-38 and revealed a very high  $IC_{50}$  values 178.36 and 194.26  $\mu$ M respectively which was even higher than the reference drugs. Thus the observations suggested that the compounds are safer to the normal cells. The overall study suggested that the synthesized molecules can serve as potential leads for drug development against cancers.

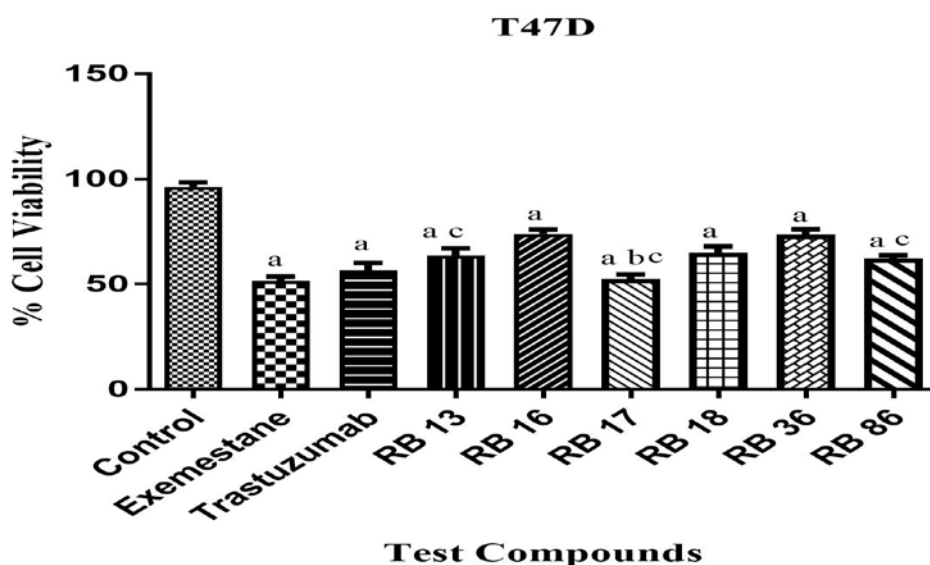
The cell viability of best six compounds was also assessed using all the above mentioned cell lines. By employing the MTT assay cell viability was determined by using the optical density of the control as 100% viability. The cancer cell lines were treated with the synthesized compounds and were further incubated for 4 hours followed by measurement of the optical density for all the treated cell lines. The cell viability against breast cancer cell lines (MCF7 and T47D) varied from 51.3-67.4% after four hours of incubation. Similarly against lung cancer cell lines (A549) the cell viability was found between 52.9-68.3%. For liver cancer cell lines (HepG2) it was found between 53.7-70.08%. The viability of the six best compounds was tested against all the four cancer cell lines and the obtained results have been presented in Figures 4.38-4.41. The results were compared with reference drugs exemestane, trastuzumab and doxorubicin.

Table 4.20: IC<sub>50</sub> values of coumarin-quinoxaline hybrids against cancer and normal cell lines

| Compound    | IC <sub>50</sub> (μM) |              |              |              |               |
|-------------|-----------------------|--------------|--------------|--------------|---------------|
|             | MCF7                  | T47D         | A549         | HepG2        | WI-38         |
| RB13        | 16.80 ± 2.18          | 18.32 ± 1.06 | 14.32 ± 0.18 | 44.32 ± 2.18 | NT            |
| RB14        | 22.38 ± 1.18          | 38.82 ± 2.46 | 32.18 ± 0.98 | 42.22 ± 1.88 | NT            |
| RB16        | 36.8 ± 1.26           | 29.38 ± 1.02 | >50          | >50          | NT            |
| RB17        | 3.8 ± 0.78            | 6.52 ± 0.82  | 3.2 ± 0.28   | 5.12 ± 0.82  | 178.36 ± 2.16 |
| RB18        | 17.82 ± 1.76          | 24.12 ± 1.48 | 19.32 ± 0.86 | >50          | NT            |
| RB19        | 42.12 ± 2.08          | 46.80 ± 2.08 | >50          | >50          | NT            |
| RB36        | 12.8 ± 1.12           | 32.2 ± 1.82  | 16.34 ± 1.42 | 18.4 ± 1.26  | NT            |
| RB37        | 37.08 ± 1.82          | >50          | 29.18 ± 1.32 | 39.18 ± 1.24 | NT            |
| RB86        | 7.82 ± 0.26           | 18.6 ± 1.12  | 9.46 ± 1.16  | 6.86 ± 0.78  | 194.26 ± 1.62 |
| RB87        | 38.26 ± 0.92          | 36.92 ± 2.86 | 28.26 ± 1.02 | 37.16 ± 2.32 | NT            |
| RB88        | 40.13 ± 1.22          | 48.18 ± 1.86 | 30.06 ± 0.68 | >50          | NT            |
| RB89        | >50                   | >50          | 42.13 ± 2.26 | >50          | NT            |
| Exemestane  | 2.16 ± 0.32           | 8.38 ± 0.92  | NT           | NT           | 123.22 ± 0.86 |
| Trastuzumab | 9.18 ± 1.02           | 11.26 ± 1.32 | NT           | NT           | 132.26 ± 0.92 |



**Figure 4.38:** Percentage cell viability versus experimental trials using MTT assay against MCF-7 cell line. Data was shown as Mean  $\pm$  SD and statistically analyzed by one way ANOVA followed by tukey's post hoc test.  $p^a \leq 0.05$  vs. control was considered to be statistically significant,  $p^b \geq 0.05$  vs. exemestane and  $p^c \geq 0.05$  vs. trastuzumab was considered to be statistically insignificant.



**Figure 4.39:** Percentage cell viability versus experimental trials using MTT assay against T47D cell line. Data was shown as Mean  $\pm$  SD and statistically analyzed by one way ANOVA followed by tukey's post hoc test.  $p^a \leq 0.05$  vs. control was considered to be statistically significant,  $p^b \geq 0.05$  vs. exemestane and  $p^c \geq 0.05$  vs. trastuzumab was considered to be statistically insignificant

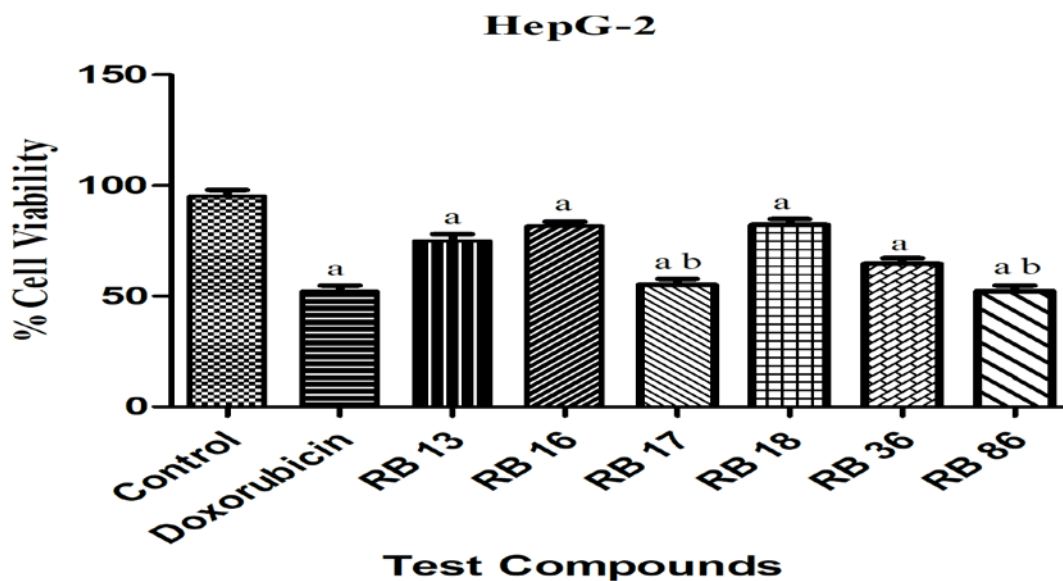


**Figure 4.40:** Percentage cell viability versus experimental trials using MTT assay against HepG-2 cell line. Data was shown as Mean  $\pm$  SD and statistically analyzed by one way ANOVA followed by tukey's post hoc test.  $p^a \leq 0.05$  vs. control was considered to be statistically significant and  $p^b \geq 0.05$  vs. doxorubicin was considered to be statistically insignificant

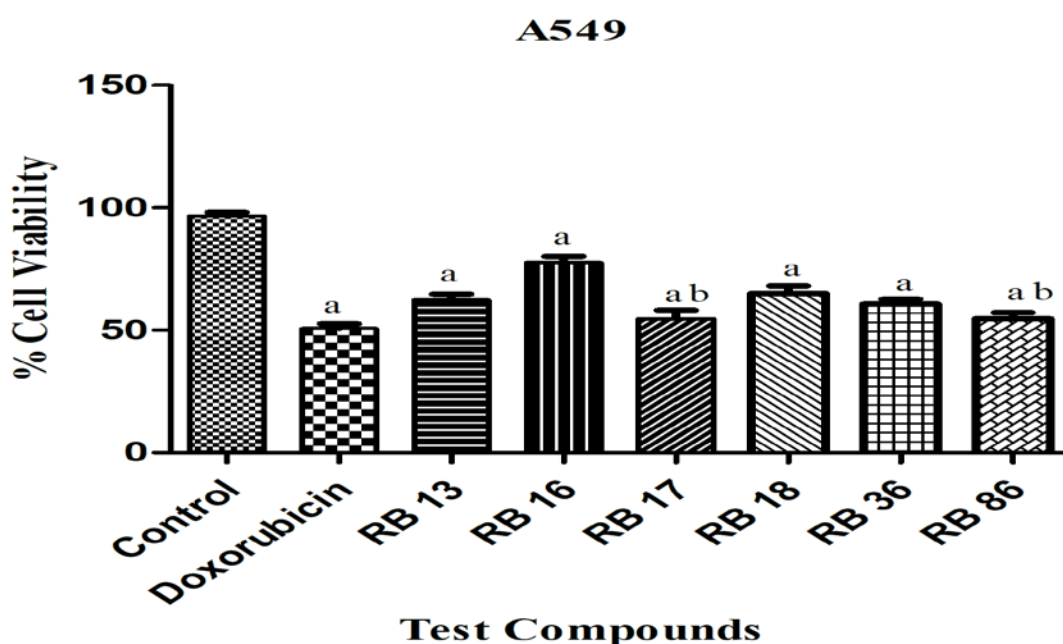


**Figure 4.41:** Percentage cell viability versus experimental trials using MTT assay against A549 cell line. Data was shown as Mean  $\pm$  SD and statistically analyzed by one way ANOVA followed by tukey's post hoc test.  $p^a \leq 0.05$  vs. control was considered to be statistically significant and  $p^b \geq 0.05$  vs. doxorubicin was considered to be statistically insignificant

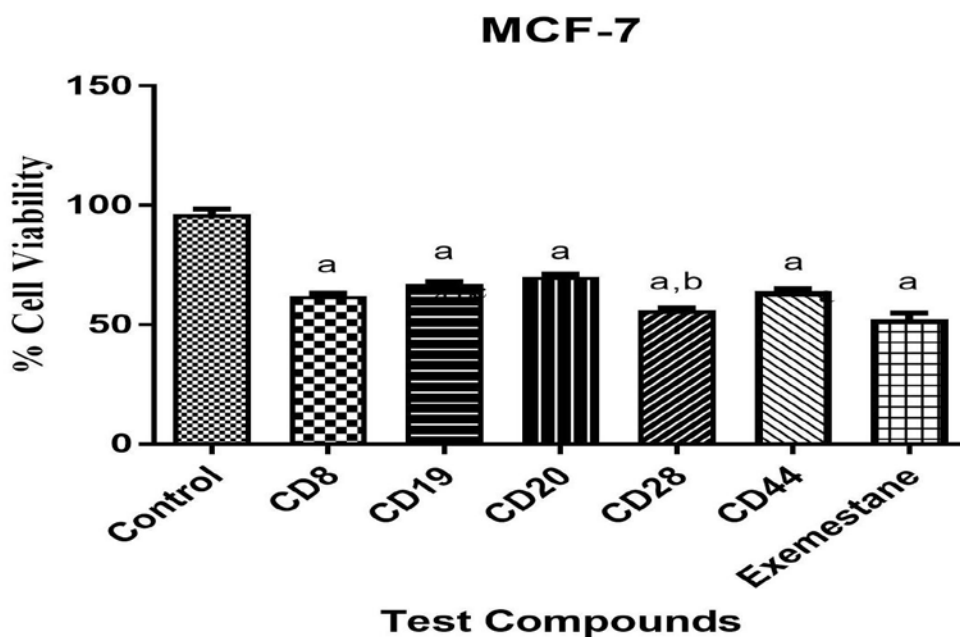
#### **4.3.2 *In vitro* antiproliferative evaluation of the synthesized coumarin-dihydropyrimidinone hybrids**

Twelve synthesized coumarin-dihydropyrimidinone hybrid molecules were evaluated for anticancer activity against breast cancer (MCF7, T47D), liver cancer (HepG2) and lung cancer (A549) cell lines. The compounds exhibited the IC<sub>50</sub> values at micromolar ranges (Table 4.21). Exemestane was used as reference drugs against breast cancer cell lines whereas doxorubicin was used against liver and lung cancer cell lines. Compound CD28 displayed maximum potency against breast cancer cell lines with IC<sub>50</sub>= 8.82 and 13.82 μM, which was almost comparable to reference drugs Exemestane; IC<sub>50</sub>= 7.32 and 28.28 μM, against breast cancer cell lines. On the other hand, compounds CD10 and CD8 displayed maximum potency against the liver and lung cancer cell lines in the range of IC<sub>50</sub>=3.68-14.12 μM in comparison to the reference drug Doxorubicin (IC<sub>50</sub>=3.36-5.08 μM). Rest of the compounds revealed good to moderate activity against breast cancer cell lines and moderate to poor activity against lung and liver cancer cell lines. The most potent compounds CD28 and CD10 were also evaluated for normal cell toxicity against human lung fibroblast cell lines WI-38 and revealed a very high IC<sub>50</sub> values 144.42 and 188.42 μM respectively which was even higher than the reference drugs. Thus the observations suggested that the compounds are safer to the normal cells. The overall study suggested that the synthesized molecules can serve as potential leads for drug development against cancers.

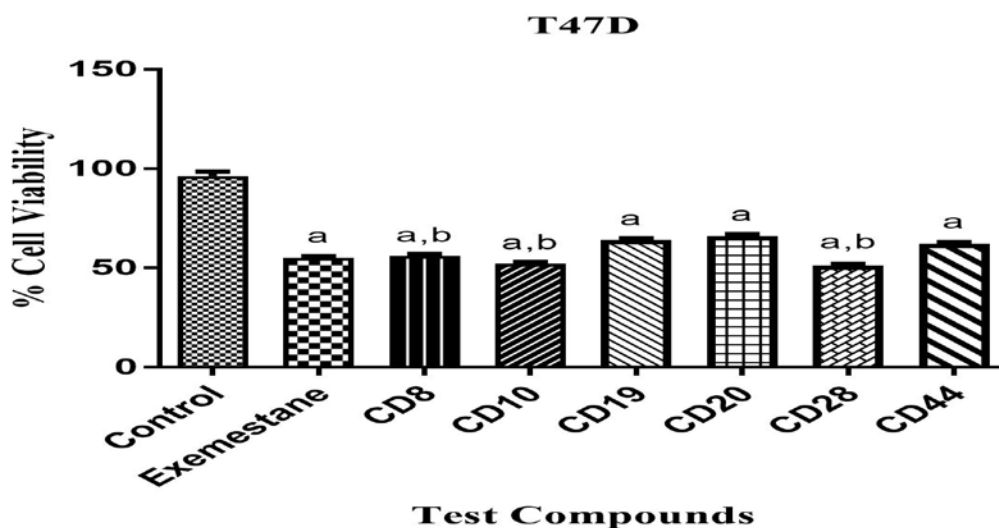
The cell viability of best six compounds was also assessed using all the above mentioned cell lines. By employing the MTT assay cell viability was determined by using the optical density of the control as 100% viability. The cancer cell lines were treated with the synthesized compounds and were further incubated for 4 hours followed by measurement of the optical density for all the treated cell lines. The cell viability against breast cancer cell lines (MCF7 and T47D) varied from 53.3-68.4% after four hours of incubation. Similarly against lung cancer cell lines (A549) the cell viability was found between 51.2-69.3%. For liver cancer cell lines (HepG2) it was found between 50.7-68.18%. The viability of the six best compounds was tested against all the four cancer cell lines and the obtained results have been presented in Figures 4.42-4.45. The results were compared with reference drugs exemestane and doxorubicin.

Table 4.21: IC<sub>50</sub> values of coumarin-dihydropyrimidinone hybrids against cancer and normal cell lines

| Compound    | IC <sub>50</sub> (μM) |              |              |              |               |
|-------------|-----------------------|--------------|--------------|--------------|---------------|
|             | MCF7                  | T47D         | A549         | HepG2        | WI-38         |
| CD6         | 22.8 ± 2.18           | 38.82 ± 2.46 | 24.26 ± 0.48 | 32.48 ± 2.16 | NT            |
| CD8         | 16.8 ± 0.96           | 22.38 ± 1.02 | 12.02 ± 0.86 | 14.12 ± 1.28 | NT            |
| CD9         | 34.8 ± 2.26           | 39.38 ± 1.12 | >50          | 41.34 ± 0.82 | NT            |
| CD10        | 30.8 ± 1.78           | 16.42 ± 0.62 | 3.68 ± 0.48  | 5.22 ± 0.42  | 188.42 ± 0.76 |
| CD19        | 24.8 ± 1.12           | 28.2 ± 1.82  | 29.22 ± 0.62 | 31.35 ± 0.72 | NT            |
| CD20        | 27.82 ± 1.76          | 32.6 ± 1.42  | >50          | 48.56 ± 1.62 | NT            |
| CD28        | 8.82 ± 0.26           | 13.82 ± 1.08 | 5.47 ± 1.02  | 7.4 ± 0.64   | 144.42 ± 2.06 |
| CD32        | 42.18 ± 1.62          | >50          | 39.28 ± 1.56 | 42.23 ± 1.14 | NT            |
| CD42        | 46.22 ± 0.26          | 38.6 ± 1.12  | >50          | >50          | NT            |
| CD43        | 38.26 ± 0.92          | >50          | 28.26 ± 1.02 | 37.16 ± 2.32 | NT            |
| CD44        | 23.82 ± 1.28          | 26.82 ± 2.16 | 30.06 ± 0.68 | >50          | NT            |
| CD49        | >50                   | 48.24 ± 2.12 | 37.24 ± 1.34 | >50          | NT            |
| Exemestane  | 7.32 ± 0.32           | 18.28 ± 0.92 | NT           | NT           | 123.22 ± 0.86 |
| Doxorubicin | NT                    | NT           | 3.36 ± 0.26  | 5.08 ± 0.34  | 89.13 ± 1.12  |



**Figure 4.42:** Percentage cell viability versus experimental trials using MTT assay against MCF-7 cell line. Data was shown as Mean  $\pm$  SD and statistically analyzed by one way ANOVA followed by tukey's post hoc test.  $p^a \leq 0.05$  vs. control was considered to be statistically significant,  $p^b \geq 0.05$  vs. exemestane was considered to be statistically insignificant.



**Figure 4.43:** Percentage cell viability versus experimental trials using MTT assay against T47D cell line. Data was shown as Mean  $\pm$  SD and statistically analyzed by one way ANOVA followed by tukey's post hoc test.  $p^a \leq 0.05$  vs. control was considered to be statistically significant,  $p^b \geq 0.05$  vs. exemestane was considered to be statistically insignificant.

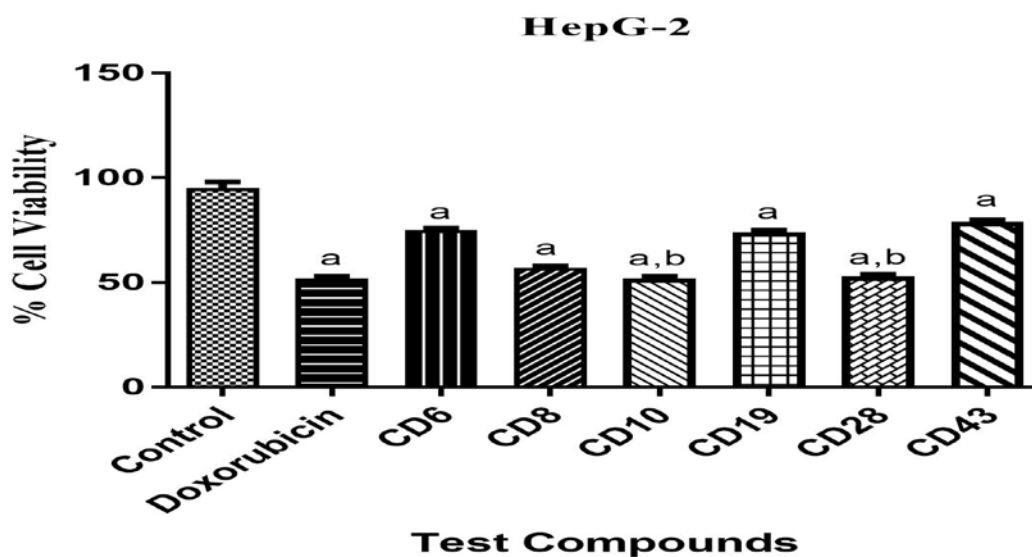


**Figure 4.44:** Percentage cell viability versus experimental trials using MTT assay against HepG2 cell line. Data was shown as Mean  $\pm$  SD and statistically analyzed by one way ANOVA followed by tukey's post hoc test.  $p^a \leq 0.05$  vs. control was considered to be statistically significant,  $p^b \geq 0.05$  vs. doxorubicin was considered to be statistically insignificant.

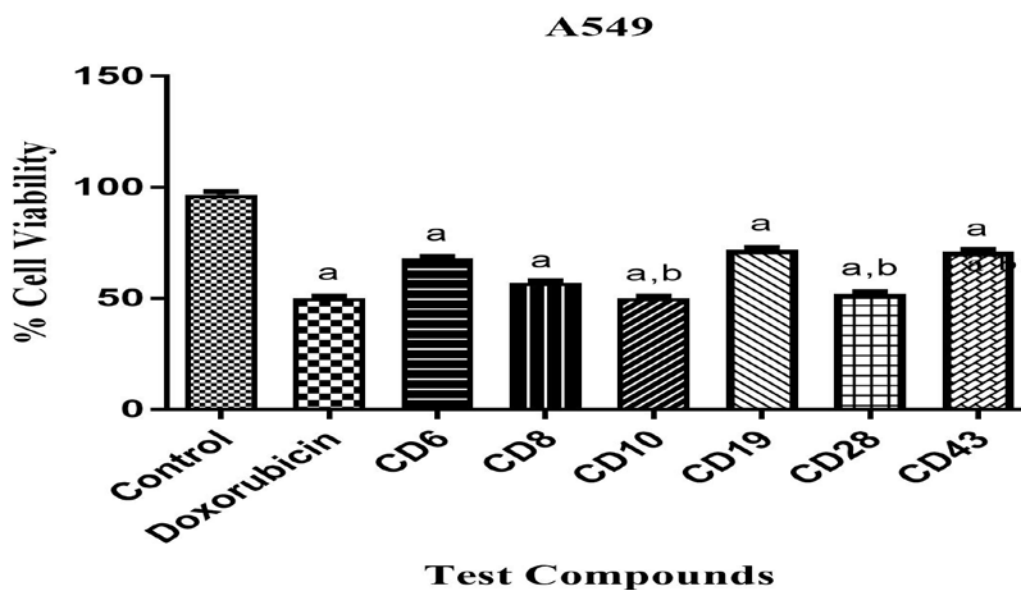


**Figure 4.45:** Percentage cell viability versus experimental trials using MTT assay against A549 cell line. Data was shown as Mean  $\pm$  SD and statistically analyzed by one way ANOVA followed by tukey's post hoc test.  $p^a \leq 0.05$  vs. control was considered to be statistically significant,  $p^b \geq 0.05$  vs. doxorubicin was considered to be statistically insignificant.

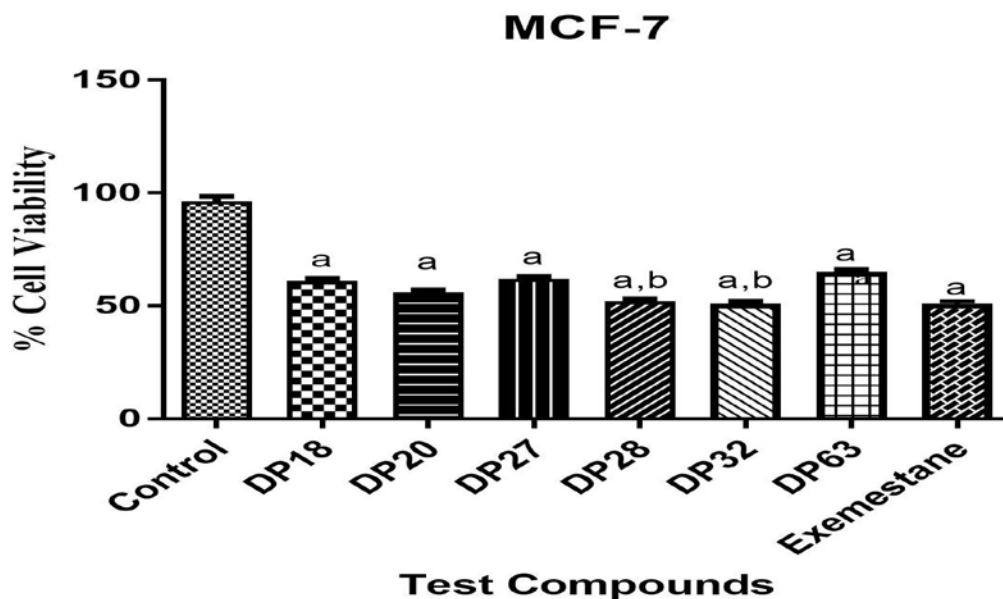
#### **4.3.3 *In vitro* antiproliferative evaluation of the synthesized coumarin-dihydropyridine hybrids**

Twelve synthesized coumarin-dihydropyridine hybrid molecules were evaluated for anticancer activity against breast cancer (MCF7, T47D), liver cancer (HepG2) and lung cancer (A549) cell lines. The compounds exhibited the IC<sub>50</sub> values at micromolar ranges (Table 4.23). Exemestane was used as reference drugs against breast cancer cell lines whereas doxorubicin was used against liver and lung cancer cell lines. Compound DP32, DP28 and DP20 displayed maximum potency against all the four cancer cell lines with IC<sub>50</sub>= 5.22-15.42 μM, which was almost comparable to reference drugs Exemestane; IC<sub>50</sub>= 7.32 and 18.28 μM, against breast cancer cell lines. And Doxorubicin; IC<sub>50</sub>= 3.36 and 5.08 μM, against liver and lung cancer cell lines. Also compounds DP17, DP28 and DP63 good potency against all the cancer cell lines. Rest of the compounds revealed good to moderate activity. The most potent compounds DP28 and DP32 were also evaluated for normal cell toxicity against human lung fibroblast cell lines WI-38 and revealed a very high IC<sub>50</sub> values 118.61 and 121.42 μM respectively which was even higher than the reference drugs. Thus the observations suggested that the compounds are safer to the normal cells. The overall study suggested that the synthesized molecules can serve as potential leads for drug development against cancers.

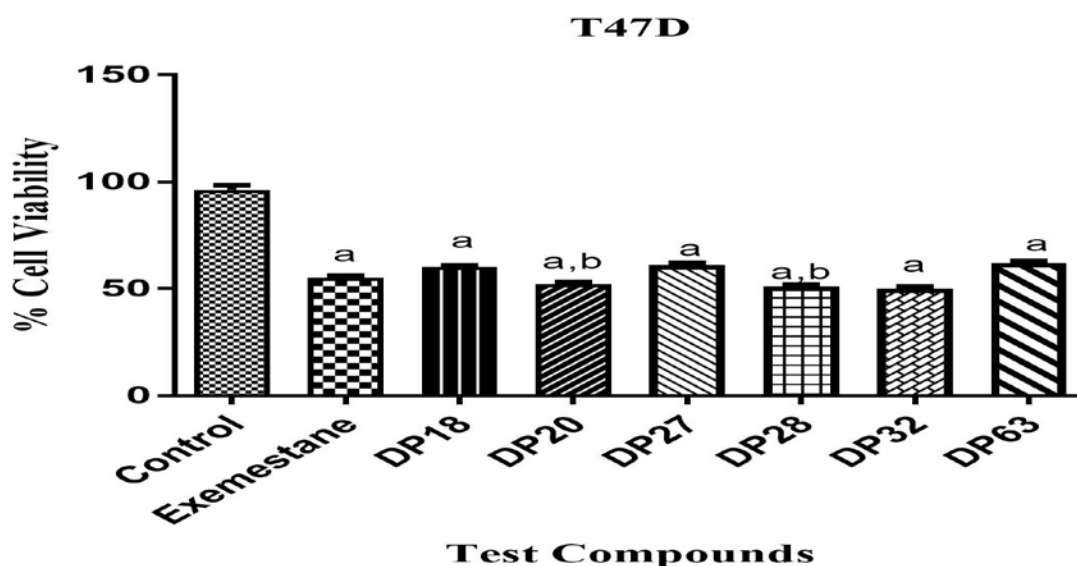
The cell viability of best six compounds was also assessed using all the above mentioned cell lines. By employing the MTT assay cell viability was determined by using the optical density of the control as 100% viability. The cancer cell lines were treated with the synthesized compounds and were further incubated for 4 hours followed by measurement of the optical density for all the treated cell lines. The cell viability against breast cancer cell lines (MCF7 and T47D) varied from 50.3-62.4% after four hours of incubation. Similarly against lung cancer cell lines (A549) the cell viability was found between 56.2-68.3%. For liver cancer cell lines (HepG2) it was found between 51.7-70.18%. The viability of the six best compounds was tested against all the four cancer cell lines and the obtained results have been presented in Figures 4.46-4.49. The results were compared with reference drugs exemestane and doxorubicin.

Table 4.23: IC<sub>50</sub> values of coumarin-dihydropyridine hybrids against cancer and normal cell lines

| Compound           | IC <sub>50</sub> (μM) |              |              |              |               |
|--------------------|-----------------------|--------------|--------------|--------------|---------------|
|                    | MCF7                  | T47D         | A549         | HepG2        | WI-38         |
| <b>DP12</b>        | 24.8 ± 1.48           | 28.62 ± 1.46 | 29.64 ± 0.48 | 37.38 ± 1.64 | NT            |
| <b>DP18</b>        | 16.28 ± 0.86          | 22.32 ± 1.42 | 18.22 ± 0.66 | 29.22 ± 0.88 | NT            |
| <b>DP19</b>        | 39.8 ± 2.26           | 42.38 ± 1.12 | 36.82 ± 2.16 | 45.34 ± 0.82 | NT            |
| <b>DP20</b>        | 12.28 ± 0.78          | 15.46 ± 0.82 | 7.48 ± 0.68  | 8.26 ± 0.92  | NT            |
| <b>DP26</b>        | 26.8 ± 1.12           | 27.2 ± 1.82  | 31.12 ± 0.42 | 33.25 ± 0.82 | NT            |
| <b>DP27</b>        | 17.82 ± 1.46          | 26.62 ± 1.72 | 16.82 ± 1.16 | 24.56 ± 0.62 | NT            |
| <b>DP28</b>        | 7.82 ± 1.16           | 15.02 ± 0.98 | 7.47 ± 0.86  | 7.14 ± 0.64  | 118.61 ± 1.72 |
| <b>DP32</b>        | 5.22 ± 0.62           | 10.14 ± 1.34 | 3.82 ± 0.56  | 7.24 ± 0.44  | 121.42 ± 2.06 |
| <b>DP56</b>        | 36.28 ± 0.46          | 34.16 ± 1.72 | 38.42 ± 1.96 | 30.82 ± 1.16 | NT            |
| <b>DP58</b>        | 40.26 ± 0.92          | 36.82 ± 2.16 | 38.26 ± 1.22 | 47.16 ± 1.32 | NT            |
| <b>DP61</b>        | 39.82 ± 1.28          | 46.82 ± 2.16 | 39.06 ± 0.58 | 36.82 ± 2.26 | NT            |
| <b>DP63</b>        | 22.82 ± 2.16          | 28.24 ± 2.12 | 27.24 ± 1.34 | 29.82 ± 1.26 | NT            |
| <b>Exemestane</b>  | 7.32 ± 0.32           | 18.28 ± 0.92 | NT           | NT           | 123.22 ± 0.86 |
| <b>Doxorubicin</b> | NT                    | NT           | 3.36 ± 0.26  | 5.08 ± 0.34  | 89.13 ± 1.12  |



**Figure 4.46:** Percentage cell viability versus experimental trials using MTT assay against MCF-7 cell line. Data was shown as Mean  $\pm$  SD and statistically analyzed by one way ANOVA followed by tukey's post hoc test.  $P^a \leq 0.05$  vs. control was considered to be statistically significant,  $p^b \geq 0.05$  vs. exemestane was considered to be statistically insignificant.



**Figure 4.47:** Percentage cell viability versus experimental trials using MTT assay against T47D cell line. Data was shown as Mean  $\pm$  SD and statistically analyzed by one way ANOVA followed by tukey's post hoc test.  $P^a \leq 0.05$  vs. control was considered to be statistically significant,  $p^b \geq 0.05$  vs. exemestane was considered to be statistically insignificant.

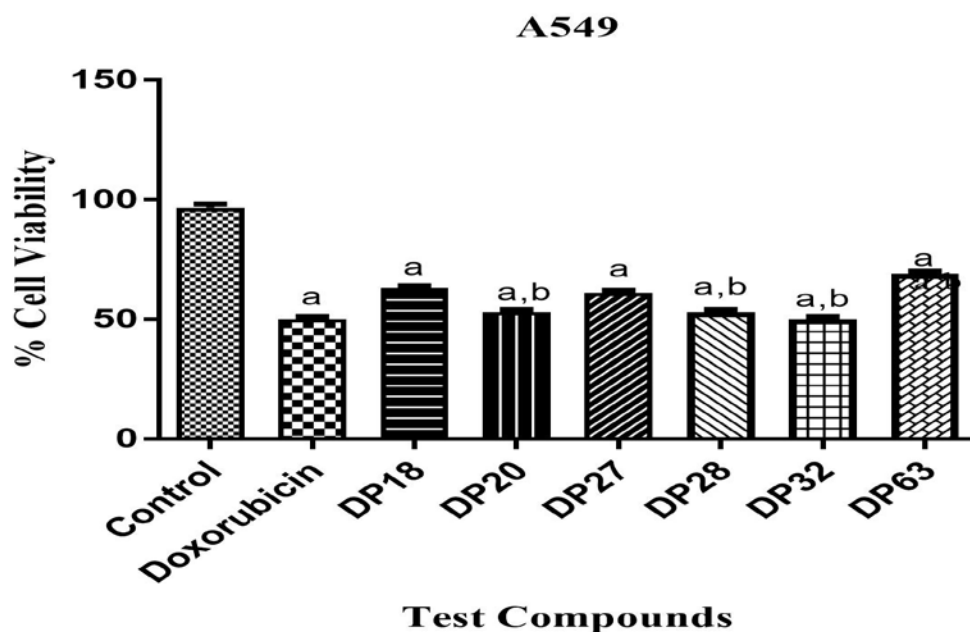


**Figure 4.48:** Percentage cell viability versus experimental trials using MTT assay against A549 cell line. Data was shown as Mean  $\pm$  SD and statistically analyzed by one way ANOVA followed by tukey's post hoc test.  $P^a \leq 0.05$  vs. control was considered to be statistically significant,  $p^b \geq 0.05$  vs. doxorubicin was considered to be statistically insignificant.

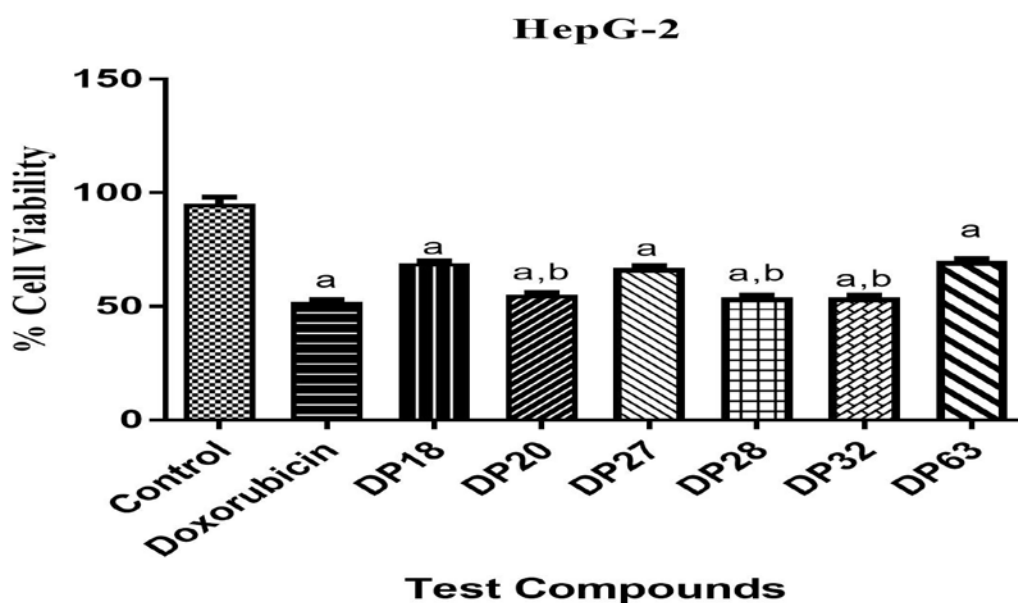


**Figure 4.49:** Percentage cell viability versus experimental trials using MTT assay against HepG2 cell line. Data was shown as Mean  $\pm$  SD and statistically analyzed by one way ANOVA followed by tukey's post hoc test.  $P^a \leq 0.05$  vs. control was considered to be statistically significant,  $p^b \geq 0.05$  vs. doxorubicin was considered to be statistically insignificant.

#### 4.3.4 Normal Cell Toxicity

As stated in antiproliferative activity, two most potent compounds from each series were also evaluated to check their toxicity on normal human cells. The normal cell cytotoxicity was assessed against human normal lung fibroblast cell lines WI-38. The  $IC_{50}$  values were compared to all the three reference drugs exemestane, trastuzumab and doxorubicin (Figure 4.50). The results evidenced that the  $IC_{50}$  values for all the compounds (RB17, RB86, CD10, CD28, DP28 and DP32) were quite high in the range of 125.0-190.0  $\mu\text{M}$  which was higher even than the reference drugs. These observations indicated that the synthesized compounds are specific to the cancer cells only and are safer to the normal human cells.

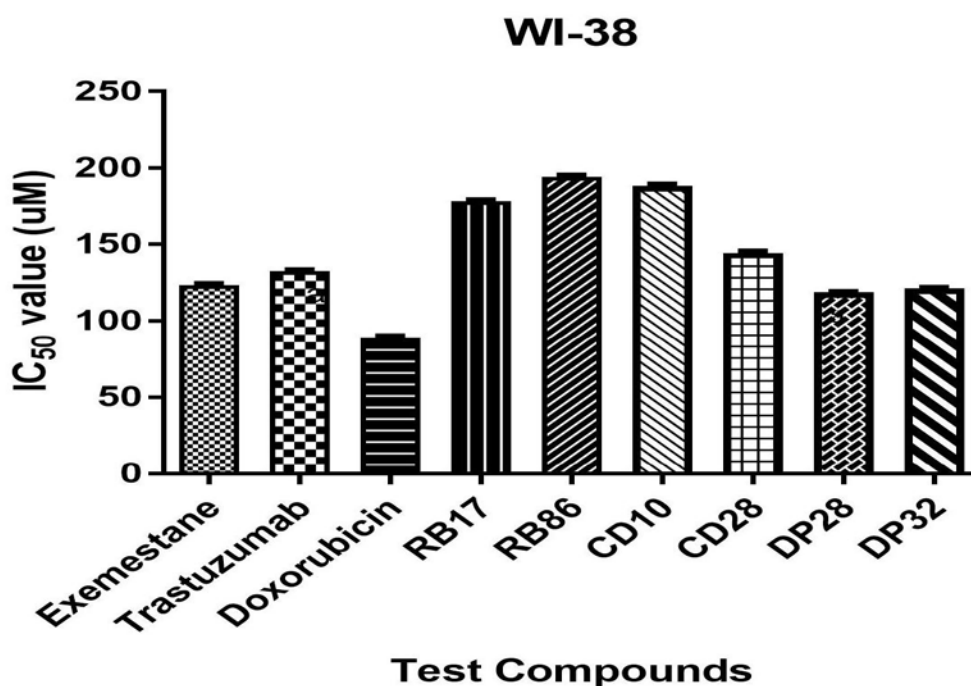


Figure 4.50. Cytotoxic effects of most potent compounds on normal human cells

#### 4.4 Structural Activity Relationships (SAR)

##### 4.4.1 SAR of coumarin-quinoxaline hybrids

Important aspects found about structural activity relationship of coumarin-quinoxaline hybrids are as follows:

- A. Substitution of pyrone ring at 4<sup>th</sup> position with  $-\text{CH}_3$ ,  $-\text{C}_6\text{H}_5$  and  $-\text{OH}$  produced compounds with good to moderate activity (RB17, RB36).

- B. Substitution of coumarin ring at 5<sup>th</sup> position with  $-\text{OCH}_3$  group revealed excellent activity (RB86).
- C. Substitution of phenyl ring of quinoxaline moiety at 5<sup>th</sup> position with  $-\text{OCH}_3$  and 5<sup>th</sup> and 6<sup>th</sup> position with  $-(\text{OCH}_3)_2$  displayed maximum potency whereas substitution at 5<sup>th</sup> position with halogens displayed moderate activity.
- D. Docking studies revealed that the keto group of coumarin was essential for aromatase binding whereas quinoxaline moiety also displayed arene-cation interactions with the aromatase.
- E. It was also worth notable that pyrrolidine moiety bridging the coumarin and quinoxaline displayed significant interactions with both aromatase and HER2. Figure 4.51 depicts important points of observed structural activity relationship.

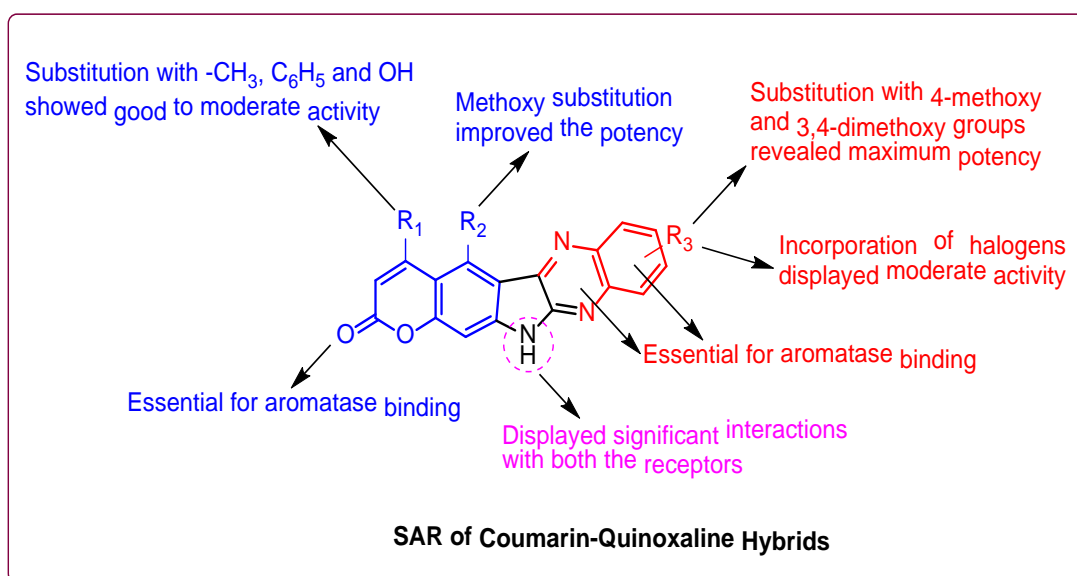


**Figure 4.51: SAR of coumarin-quinoxaline hybrids**

#### 4.4.2 SAR of coumarin-dihydropyrimidinone hybrids

Important aspects found about structural activity relationship of coumarin-dihydropyrimidinone hybrids are as follows:

- A. Substitution of phenyl ring of coumarin at 7<sup>th</sup> position with  $-\text{OCH}_3$  and  $-\text{NO}_2$  revealed maximum potency (CD28 and CD8) whereas attachment of halogens at the same position lowered the activity (CD19, CD20).

- B. Incorporation of  $-OCH_3$ ,  $-CH_3$  and  $-F$  on the 4<sup>th</sup> position of phenyl ring revealed improved activity (CD8, CD28, CD10).
- C. Substitution of phenyl ring at 4<sup>th</sup> position with higher halogens Cl, Br and  $-NH_2$  displayed slightly lower activity (CD32, CD42, CD44).
- D. Docking studies revealed that the keto group of coumarin was essential for aromatase binding whereas phenyl ring also displayed arene-cation interactions with the aromatase.
- E. The amino groups of dihydropyrimidinone moiety displayed significant hydrogen bonding interactions with the amino acids.

Figure 4.52 depicts important points of SAR observed for coumarin-dihydropyrimidinone hybrids.

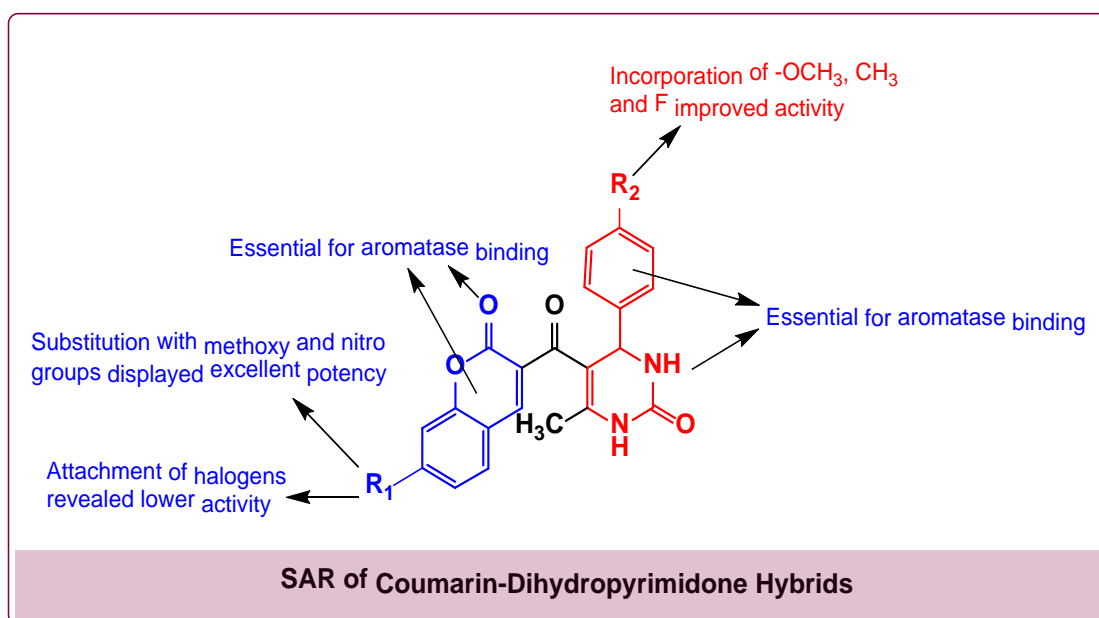


**Figure 4.52: SAR of coumarin-dihydropyrimidinone hybrids**

#### 4.4.3 SAR of coumarin-dihydropyridine hybrids

Important aspects found about structural activity relationship of coumarin-dihydropyridine hybrids are as follows:

- A. Unsubstituted phenyl ring of coumarin moiety displayed maximum potency (DP18, DP20).

- B. Also substitution of phenyl ring of coumarin moiety at 7<sup>th</sup> position with –Cl, –OH and –NH<sub>2</sub> displayed good to excellent activity (DP28, DP32, DP63).
- C. It was also worth notable that substitution of phenyl ring of coumarin on the 7<sup>th</sup> position with –CH<sub>3</sub> and –OCH<sub>3</sub> revealed slightly lower activity (DP61, DP63).
- D. Incorporation of electron withdrawing groups (–Cl, –NO<sub>2</sub>) on 4<sup>th</sup> position of phenyl ring displayed maximum potency (DP18, DP28).
- E. The dihydropyridine moiety displayed significant binding with the aromatase through its –NH group.
- F. Docking studies revealed that the keto group of coumarin was essential for aromatase binding.

Figure 4.53 depicts important points of SAR observed for coumarin-dihydropyridine hybrids.

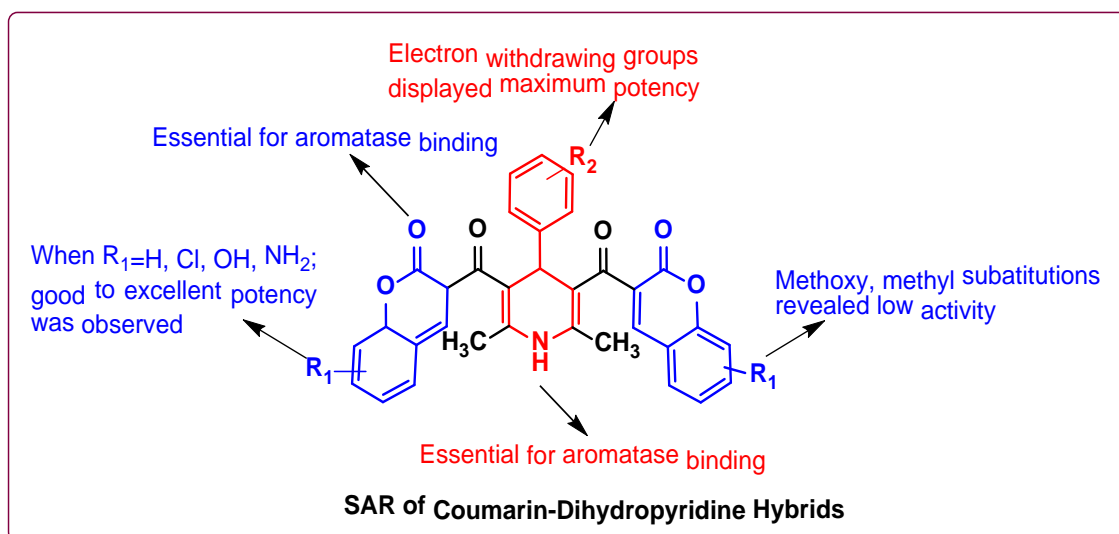


**Figure 4.53: SAR Of coumarin-dihydropyridine hybrids**